

# **Micellar- and Polymer-Enhanced Ultrafiltration for Heavy Metal and Sulfate Removal from Aqueous Solutions**

by ©  
Weiyun Lin

A Thesis Submitted to the School of Graduate Studies  
in partial fulfillment of the requirement for the degree of

Doctor of Philosophy

Faculty of Engineering and Applied Science  
Memorial University of Newfoundland

**March 2020**

St. John's

Newfoundland and Labrador

## Abstract

Micellar-enhanced ultrafiltration (MEUF) and polymer-enhanced ultrafiltration (PEUF) show potential as promising techniques to remove dissolved ions from wastewater, but they remain inadequately understood. In this thesis, the MEUF removal of copper, nickel, and cobalt ions from aqueous solutions was investigated. The effect of surfactant-to-metal (S/M) ratio and pH on MEUF performance (i.e., metal rejection rate and permeate flux) were examined to obtain the preferred operational conditions. A resampling-based artificial neural network (ANN) modeling was proposed as a promising tool to predict the MEUF performance and to reveal the importance of process parameters. The model-predicted values showed good agreement with experimental data ( $R^2 > 0.99$ ). S/M ratio and pH had relatively greater contributions to the system performance, whereas sampling time contributed less. A high MEUF efficiency (Rejection  $> 99\%$ ) was achieved.

To optimize the system performance and to observe the interactions among operational parameters, the statistical-based response surface methodology (RSM) was used to overcome the drawbacks of the commonly used one-factor-at-a-time method. The thesis is the first study to use an RSM method based on a Box-Behnken design to examine nickel ion removal in a MEUF system while combine with an ANN model. The generated RSM models described the relationship between each performance indicator (nickel rejection rate or permeate flux) and process variables (transmembrane pressure, feed nickel concentration, feed surfactant concentration, and membrane molecular weight

cut-off (MWCO) of the membrane). Both RSM and ANN methods adequately described the performance indicators within the examined ranges of the process variables.

Next, the thesis targets on sulfate ions, a dissolved anion of increasing concern but not tackled in the MEUF/PEUF field. The thesis is the first study to use MEUF and PEUF to remove sulfate ions as the target component from aqueous solutions. It is also the first to examine the adsorption mechanism of sulfate to surfactant/polymer in such systems. Both MEUF and PEUF were found technically viable to remove sulfate from aqueous streams, with the highest rejection rate (Rejection > 99%) found in dilute sulfate solutions. Further, adsorption equilibrium and kinetics studies show that Freundlich isotherm and pseudo-second-order kinetics can describe the adsorption process.

This thesis adds knowledge to the existing MEUF/PEUF techniques by improving system operation, conducting system optimization, and exploring new components (i.e., sulfate ions) that can be removed. It also provides treatment information and potentially facilitates reservoir souring control and mining wastewater treatment.

## Acknowledgments

This Ph.D. has been the most memorable journey in my life. My biggest thanks go out to my supervisor, Dr. Baiyu (Helen) Zhang, who taught me what research is, provided me valuable chances to be involved in different projects, mentored me in both research and life, never lost faith in me, and encouraged me over the years. I am very lucky to be her student and proud to be a member of the Northern Region Persistent Organic Pollution Control (NRPOP) research group.

Many thanks to my supervisory committee, Drs. Kelly Hawboldt and Zhendi Wang, for their valuable advice and continued support for my research, and detailed revision of my manuscripts and thesis; to my role model Dr. Leonard Lye, who pushed me out of my comfort zone on many occasions, and who greatly enhanced my transferable skills.

I am grateful to my parents for their unconditional love and lifelong support in every single way; to my as-good-as-family friends Zhiwen (Joy) Zhu, Junjie (Grace) Hu, Ming Liu, and Nicholas Larocque for their understanding and always being there during my hard times.

Much appreciation goes to all my colleagues in the NRPOP lab, for every proposal, project, and manuscript we worked together; for the discussions in our weekly meetings; for the questions they asked in presentations; for their companionship in labs, daytime and after hours, weekdays and weekends; for their help to lift heavy equipment and troubleshoot problems in the lab, and so much more.

I feel grateful to Memorial University of Newfoundland, which made my dream of studying in Canada come true; to Faculty of Engineering and Applied Science, which provided so many opportunities to build up my technical and soft skills; to Core Research Equipment and Instrument Training (CREAIT) Network, which provided equipment and technical support to test my laboratory samples; to our renowned QE II library, which never failed to find any reference I was looking for; to our lab instructor Lidan Tao, who made our lab work ten times more efficient; and to Adam Taylor and Shawn Beson, who ordered our lab consumables and equipment items most efficiently. Finally, thanks go to the Natural Sciences and Engineering Research Council of Canada (NSERC) and the Canada Foundation for Innovation (CFI) for financing and supporting my research.

## Research contributions

(1) The study improves the understanding of the effect of system parameters and the relative importance between the examined parameters through using a resampling-based artificial neural network (ANN) tool, showing micellar-enhanced ultrafiltration (MEUF) as a potential treatment technique for metal-containing wastewater.

(2) This study is the first report to use a response surface methodology for system optimization of nickel ions removal using MEUF, combined with ANN modeling. The optimization results further enhance the understanding of different parameters and their interactions in a MEUF system.

(3) The study conducted the first investigation for the removal of sulfate as the target solute (from low to high concentrations) under different system conditions in MEUF and PEUF systems. It is also the first report of sulfate-colloid interaction in these systems. The obtained adsorption isotherm and kinetic equations provide information for sulfate removal in mining and offshore oil and gas industries.

# Table of Contents

<b>Abstract.....</b>	<b>ii</b>
<b>Acknowledgments .....</b>	<b>iv</b>
<b>Research contributions .....</b>	<b>vi</b>
<b>Table of Contents .....</b>	<b>vii</b>
<b>List of Tables .....</b>	<b>xii</b>
<b>List of Figures.....</b>	<b>xiv</b>
<b>List of Symbols .....</b>	<b>xx</b>
<b>List of Abbreviations .....</b>	<b>xxii</b>
 <b>Chapter 1. Introduction.....</b>	 <b>1</b>
1.1. Background.....	2
1.1.1. Heavy metal pollution, impact, and treatment.....	2
1.1.2. Sulfate pollution, impact, and treatment.....	7
1.2. Statement of Problems .....	9
1.3. Research Objective .....	11
1.4. Thesis Structure .....	11
 <b>Chapter 2. Literature Review .....</b>	 <b>13</b>
2.1. Membrane Separation Techniques for Wastewater Treatment.....	14
2.2. Micellar-Enhanced Ultrafiltration (MEUF).....	18
2.2.1. Mechanism and advantages of MEUF.....	18
2.2.2. Major components and parameters of MEUF .....	19

2.2.3.	Existing MEUF studies for dissolved ion removal.....	28
2.3.	Polymer-Enhanced Ultrafiltration (PEUF) .....	32
2.3.1.	Background and mechanisms of PEUF .....	32
2.3.2.	Existing PEUF studies for dissolved ion removal .....	33
2.4.	Ion Adsorption onto Surfactant Micelles/Polymers in MEUF/PEUF .....	34
2.4.1.	Adsorption isotherm models.....	41
2.4.2.	Adsorption kinetic models.....	42
2.4.3.	Adsorption in MEUF and PEUF systems .....	42
2.5.	System Optimization and Modeling .....	44
2.6.	Summary .....	49

<b>Chapter 3.</b>	<b>Removal of Heavy Metals from Mining Wastewater by Micellar-</b>	
	<b>enhanced Ultrafiltration (MEUF): Experimental Investigation and Artificial Neural</b>	
	<b>Network Modeling .....</b>	<b>50</b>
3.1.	Introduction.....	51
3.2.	Material and Methods .....	54
3.2.1.	Materials .....	54
3.2.2.	Experimental set-up .....	54
3.2.3.	MEUF procedure .....	55
3.2.4.	Sample analysis .....	58
3.2.5.	Artificial neural networks (ANN) modeling.....	59
3.2.6.	Resampling-based ANN modeling.....	60
3.2.7.	Statistical analysis.....	60



3.3.	Results and Discussion .....	61
3.3.1.	MEUF performance in different conditions .....	61
3.3.2.	Monitoring of parameter changes over time in MEUF runs.....	66
3.3.3.	ANN modeling and parameter importance.....	68
3.3.4.	Statistical analysis.....	71
3.3.5.	Discussion.....	74
3.4.	Summary .....	78
3.5.	Supplemental Materials .....	80

#### **Chapter 4. Micellar-Enhanced Ultrafiltration to Remove Nickel: A Response**

<b>Surface Method and Artificial Neural Network Optimization.....</b>	<b>90</b>
4.1. Introduction.....	91
4.2. Material and Methods .....	95
4.2.1. Materials .....	95
4.2.2. Dead-end ultrafiltration experiments .....	95
4.2.3. Sample and data analysis .....	97
4.2.4. Response surface modeling .....	98
4.2.5. Artificial neural network (ANN) modeling .....	101
4.3. Results and Discussion .....	102
4.3.1. Ultrafiltration experimental results.....	102
4.3.2. RSM models .....	105
4.3.3. Effect of factors on rejection rate and permeate flux .....	109
4.3.4. RSM optimization.....	115

4.3.5.	ANN modeling.....	116
4.4.	Summary .....	119
 <b>Chapter 5. Sulfate Removal Using Colloid-Enhanced Ultrafiltration: Performance Evaluation and Adsorption Studies.....120</b>		
5.1.	Introduction.....	121
5.2.	Material and Methods .....	123
5.2.1.	Chemicals .....	123
5.2.2.	Ultrafiltration membranes.....	123
5.2.3.	Experimental set-up .....	124
5.2.4.	Examination of ultrafiltration performance .....	128
5.2.5.	Adsorption studies .....	132
5.2.6.	Quality Assurance/quality control (QA/QC) .....	136
5.3.	Results and Discussion .....	137
5.3.1.	Performance of ultrafiltration .....	137
5.3.2.	Adsorption studies .....	148
5.3.3.	Ultrafiltration performance during experimental runs.....	152
5.3.4.	Membrane characteristics .....	153
5.3.5.	MEUF and PEUF comparison .....	158
5.4.	Summary .....	162
 <b>Chapter 6. Conclusions, Research Contributions, and Future work .....165</b>		
6.1.	Conclusions.....	166
6.2.	Contribution to Knowledge .....	168

6.3. Recommendations and Future Work .....	168
<b>Appendix A .....</b>	<b>170</b>
<b>Appendix B .....</b>	<b>177</b>
<b>References .....</b>	<b>179</b>

## List of Tables

Table 1-1 Toxic effect of heavy metals on humans .....	5
Table 1-2 Authorized limits of deleterious substances in metal mining effluent .....	6
Table 1-3 Comparisons of sulfate removing techniques.....	10
Table 2-1 Comparison of membrane separation technologies.....	16
Table 2-2 Specifications of commonly used ionic surfactants .....	26
Table 2-3 Summary of MEUF removal of dissolved ions from aqueous streams (selected examples) .....	30
Table 2-4 Summary of commonly used water-soluble polymers in PEUF studies .....	35
Table 2-5 Summary of PEUF removal of dissolved ions from aqueous streams .....	37
Table 2-6 Summary of RSM studies in MEUF and PEUF .....	46
Table 2-7 Summary of studies using RSM combined with other mathematical models...	48
Table 3-1 Experimental runs of ultrafiltration tests .....	57
Table 3-2 Summary of statistical results.....	72
Table 3-3 Results of analysis of variance (rank-approximation method).....	73
Table 4-1 Summary of MEUF studies integrating RSM and other optimization models .	94
Table 4-2 Properties of the surfactant used in this study .....	96
Table 4-3 Factors and levels set by Box-Behnken design (BBD) .....	100
Table 4-4 Design layout and experimental results of the BBD design.....	103
Table 4-5 ANOVA for reduced quadratic model (response: rejection).....	106
Table 4-6 ANOVA for reduced quadratic model (response: flux) .....	107
Table 5-1 Specifications of the surfactant and polymer used in this study .....	125

Table 5-2 Specifications of the membrane used in this study .....	126
Table 5-3 Experimental runs: effect of feed concentrations on ultrafiltration performance .....	129
Table 5-4 Summary of results for regression analysis .....	147
Table 5-5 Pseudo-second-order kinetic constants for adsorption of sulfate ion in MEUF and PEUF systems .....	154
Table 5-6 Summary of MEUF vs PEUF performance in this study .....	164
Table A-0-1 Input and output data for ANN models (Chapter 3).....	170
Table B-0-1 Relationship between variables (sulfate concentration, surfactant concentration) and responses (rejection, flux, sulfate concentration in permeate) .....	177
Table B-0-2 Relationship between variables (sulfate concentration, polymer concentration) and responses (rejection, flux, sulfate concentration in permeate) .....	178

## List of Figures

Figure 2-1 Ultrafiltration mode: (a) unstirred batch system, (b) stirred batch system, (c) stirred batch system with feed reservoir, (d) cross-flow system, and (e) cross-flow system with retentate recycling .....	21
Figure 2-2 A typical flux vs. pressure plot for distilled water as feed. Membrane permeability ( $L_p = Jw/\Delta P$ ) indicates how porous a membrane is. Higher $L_p$ values indicate more porous membranes. ....	22
Figure 3-1 A Schematic diagram of (a) SDS monomer, (b) SDS micelle (when SDS concentration > CMC) (c) micellar-enhance ultrafiltration (MEUF) setup, and (d) mechanism of MEUF removal of metal ions .....	56
Figure 3-2 Flow chart of the statistical analysis method .....	63
Figure 3-3 Effect of (a) S/M ratio (pH not adjusted) and (b) pH (S/M = 8.5) on metal rejection rate and effect of (c) S/M ratio (pH not adjusted) and (d) pH (S/M = 8.5) on permeate flux. $[Cu^{2+}/Ni^{2+}/Co^{2+}]_f = 1 \text{ mM}$ , $\Delta P = 40 \text{ psi}$ , and $T = \text{room temperature}$ .....	64
Figure 3-4 Metal concentrations in the permeate at the end of UF tests with the effect of (a) S/M ratio and (b) pH. $[Cu^{2+}/Ni^{2+}/Co^{2+}]_f = 1 \text{ mM}$ , $\Delta P = 40 \text{ psi}$ , and $T = \text{room temperature}$ .....	65
Figure 3-5 Change of (a) rejection rate and permeate concentrations of metal in single system and change of (b) sampling time and permeate flux during a UF run.	

[Cu <sup>2+</sup> /Ni <sup>2+</sup> /Co <sup>2+</sup> ] <sub>f</sub> = 1 mM, [SDS] <sub>f</sub> = 8.5 mM, pH = 10, ΔP = 40 psi, and T = room temperature .....	67
Figure 3-6 Comparison between ANN modeled (Output) and experimental (Target) results on the rejection rate and permeate flux for Cu system using (a) training, (b) validation, (c) testing, and (d) overall datasets .....	69
Figure 3-7 The relative contributions of sampling volume, S/M ratio, and pH to (a) rejection rate and (b) permeate flux for Cu system.....	70
Figure 3-8 Change of rejection rate during UF runs (Cu system) examining the effect of S/M ratio (pH not adjusted) and pH value (S/M = 8.5). [Cu <sup>2+</sup> ] <sub>f</sub> = 1 mM, ΔP = 40 psi, T = room temperature .....	80
Figure 3-9 Change of permeate flux during UF runs (Cu system) examining the effect of S/M ratio (pH not adjusted) and pH value (S/M = 8.5). [Cu <sup>2+</sup> ] <sub>f</sub> = 1 mM, ΔP = 40 psi, T = room temperature .....	81
Figure 3-10 Change of rejection rate during UF runs (Ni system) examining the effect of S/M ratio (pH not adjusted) and pH value (S/M = 8.5). [Ni <sup>2+</sup> ] <sub>f</sub> = 1 mM, ΔP = 40 psi, T = room temperature .....	82
Figure 3-11 Change of permeate flux during UF runs (Ni system) examining the effect of S/M ratio (pH not adjusted) and pH value (S/M = 8.5). [Ni <sup>2+</sup> ] <sub>f</sub> = 1 mM, ΔP = 40 psi, T = room temperature .....	83

Figure 3-12 Change of rejection rate during UF runs (Co system) examining the effect of S/M ratio (pH not adjusted) and pH value (S/M = 8.5). $[\text{Co}^{2+}]_f = 1 \text{ mM}$ , $\Delta P = 40 \text{ psi}$ , T = room temperature .....	84
Figure 3-13 Change of permeate flux during UF runs (Co system) examining the effect of S/M ratio (pH not adjusted) and pH value (S/M = 8.5). $[\text{Co}^{2+}]_f = 1 \text{ mM}$ , $\Delta P = 40 \text{ psi}$ , T = room temperature .....	85
Figure 3-14 Comparison between ANN modeled (Output) and experimental (Target) results on the rejection rate and permeate flux for Ni system using (a) training, (b) validation, (c) testing, and (d) overall datasets .....	86
Figure 3-15 Comparison between ANN modeled (Output) and experimental (Target) results on the rejection rate and permeate flux for Co system using (a) training, (b) validation, (c) testing, and (d) overall datasets .....	87
Figure 3-16 The relative contributions of sampling volume, S/M ratio, and pH to (a) rejection rate and (b) permeate flux for Ni system .....	88
Figure 3-17 The relative contributions of sampling volume, S/M ratio, and pH to (a) rejection rate and (b) permeate flux for Co system.....	89
Figure 4-1 Response surface (a) and contour (b) showing the effect of pressure and MWCO on rejection rate. $C_{\text{Ni}} = 1.25 \text{ mM}$ , $C_{\text{SDS}} = 16.6 \text{ mM}$ .....	112



Figure 4-2 Response surface (a) and contour (b) showing the effect of nickel and SDS concentrations on rejection rate. Pressure = 40 psi, MWCO = 5 kDa. ....	113
Figure 4-3 Response surface (a) and contour (b) showing the effect of SDS concentration and MWCO on rejection rate. Pressure = 40 psi, $C_{Ni} = 1.25$ mM.....	114
Figure 4-4 The scatter plots of ANN model predicted values (rejection rate of nickel ions) versus experimental values for (a) training, (b) validation, (c) testing, and (d) all data sets .....	117
Figure 4-5 The scatter plots of ANN model predicted values (permeate flux) versus experimental values for (a) training, (b) validation, (c) testing, and (d) all data sets .....	118
Figure 5-1 Schematic of micellar-enhanced ultrafiltration (MEUF) and polymer-enhanced ultrafiltration (PEUF) setups. 1, nitrogen gas; 2, regulator; 3, pressure control valve; 4, UF cell; 5, magnetic stirrer; 6, feed solution; 7, UF membrane; 8, permeate; 9, volumetric cylinder; 10, sulfate ions; 11, surfactant monomer; 12, surfactant micelle binding sulfate ions; 13, polymer binding sulfate ions. ....	127
Figure 5-2 Sulfate rejection and permeate flux at different (a) initial CTAB/PDADMAC concentration ( $[SO_4^{2-}]_f = 10$ mM, and (b) initial sulfate concentration ( $[CTAB/PDADMAC]_f = 15$ mM). $\Delta P = 40$ psi. ....	140
Figure 5-3 Effect of initial CTAB/PDADMAC concentration on the quantity of surfactant micelles/polymer ligands formed. $[SO_4^{2-}]_f = 10$ mM. $\Delta P = 40$ psi .....	141

Figure 5-4 Effect of (a) initial CTAB/PDADMAC concentration ( $[\text{SO}_4^{2-}]_f = 10 \text{ mM}$ ) and (b) initial sulfate concentration ( $[\text{CTAB/PDADMAC}]_f = 15 \text{ mM}$ ) on permeate quality	145
Figure 5-5 (a) Effect of CTAB/PDADMAC concentration on micelle loading ( $L_c$ ) and adsorption amount ( $\Gamma_e$ ), $[\text{SO}_4^{2-}]_f = 10 \text{ mM}$ , (b) Effect of sulfate concentration on micelle loading and adsorption capacity $[\text{CTAB/PDADMAC}]_f = 15 \text{ mM}$	146
Figure 5-6 Regression analysis fitting experimental data to linearized (a) Langmuir and (b) Freundlich equilibrium isotherms in MEUF and PEUF systems. $[\text{SO}_4^{2-}]_f = 1\text{-}20 \text{ mM}$ , $[\text{CTAB/PDADMAC}]_f = 15 \text{ mM}$	149
Figure 5-7 Comparison of experimental and calculated Freundlich isotherms of sulfate ions onto colloid. $[\text{SO}_4^{2-}]_f = 1\text{-}20 \text{ mM}$ , $[\text{CTAB/PDADMAC}]_f = 15 \text{ mM}$	150
Figure 5-8 Sulfate rejection as a function of the accumulative amount of filtrate at different initial sulfate and colloid concentrations. (a) $[\text{SO}_4^{2-}]_f = 10 \text{ mM}$ , $[\text{CTAB}]_f = 10\text{-}100 \text{ mM}$ ; (b) $[\text{SO}_4^{2-}]_f = 10 \text{ mM}$ , $[\text{PDADMAC}]_f = 10\text{-}100 \text{ mM}$ ; (c) $[\text{SO}_4^{2-}]_f = 0\text{-}20 \text{ mM}$ , $[\text{CTAB}]_f = 15 \text{ mM}$ ; (d) $[\text{SO}_4^{2-}]_f = 0\text{-}20 \text{ mM}$ , $[\text{PDADMAC}]_f = 15 \text{ mM}$ . $\Delta P = 40 \text{ psi}$	155
Figure 5-9 Permeate fluxes as a function of the accumulative amount of filtrate at different initial sulfate and colloid concentration. a) $[\text{SO}_4^{2-}]_f = 10 \text{ mM}$ , $[\text{CTAB}]_f = 10\text{-}100 \text{ mM}$ ; (b) $[\text{SO}_4^{2-}]_f = 10 \text{ mM}$ , $[\text{PDADMAC}]_f = 10\text{-}100 \text{ mM}$ ; (c) $[\text{SO}_4^{2-}]_f = 0\text{-}20 \text{ mM}$ , $[\text{CTAB}]_f = 15 \text{ mM}$ ; (d) $[\text{SO}_4^{2-}]_f = 0\text{-}20 \text{ mM}$ , $[\text{PDADMAC}]_f = 15 \text{ mM}$ . $\Delta P = 40 \text{ psi}$	156
Figure 5-10 Logarithm plot of permeate flux over (a) CTAB and (b) PDADMAC concentrations in retentate	157

Figure 5-11 Summary of membrane permeability test (a) water flux on new membranes (b) feed solution containing 5 mM $\text{SO}_4^{2-}$ and 15 mM CTAB. All values are the average of triplicate measurements.....	159
Figure 5-12 Change of water flux: membrane for (a) MEUF use and (b) PEUF use. Values are the mean and standard deviations of triplicate tests. Retaining 90% of $J_{w\text{-new}}$ deems membrane reusable. ....	160
Figure 5-13 Scanning electron micrographs (SEM) of (a) back and (b) cross-section views of a new regenerated cellulose membrane; (c) back and (d) cross-section view of a membrane after 9 MEUF runs; (e) back and (f) cross-section view of membrane after 14 PEUF runs. (▲) trapped micelle-sulfate complex.....	161

## List of Symbols

$A_m$	Effective membrane area ( $m^2$ )
$C/S$	Initial molar ratio of colloid (surfactant or polymer) to sulfate in feed solutions
$C_e$	Equilibrium sulfate concentration (mg/L)
$h_0$	The initial sorption rate (mg/g·min)
$J$	Flux of the ultrafiltration permeate ( $L/m^2 \cdot h$ )
$J_w$	Flux of deionized water ( $L/m^2 \cdot h$ )
$K_1$	Pseudo-first-order rate constant ( $min^{-1}$ )
$K_2$	Pseudo-second-order rate constant (g/mg·min)
$K_F$	Freundlich constant ( $mg^{1-1/n} L^{1/n}/g$ )
$K_L$	Langmuir equilibrium constant (L/mg)
$L_c$	Colloid loading (mM/mM)
$n_F$	Freundlich exponent
$R$	Rejection rate (%)
$R^2$	Coefficient of determination
$R^2\text{-adj}$	Adjusted R squared
$R^2\text{-pre}$	Predicted R squared
$R_m$	Resistance of membrane ( $m^{-1}$ )
$S/M$	Initial molar ratio of surfactant to metal ions in feed solutions
$S'$	Amount of surfactant micelle or polymer ligands formed per unit time (g/h)
$\Gamma_e$	Adsorption amount of sulfate ions per unit mass of colloid at equilibrium (mg/g)
$\Gamma_t$	Adsorption amount of sulfate ions per unit mass of colloid at time t (mg/g)

$\Gamma_{max}$     The maximum amount of sulfate adsorbed per unit mass of colloid at equilibrium  
(mg/g)

*Subscript*

f        Feed

p        Permeate

r        Retentate

*Greek letters*

$\eta$         viscosity of the solvent

## List of Abbreviations

### *Membrane technology*

CEUF	Colloid-enhanced ultrafiltration
Da	Dalton
MEUF	Micellar-enhanced ultrafiltration
MF	Microfiltration
MWCO	Molecular weight cut-off
NF	Nanofiltration
PEUF	Polymer-enhanced ultrafiltration
RO	Reverse osmosis
TMP	Transmembrane pressure
UF	Ultrafiltration

### *Surfactant, polymers, and membrane materials*

CA	Cellulose acetate
CMC	Critical micellar concentration
CPC	Cetylpyridinium chloride
CTAB	Cetyltrimethylammonium
PA	Polyamide
PAA	Polyacrylic acid
PAN	Polyacrylonitrile
PDADMAC	Poly(diallyldimethyl ammonium chloride)

PEI	Polyethylenimine
PES	Polyethersulfone
PONPEs	Polyoxyethylene nonyl phenyl ethers
PS	Polysulfone
PSS	Sodium poly(styrene sulfonate)
PVAm	Polyvinylamine
PVDF	Polyvinylidene fluoride
RC	Regenerated cellulose
SDS	Sodium dodecyl sulfate

*Statistics and modeling*

ANFIS	Adaptive neuro-fuzzy inference system
ANN	Artificial neural network
ANOVA	Analysis of variance
APE	Average percentage errors
BBD	Box–Behnken designs
CCD	Central composite design
DF	Degree of freedom
FFD	Full factorial design
MLR	Multiple linear regression
MS	Mean of squares
MSE	Mean squared error
RSM	Response surface methodology

SS	Sum of squares
----	----------------

*Characterizations*

BOD	Biological oxygen demand
-----	--------------------------

COD	Chemical oxygen demand
-----	------------------------

FAA	Flame Atomic Absorption
-----	-------------------------

SEM	Scanning electron microscopy
-----	------------------------------

TOC	Total organic carbon
-----	----------------------



## **Chapter 1.**

### **Introduction**

## **1.1. Background**

### **1.1.1. Heavy metal pollution, impact, and treatment**

Heavy metals commonly refer to a group of metals and metalloids having specific densities over  $5 \text{ g/cm}^3$ , such as copper (Cu), nickel (Ni), cobalt (Co), lead (Pb), cadmium (Cd), arsenic (As), chromium (Cr), and mercury (Hg) (Gadd and Griffiths, 1977; Järup, 2003; Li et al., 2014). They have been widely used in industrial, agricultural, domestic, and technological applications. Major environmental pollution of heavy metals comes from mining, foundries and smelters, and other metal-based industrial sources (Tchounwou et al., 2012). Mining is a major economic activity in Newfoundland and Labrador (NL). In 2015, the Voisey's Bay mine produced 53,000 tonnes of nickel, 32,000 tonnes of copper, and 849 tonnes of cobalt (Government of NL, 2016). Among them, copper and nickel are priority pollutants listed in the Clean Water Act (USEPA, 1972), where their environmental impact and pollution control are of top concern.

Heavy metals are nondegradable and highly soluble in the aquatic environment. They exist in surface water in forms of ions or chemical complexes and eventually reach the groundwater. Dissolved heavy metals can affect microbial activities and disturb aquatic lives (Jaishankar et al., 2014). They can also be ingested by living organisms, accumulate in the food chain, and cause serious health problems (Pezhhan and Pezhhan, 2015). Excessive exposure to heavy metals can reduce growth and development, damage organ and nervous systems, or even cause death (Pezhhan and Pezhhan, 2015). Typically, arsenic, cadmium, chromium, and nickel are carcinogenic and associated with mutation, deletion, or oxygen radical attack on DNA (Tchounwou et al., 2012).

Table 1-1 summarizes the toxic effect of heavy metals that raise health concerns. Heavy metals are toxic to humans and the aquatic environment even at low concentrations. Therefore, stringent water and wastewater regulations have been established to minimize human exposure and restrict the discharge of metal-containing effluents to the environment. For example, the Canadian Metal Mining Effluent Regulations (MMER) restricts most metal concentrations in the effluent to <1 mg/L (MMER, 2012), as listed in Table 1-2. More stringent regulations are set for portable water. For example, the European Community set the maximum concentration of nickel in portable water as 50 µg/L (Danis and Aydiner, 2009).

Heavy metals can be removed from wastewater streams using conventional techniques (e.g., chemical precipitation, ion exchange, sorption) and more advanced techniques such as membrane separation. Precipitation is a separation operation that generates a solid from a supersaturated solution, commonly using hydroxide or sulfide. It serves as an economical method for the treatment of industrial wastewater containing high concentrations of heavy metals (Fu and Wang, 2011). Ion exchange can effectively treat high concentrations of heavy metals, though the generation of resins may cause serious secondary pollution (Fu and Wang, 2011). Adsorption (most effectively activated carbon sorption) is a recognized method to remove low-concentration heavy metals from water but the high capital and regeneration cost of activated carbon limit its wide application (Bhatnagar et al., 2010). Membrane filtration is more advanced and has been widely used in recent decades, showing advantages of high treatment efficiency, easy operation, and taking less space (Purkayastha et al., 2014). Commonly used membranes

technologies include microfiltration (MF), ultrafiltration (UF), nanofiltration (NF), and reverse osmosis (RO). RO and NF are capable of removing dissolved metals in water but require high operational costs. Though UF has advantages of lower pressure requirement, it cannot retain heavy metal ions. When treating large volumes of wastewater containing heavy metals with relatively low concentrations, the above treatment methods have disadvantages such as large volumes of sludge generation, high energy or chemical cost, incomplete removal, or lack of selectivity.

To tackle the above disadvantages of treatment technologies to remove relatively low concentrations of heavy metal from the aqueous effluent, a more effective treatment method has received attention in recent years, namely the colloid-enhanced ultrafiltration (CEUF). The CEUF is a novel membrane-based separation process to remove dissolved ions (such as metal ions) from aqueous streams (Fu and Wang, 2011; Schwarze, 2017). A CEUF technique makes use of charged macromolecules to bind the oppositely charged pollutant ions by electrostatic interaction. This technique includes the use of surfactant micelles (a spherical form when surfactant monomers aggregate) in the process of micellar-enhanced ultrafiltration (MEUF) or the use of a polymer in the polymer-enhanced ultrafiltration (PEUF). The pollutant-colloid complex is then concentrated and retained by a UF membrane while generating relative clean effluents (Roach and Zapien, 2009). The main advantage of CEUF over the conventional UF separation is the ability to retain the low-molecular-weight pollutants that are too small for regular UF membranes. Besides, the CEUF separation can provide higher permeate flux and consumes less energy than those associated with NF and RO.

Table 1-1 Toxic effect of heavy metals on humans

Heavy metal	Toxic effects on humans
Arsenic	Skin irritation, vascular disease, carcinogenic
Cadmium	Kidney disorder and damage, carcinogenic
Chromium	Headache, nausea, diarrhea, carcinogenic, corrosive to tissue, skin sensitization, kidney damage
Cobalt	Asthma-like allergy, heart failure, damage to the thyroid and liver, carcinogenic
Copper	Insomnia, liver damage, Wilson disease
Lead	Kidney diseases, damage to the fetal brain, damages to the circulatory and nervous system
Mercury	Rheumatoid arthritis, kidney diseases, damages to the circulatory and nervous system
Nickel	Skin irritation, coughing, nausea, chronic asthma, carcinogenic
Zinc	Increased thirst, lethargy, depression, neurological problems

Sources: (Rengaraj and Moon, 2002; Kamble and Marathe, 2005; Pezhhan and Pezhhan, 2015)

Table 1-2 Authorized limits of deleterious substances in metal mining effluent

<b>Deleterious substance</b>	<b>Maximum authorized concentration in a grab sample</b>
Arsenic	1.00 mg/L
Copper	0.60 mg/L
Lead	0.40 mg/L
Nickel	1.00 mg/L
Zinc	1.00 mg/L

Source: (MMER, 2012)

### **1.1.2. Sulfate pollution, impact, and treatment**

Sulfates are common components in industrial wastewater, and naturally present in mining and metal-refining effluents when processing sulfur-containing minerals such as barite ( $\text{BaSO}_4$ ), epsomite ( $\text{MgSO}_4 \cdot 7\text{H}_2\text{O}$ ), gypsum ( $\text{CaSO}_4 \cdot 2\text{H}_2\text{O}$ ), and metal sulfides (mainly Fe, Cu, and Mo) (Silva et al., 2010). Sulfate-containing wastewater can also be generated during productions of fertilizers, paper, glass, dyes, textiles, and other industrial products (Greenwood and Earnshaw, 2012). In natural environments, sulfates can exist in groundwater at 10 mg/L (Pookrod et al., 2005) and in common seawater at 2700 mg/L (Canfield and Farquhar, 2009). The sulfate concentrations from industrial effluents could vary from hundreds to thousands of ppm (Maree et al., 2004; Bader, 2007; Agboola et al., 2017).

Sulfates can cause various problems depending on the concentration, often associated with altered taste of water, digestion problems in animals and humans, scaling, oil and water acidification, and corrosion problems (Silva et al., 2010). Excessive consumption of sulfates in drinking water can cause acute diarrhea and dehydration on human and livestock (Sadeghalvad et al., 2016). In industrial activities, sulfates are one of the major contributors to water mineralization. They raise the conductivity of water and the scaling potential of pipes, fouling and deposition in boilers, blockage of soil pores, and retarding irrigation or water drainage (Silva et al., 2010). Anaerobic treatment of sulfate-containing wastewater or injection of sulfate-containing seawater in enhanced oil recovery can promote sulfide generation by the activities of sulfate-reducing bacteria. The gaseous hydrogen sulfide ( $\text{H}_2\text{S}$ ) is poisonous and poses health and safety hazards. Sulfide

in wastewater increases the biological oxygen demand (BOD) and chemical oxygen demand (COD). It is also corrosive to equipment and infrastructures, and further acidify the receiving soil and water (Tait et al., 2009).

Conventionally, the treatment of dissolved sulfates receives less attention due to its lower toxicity and therefore looser regulatory standards than that of other compounds such as heavy metals. However, sulfate contamination has been increasingly considered as a long term environmental problem, especially for mining-dependent countries with limited freshwater supply, such as South Africa (Bowell, 2004). Environmental agencies have been increasingly concerned with elevated sulfate concentrations in water. The World Health Organization (WHO) and Health Canada recommend a maximum of 500 mg/L sulfate in water. Regulatory agencies in some mining countries set sulfate restrictions between 250 and 500 mg/L in mining effluents (INAP, 2003). Although the USPEA does not single out sulfate under the *National Recommended Water Quality Criteria*, it recommends a 250 mg/L of Total Dissolved Solids (TDS) (i.e., the maximum sulfate concentration should be less than this value) (USEPA, 2002).

The removal of sulfates from aqueous streams remains challenging for the mining, metallurgical, oil and gas, and chemical industries. Commonly used techniques include the following (INAP, 2003; Silva et al., 2010): (1) *Chemical treatment*: precipitation (such as by dosing lime) is a simple way to treat wastewater with high sulfate concentration (1500-2000 mg/L and above); (2) *Biological treatment*: sulfate-reducing bacteria produces metal sulfide precipitation if metal exist; and (3) *Physical treatment*: membrane filtration such as NF and RO, and ion exchange that can be a polishing step after lime precipitation. Table 1-3 compares the above technologies. Among them, RO



and NF are used to remove sulfates from seawater for oil reservoir seawater injection, for reservoir souring control and scale prevention. However, the practice can involve enormous operational and maintenance costs.

## **1.2. Statement of Problems**

Although a number of studies report the MEUF and PEUF removal of dissolved ions from aqueous streams, this separation technique remains inadequately understood and has not been employed in most industrial applications. Continued efforts are needed to:

- (1) Expand the knowledge of MEUF removal for different species of dissolved metal under different operational parameters. A modeling method has to be incorporated to interpret and predict the MEUF system performance as well as to understand the relative importance of operating parameters.
- (2) Better understand the MEUF systems, especially when multiple variable and responses are involved. Studies of MEUF system optimization are rare. To overcome the drawbacks of the traditional one-factor-at-a-time method, statistical models are desired to optimize the system. Interactions between process variables and performance prediction are crucial information to be obtained.
- (3) Explore the technical efficacy of MEUF and PEUF to remove sulfate ions. A study on sulfate (an anion of increasing concern) removal has not been conducted. The underlying mechanism of sulfate-colloid interaction needs to be explored. Although adsorption between solute and surfactant/polymer are the key factors behind a successful MEUF/PEUF, very few works have been carried out focusing on the adsorption behavior and mechanism.

Table 1-3 Comparisons of sulfate removing techniques

<b>Treatment methods</b>	<b>Advantages</b>	<b>Disadvantages</b>
Chemical precipitation (e.g., barium sulfate precipitation, ettringite precipitation)	- High efficiency	- High chemical costs - Large-volume of sludge generation - Residual barium
Biological reduction	- Low costs - Easy operation	- Long residence time - Organic material residuals - Large space
Adsorption and/or ion exchange	- High efficiency - Low concentrations of sulfate treatment - Relatively low costs (lower than RO)	- Requires bed generation - Tailing generation during resin regeneration
Membrane filtration (e.g., NF, RO)	- High removal and time efficiency - Save space	- High operational and maintenance costs - Membrane fouling problem

Source: (Silva et al., 2010)

### **1.3. Research Objective**

This thesis has three main objectives (1) the MEUF removal of heavy metals (copper, nickel, and cobalt ions, main components generated by the local mining industry) from aqueous streams, including examining the effect of crucial process parameters (i.e., surfactant to metal ratio and feed pH) on the MEUF performance, and modeling the performance and the relative importance of process parameters; (2) the MEUF removal of nickel ion using statistical models, including a response surface methodology and artificial neural network for system optimization; and (3) technical viability of MEUF and PEUF removal of sulfate from water, as well as the associated equilibrium and kinetic studies. This thesis adds and enhances knowledge in the field of MEUF/PEUF and provide a treatment alternative in industries such as oil and gas (to prevent sulfate-induced scales and reservoir souring) and mining (to treat metal- and sulfate-containing wastewater).

### **1.4. Thesis Structure**

This thesis focuses on MEUF and PEUF removal of cationic and anionic pollutants from aqueous solutions. It has 6 chapters. Chapter 2 reviews the research status of MEUF and PEUF technologies in removing ionic pollutants. Chapter 3 investigates the MEUF removal of copper, nickel, and cobalt under different operational conditions. To further understand the optimal condition, Chapter 4 applies a design-of-experiment method and computer modeling to determine the optimal condition for MEUF removal of nickel ions from water. To investigate the anionic pollutant removal, Chapter 5 explores the technical viability of a MEUF and a PEUF process for sulfate removal. Adsorption isotherm and

kinetics studies are conducted to understand the underlying mechanism. Finally, Chapter 6 summarizes and concludes these studies and recommends future work.

## **Chapter 2.**

### **Literature Review**

## **2.1. Membrane Separation Techniques for Wastewater Treatment**

Membrane separation techniques are processes where a membrane (driven by pressure, concentration, electrical potential, or temperature gradients) selectively restricts the passage of pollutants (such as organics, nutrients, turbidity, microorganisms, and inorganic ions) and allows the relatively clean water to pass through (Mulder, 1996).

They are widely used in water and wastewater treatment, having advantages such as easy operation and control, and with few chemical additives requirements (Rivas et al., 2011).

A membrane process separates a feed stream into permeate (or filtrate, i.e., the stream relatively clean) and retentate (or concentrate, i.e., the stream containing concentrated target pollutants) by a semipermeable membrane. Depending on the direction of flow, the filtration system of dead-end or cross-flow mode (where the feed stream flows perpendicular or parallel to the membrane surface, respectively) are most commonly used (Rivas et al., 2011). In the laboratory scale, the conventional dead-end filtration has been widely used (Akita et al., 1997; Pookrod et al., 2005; Chhatre and Marathe, 2006; Xiarchos et al., 2008; Cojocarui et al., 2009a; Landaburu-Aguirre et al., 2010; Almutairi et al., 2011; Huang et al., 2015; Bahmani et al., 2019). Membrane systems can be operated with either a constant permeate flux or a constant feed pressure. The constant-flux operation filters the feed stream (assuming constant composition) in a fixed time, where the amount of permeate, retentate, and the fouling load are constant. The concentrated solute in the retentate increases the membrane resistance during the filtration process; therefore the feed pressure shall be increased accordingly to maintain a constant flux. Industrial applications generally employ this constant flux mode. In the laboratory scale,

however, the constant-pressure filtration is more commonly used to track the system mechanism, since the feed pressure is constant and the flux decreases with the filtration time (Van de Ven et al., 2008).

Industrial membrane processes include MF, UF, NF, and RO, classified by the size of solute that can be rejected by a membrane. Table 2-1 compares the specifications of these membranes, showing that UF is an intermediate technique in terms of separation effectiveness, efficiency, and cost. The UF technique was developed in the late 1960s and typically retain substances with molecular weights of 1000 Daltons (Da) and more (Cheryan, 1986; Sriratana et al., 1996). Ultrafiltration serves as a cost-effective technology that generates high flux with relatively low pressures (and therefore lower energy costs), but it cannot retain a solute with a low molecular weight (Sriratana et al., 1996). That is, heavy metal or sulfate ions cannot be retained by ordinary UF membranes, and their removal requires the more costly NF or RO. As such, the more advanced MEUF and PEUF were proposed as techniques to remove dissolved metal ions using the regular UF membranes under moderate operating conditions. Though their efficacy of removing some metal ions have been reported, many aspects (such as performance-governing factors, system optimization tools, the potential for sulfate removal, and the underlying mechanism) remain unknown.

Table 2-1 Comparison of membrane separation technologies

	<b>Microfiltration (MF)</b>	<b>Ultrafiltration (UF)</b>	<b>Nanofiltration (NF)</b>	<b>Reverse Osmosis (RO)</b>
Pore size	0.1-10 $\mu\text{m}$	0.01-0.1 $\mu\text{m}$	0.001-0.01 $\mu\text{m}$ (most typical 1 nm of pore size)	0.0001-0.001 $\mu\text{m}$
Particle MW	>1000 kDa	1000-100,000 Da	200-1000 Da	<200 Da
Pressure range	0.5-5 bar	1-10 bar	7-30 bar	20-100 bar
Typical solution for treatment	Substances contribute to turbidity (e.g., particles, sediments, algae, large bacteria)	Colloids, macromolecules, microorganisms	Most multivalent ions (e.g., hardness)	Practically all substances, including monovalent ions (e.g., $\text{Na}^+$ , $\text{Cl}^-$ )
Cannot remove	Dissolved organic matter, colloids, viruses, etc.	Solvents, ionized contaminants	Monovalent ions	-
Advantage	Lowest pressure; highest flux	Low pressure; High flux; More efficient than MF;	Can remove some dissolved ions	Most efficient in removing aqueous pollutants



	<b>Microfiltration (MF)</b>	<b>Ultrafiltration (UF)</b>	<b>Nanofiltration (NF)</b>	<b>Reverse Osmosis (RO)</b>
		More economical than NF and RO		
Disadvantage	Cannot disinfect the feed stream	Cannot remove dissolved ions	High pressure; High cost	Highest pressure; Highest cost
Applications	Less used because it cannot effectively treat wastewater or drinking water; Pre-treatment before RO	Clean and disinfect river water; Pre-treatment before NF and RO	Used when UF is not effective enough and RO is too costly; When high rejection rate is needed	Stringent effluent quality required; When freshwater supply is limited

Sources: (Mulder, 1996; Shon et al., 2013; Nagy, 2019)

Note: data for pore size, particle MW, and pressure range slightly vary in literature

## **2.2. Micellar-Enhanced Ultrafiltration (MEUF)**

### **2.2.1. Mechanism and advantages of MEUF**

Since the pioneering work of Leung (1980) that removed trace metal ion using MEUF, the technology has received attention in the field. In principle, MEUF is a pressure-driven membrane separation process that uses a surfactant to enable retention of multivalent ions such as heavy metal ions from the aqueous stream (Kamble and Marathe, 2005). At surfactant concentration above its critical micellar concentration (CMC), surfactant monomers can aggregate and form micelles. In these spherical micelles, the polar hydrophilic heads of the surfactant face the solvent and form the surface of micelles, and the hydrophobic tails form the core. These ionic surfactant micelles can bind the metal counterions by electrostatic attraction, forming a metal-surfactant complex that is large enough to be retained by UF membranes (Tung et al., 2002; Baek and Yang, 2004a).

Different water and wastewater treatment processes (e.g., chemical precipitation, coagulation-flocculation, electrochemical processes, ion exchange, and sorption) have been employed to remove heavy metals from aqueous streams (Landaburu-Aguirre et al., 2010). Chemical precipitation, coagulation-flocculation, and electrochemical treatment could generate a large quantity of sludge for further treatment when treating high concentrations of metals in wastewater, and these techniques become less effective when treating low concentrations (e.g., 1–100 mg/L). Effective ion exchange and sorption could be costly to treat large-volume wastewater containing low concentrations of heavy metals (Cojocaru et al., 2009a). As such, MEUF shows attractive advantages especially when

handling large volumes of low concentration streams due to its (1) ease of handling and control system; (2) high removal efficiency; (3) higher flux and lower energy costs than that of NF and RO processes; (4) small volume of retentate generation (10–30% of the feed volume) with concentrated pollutants for further treatment, which can be more cost-effective than the direct treatment of the feed stream; and (5) potential for metal and surfactant recovery (Karate and Marathe, 2008; Landaburu-Aguirre et al., 2010). As such, MEUF provides a viable alternative as a one-step or hybrid technology for dissolved ion treatment of wastewater.

### **2.2.2. Major components and parameters of MEUF**

The performance of MEUF can be affected by multiple parameters, such as the membrane (molecular weight cut-off (MWCO) and material), surfactant (types, properties, dosage, surfactant-to-solute ratio), and operating conditions (UF mode, transmembrane pressure, temperature, pH). The most important components and commonly studied parameters are described as follows.

#### **2.2.2.1. Ultrafiltration mode**

Ultrafiltration can be operated in a dead-end (unstirred batch system, stirred batch, stirred batch with feed reservoir) or cross-flow mode (with and without retentate recycling) (Figure 2-1). The transmembrane pressure is usually supplied by a nitrogen cylinder. As the UF process proceeds, the retained solute increasingly accumulates on the membrane and in the retentate, resulting in a decline of permeate flux. Therefore, the feed solution is usually stirred to minimize membrane fouling. In cross-flow systems, the retentate is either collected for further treatment or recirculated back to the feed reservoir, while the

permeate flux is constant. While continuous cross-flow filtration is popular for industrial applications, more laboratory studies prefer the stirred batch system (Figure 2-1b) because it is easy to setup and requires less equipment of feed volume (typically 50–400 mL depending on the model of the UF cell) (Schwarze, 2017).

#### **2.2.2.2. Ultrafiltration membrane**

A key component of a successful UF system is the membrane, defined as “a structure, having lateral dimensions much greater than its thickness, through which mass transfer may occur under a variety of driving forces” (Rivas et al., 2011). It is essentially a barrier that restricts the pollutants from transporting to the permeate stream. An ideal UF membrane should have (Michaels, 1968): (1) high hydraulic permeability (defined in Figure 2-2) to water, which enables high permeate flux (treatment efficiency) under a moderate transmembrane pressure; (2) sharp retention features so that the membrane can completely retain solutes with molecular weight higher than a particular MWCO value and completely release those with lower molecular weight; (3) high stability in different chemical/thermal conditions and different solute types or concentrations; (4) high resistance to fouling to ensure longer membrane life; and (5) high manufacturing reproducibility in terms of UF performance (flow rate and rejection rate).

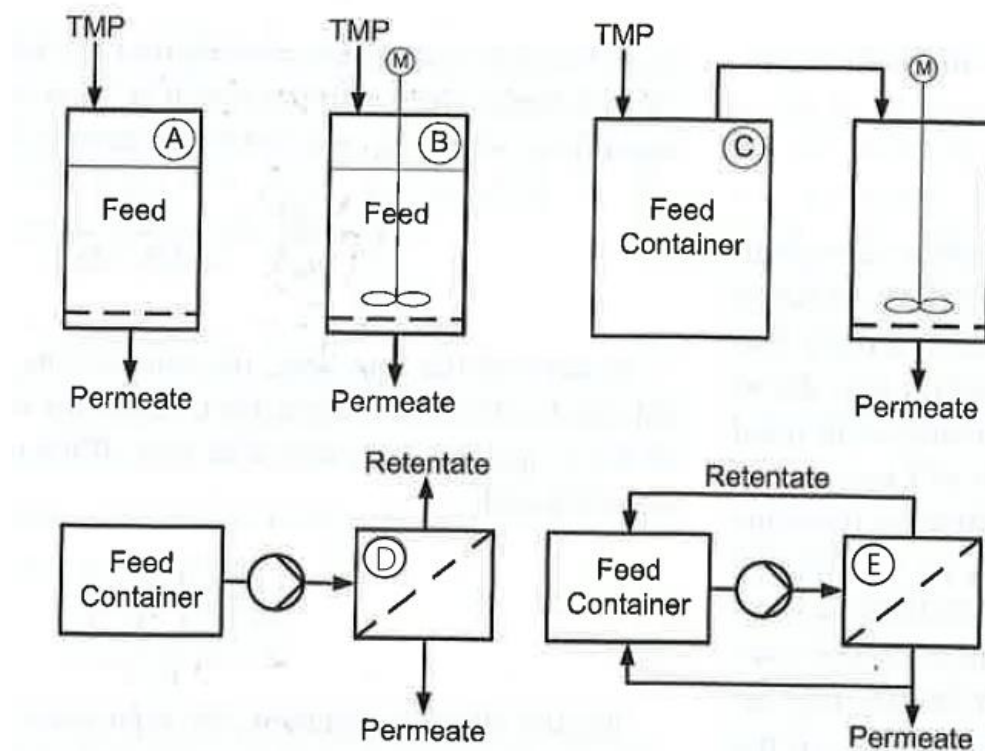


Figure 2-1 Ultrafiltration mode: (a) unstirred batch system, (b) stirred batch system, (c) stirred batch system with feed reservoir, (d) cross-flow system, and (e) cross-flow system with retentate recycling

Source: (Schwarze, 2017)

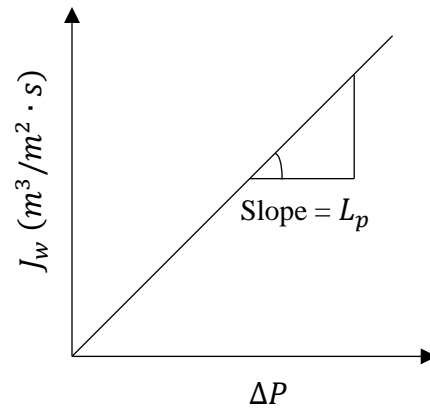


Figure 2-2 A typical flux vs. pressure plot for distilled water as feed. Membrane permeability ( $L_p = J_w/\Delta P$ ) indicates how porous a membrane is. Higher  $L_p$  values indicate more porous membranes.

A membrane can be classified based on its properties: material (polymeric or ceramic), surface property (hydrophobic, hydrophilic, or charged surface), and MWCO (implies the pore size). In general, the selection of a UF membrane is based on the physical and chemical properties of the solution. Polymeric membranes are commonly used in MEUF experiments, such as those made of regenerated cellulose (RC), cellulose acetate (CA), polyethersulfone (PES), polysulfone (PS), polyacrylonitrile (PAN), polyamide (PA), and polyvinylidene fluoride (PVDF) (Schwarze, 2017). Both hydrophobic (e.g., PES) and hydrophilic (e.g., RC, CA) membranes are used. The MWCO of the membrane should be selected depending on the micelle size, i.e., the membrane's pore size should be smaller than that of surfactant micelles.

A major operational concern with membrane use is its tendency of fouling, which results in a productivity loss (Tansel et al., 2000). Concentration polarization is a phenomenon that solute particles accumulate and build a thin boundary layer on the membrane surface. It can lead to a decline of the driving force, increased resistance against the flux, reduced membrane permeability, gel layer formation on the membrane surface, and initiation of membrane fouling (Landaburu-Aguirre et al., 2010). To tackle the problem of fouling, membranes are cleaned periodically to remove the adsorbed matter and recover membrane permeability (Shi et al., 2014). Membrane cleaning intends to restore the initial flow without disturbing the membrane surface. In MEUF, membranes are commonly cleaned by rinsing deionized water and dilute chemicals (e.g., 0.1 M NaOH, NaOCl, HCl, HNO<sub>3</sub>) (Isa et al., 2008; Li et al., 2009; El Zeftawy and Mulligan, 2011; Huang et al., 2015) and in some cases using ultrasonic cleaning (Cai et al., 2010).

### 2.2.2.3. Surfactant

Surfactants are amphiphilic molecules that consist of a hydrophilic head group and hydrophobic chain (Gelardi et al., 2016). At its critical micellar concentration (CMC), surfactants can form spherical aggregates containing 50–150 surfactant monomers (Xiarchos et al., 2008). Classified by the ionic properties of the head groups, surfactants can be anionic, cationic, and non-ionic. An ideal surfactant for MEUF should follow the criteria: (1) low CMC value, so that less surfactant is dosed (lower material cost) or lost (cleaner permeate stream); (2) cost and commercial availability; (2) ability to form large micelles; (3) less adsorption to the surface of UF membranes; (4) highly soluble for the solute, (5) biodegradable, and (6) easy for recovery (Mosler and Hatton, 1996; Vibhandik and Marathe, 2014). A good interaction (e.g., electrostatically) between a surfactant and a target pollutant and a low CMC value that enables acceptable rejection are the key criteria.

Though many surfactants are available, MEUF processes commonly used ionic surfactants include sodium dodecyl sulfate (SDS) (Juang et al., 2003; Xu et al., 2007a; Das et al., 2008a; Xiarchos et al., 2008; Landaburu-Aguirre et al., 2010; Li et al., 2011; Huang et al., 2014; Tanhaei et al., 2014; Huang et al., 2019), cetyltrimethylammonium (CTAB) (Gzara and Dhahbi, 2001; Iqbal et al., 2007; Camarillo et al., 2009; Chang et al., 2015), and cetylpyridinium chloride (CPC) (Baek and Yang, 2004b; Kim et al., 2004; Jung et al., 2008; Bahmani et al., 2019). Their properties are summarized in Table 2-2. Anionic surfactants have relatively high CMC values (Landaburu-Aguirre et al., 2010). Although non-ionic surfactants have relatively low CMC values, they cannot form ion-



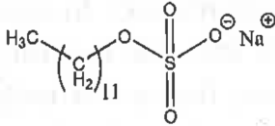
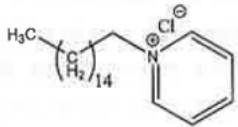
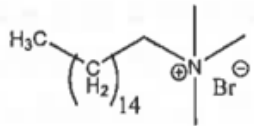
pair complexes. Hence, the function of non-ionic surfactants alone is not effective in MEUF, though in rare cases they succeeded, such as the work of Akita et al. (1997) removing gold ions using the non-ionic polyoxyethylene nonyl phenyl ethers (PONPEs).

#### **2.2.2.4. Operating conditions and parameters**

The pH affects the equilibriums of different ionic species in solution and, therefore, their electrical charges (Camarillo et al., 2009). It can also affect the interaction of solute and micelles. At lower pH values, the abundant  $H^+$  ions may hinder the binding of cations to anionic surfactant micelles; whereas at higher pH values, more binding sites are available for cations (Bade and Lee, 2007).

The driving force of a MEUF system is the pressure gradient through the membrane, namely the transmembrane pressure (TMP) (Yang et al., 2005). In a UF process filtering pure water, the water flux through the membrane is in a linear relationship with the transmembrane pressure. In a MEUF system that contains solute and surfactants, the linear relationship changes into non-linear due to the accumulation of macromolecules on the membrane (Landaburu-Aguirre et al., 2010).

Table 2-2 Specifications of commonly used ionic surfactants

Surfactant (abbreviation)	Chemical structure	Monomer MW (g/mol)	Micelle size	CMC
<b>Anionic</b>				
Sodium dodecyl sulfate (SDS)		288.32	18 kg/mol; aggregation number of 62	8.2 mM
<b>Cationic</b>				
Cetylpyridinium chloride (CPC)		358.01	27 kg/mol, aggregation number of 80	0.9 mM
Cetyltrimethylammonium bromide (CTAB)		364.45	22 kg/mol, aggregation number of 61	0.9 mM

CMC= critical micellar concentration

Sources: (Baek et al., 2003; Kamble and Marathe, 2005; Xiarchos et al., 2008; Camarillo et al., 2009)

#### 2.2.2.5. MEUF performance evaluation

The performance or efficiency of a membrane filtration system is often determined by membrane selectivity and the flow through the membrane (Mulder, 1996). The selectivity of a membrane to the feed stream is usually indicated by rejection (R), defined as the percentage of solute being retained by the membrane against the amount of solute in the feed/retentate. The value of rejection varied between 0% (solute and solvent pass through the membrane completely) and 100% (complete rejection of the solute, indicating great performance of the membrane). The flow through the membrane is indicated by flux (J), defined as the volume passing the membrane per unit area and time. Although SI units ( $\text{m}^3/\text{m}^2\cdot\text{s}$ ) are recommended, literature frequently use other units such as  $\text{L}/\text{m}^2\cdot\text{h}$  and  $\text{L}/\text{m}^2\cdot\text{d}$  (Mulder, 1996; Chakraborty et al., 2014). Rejection and flux are the most important parameters (their mathematical equations are given in Chapter 3) to evaluate MEUF performance in most studies. In the macromolecular scale, parameters such as the amount of micelles and micelle loadings are reported in a few studies to examine the solute-micelle interaction (equations are introduced in Chapter 5).

To indicate membrane properties, membrane permeability and its fouling effect are used. The former is usually indicated by the flux rate when filtering pure water through a UF membrane, described as:

$$J_w = \frac{\Delta P}{\eta_w \cdot R_M} \quad (2-1)$$

where  $J_w$  is the flux rate of pure water through the membrane (or water flux);  $\Delta P$  is the transmembrane pressure;  $\eta_w$  is the viscosity of water, and  $R_M$  is the membrane resistance.

Commonly,  $J_W$  (usually in  $m^3/m^2 \cdot s$ ) is plotted over a series of  $\Delta P$  (in Pa). The value of  $R_M$  ( $m^{-1}$ ) can be calculated from the slope of the regression line.

### **2.2.3. Existing MEUF studies for dissolved ion removal**

The compatibility (associated with surfactant rejection) of the selected UF membrane and surfactant need to be considered in the MEUF process. Researchers examined surfactant rejection by UF membranes in absence of metal ions to understand the membrane-surfactant interaction. In dead-end UF systems, Schwarze et al. (2010) filtered the micellar TX-100 solutions using cellulose membranes with MWCO from 5 to 100 kDa in a stirred cell. They found the surfactant rejection is related to its hydrophobicity properties. Urbański et al. (2002) studied the UF retention of SDS and CTAB solutions using RC membrane of 10 kDa in an AMICON 8010 (10-mL volume) and an AMICON 8050 (50-mL volume) stirred cells. In cross-flow UF units, Yang et al. (2005) used an RC membrane with 10 kDa MWCO to remove surfactants with different ionic properties (e.g., the ionic SDS, the non-ionic Tween 80). The authors reported that non-ionic surfactants led to a more severe decline in the relative flux. Also, Schwarze et al. (2009) reported over 99% of rejection of SDS and CTAB micelles (all in  $10 \times CMC$ ) using RC and PES membranes.

Studies also explored the membrane's rejection of metal ions in absence of surfactant micelles. Typically, a UF membrane cannot retain dissolved ions due to their smaller size than the membrane pores. In some cases, due to the adsorption of ions onto the membrane, marginal rejection rates were observed, such as 5% rejection of  $Zn^{2+}$  and 4% of  $Ni^{2+}$  by a RC membrane (Schwarze et al., 2015), 24% of  $Co^{2+}$  by a PES membrane

(Anthathi and Marathe, 2011), 23% of  $\text{Cu}^{2+}$  by a polyacrylonitrile (PAN) membrane (Bade and Lee, 2007), and 15% of  $\text{CrO}_4^{2-}$  by a PAN membrane (Bade et al., 2008).

A number of studies investigated the MEUF removal of dissolved ions from their single-ion solutions. Typical metal ions being studied are  $\text{Cu}^{2+}$ ,  $\text{Ni}^{2+}$ ,  $\text{Zn}^{2+}$ ,  $\text{Cd}^{2+}$ ,  $\text{Pb}^{2+}$ , As (in form of  $\text{AsO}_4^{3-}$ ), and Cr (in form of  $\text{CrO}_4^{2-}$ ), usually applying the oppositely charged surfactant (Table 2-3). Most commonly examined factors are the initial metal and surfactant concentration (or their molar ratio) and feed pH.

Still, research efforts are desirable to understand the MEUF process, predict its performance, and understand the relative contribution of different parameters. Also, most of the existing studies applied the conventional one-factor-at-a-time method to obtain an optimal condition. Such conclusions could be inaccurate if parameters interact with each other or require much extra work to find the optimal condition. A more systematic methodology is needed to understand the process parameters and their interactions in a MEUF system.

Table 2-3 Summary of MEUF removal of dissolved ions from aqueous streams (selected examples)

Ions	Surfactant	Membrane material (MWCO)	Filtration mode	Examined parameters	Highest ion rejection (%)	References
$\text{CrO}_4^{2-}$	CPC, CTAB	PS (20 kDa)	Dead-end	Feed surfactant concentration, TMP, feed chromate concentration, temperature, salt addition	99	(Kamble and Marathe, 2005)
$\text{Cu}^{2+}$ , $\text{Pb}^{2+}$ , $\text{Zn}^{2+}$	CPC	RC (10 kDa)	Dead-end	pH, feed CPC concentration	97	(Jung et al., 2008)
$\text{Ni}^{2+}$ , $\text{Co}^{2+}$	SDS	PS (20 kDa)	Cross-flow	Feed metal concentration, S/M ratio, salt addition, pH, flow rate	>99	(Karate and Marathe, 2008)
$\text{Cd}^{2+}$ , $\text{Cu}^{2+}$ , $\text{Co}^{2+}$ , $\text{Zn}^{2+}$	SDS	RC (3, 10 kDa)	Dead-end	S/M ratio	>95	(Kim et al., 2008)
$\text{Cu}^{2+}$ , $\text{MnO}_4^{2-}$	SDS, CPC	PA (5 kDa)	Cross-flow	$\text{Cu}^{2+}$ and $\text{MnO}_4^{2-}$ concentration, TMP, flow rate	90-100 ( $\text{Cu}^{2+}$ ), 96-99 ( $\text{MnO}_4^{2-}$ )	(Das et al., 2008b)

<b>Ions</b>	<b>Surfactant</b>	<b>Membrane material (MWCO)</b>	<b>Filtration mode</b>	<b>Examined parameters</b>	<b>Highest ion rejection (%)</b>	<b>References</b>
$\text{Cd}^{2+}$ , $\text{Zn}^{2+}$	SDS	RC (3, 5, 10 kDa)	Dead-end	TMP, feed metal concentration, feed SDS concentration, MWCO	98-99	(Landaburu-Aguirre et al., 2010)
$\text{Ni}^{2+}$	SDS + Tween 80 (non-ionic)	PES (10 kDa)	Cross-flow	pH, TMP, S/M ratio, TW80/SDS molar ratio	99	(Vibhandik and Marathe, 2014)

## **2.3. Polymer-Enhanced Ultrafiltration (PEUF)**

### **2.3.1. Background and mechanisms of PEUF**

Polyelectrolytes (polymer hereafter) are polymers with ionic groups (Dunaway et al., 1998). A water-soluble polymer contains a polymer backbone, which controls the solubility and stability of the polymer, and hydrophilic functional groups (e.g., ether, alcohol) that control the selectivity (Almutairi et al., 2011; Halake et al., 2014). Similar to MEUF, PEUF (polymer-enhanced ultrafiltration, or sometimes polymer-assisted ultrafiltration or polyelectrolyte-enhanced ultrafiltration) can remove dissolved ions from aqueous streams, using a water-soluble polymer as the binding agent. The polymer-ion complex is formed through electrostatic interaction and be retained by a UF membrane, while the unbound ions pass the membrane with the permeate stream.

An ideal water-soluble polymer, a key component of a successful PEUF system, should have the following characteristics: (1) sufficiently high solubility in water; (2) chemical and mechanical stability under the process conditions; (3) a large number of chelating units or functional groups; (4) high affinity to the target contaminants and inactivity to non-target compounds or the membrane; (5) adequate molecular weight that is greater than the MWCO of the UF membrane to obtain high rejection, but not too large to result in high solution viscosity or membrane fouling; (6) low toxicity to prevent any secondary pollution; (7) commercially available and low cost (i.e., easy and inexpensive to synthesize); and (8) possibility of regeneration (Geckeler and Volchek, 1996; Cañizares et al., 2005; Rivas et al., 2011). Although the synthesis of polymer with desired



chelating properties has been progressed, the selection of water-soluble polymers for PEUF is still limited (Huang et al., 2016a). Those with amine or carboxyl groups are more often used for PEUF removal of heavy metals. Table 2-4 summaries the commonly used polymers in PEUF studies. Similar to MEUF, parameters such as polymer type and properties (associated with the functional groups and charges), membrane type and MWCO, solution composition (e.g., solute and polymer concentrations and their ratio), pH, and pressure are important factors for PEUF processes (Geckeler and Volchek, 1996).

### **2.3.2. Existing PEUF studies for dissolved ion removal**

Existing PEUF studies for the removal of dissolved ions from water and wastewater mostly focus on the polymer-ion interactions, which are influenced by the polymer dosage, feed pH, transmembrane pressure, and membrane properties. Attentions are also on the observations of concentration polarization, membrane fouling, and cleaning methods. Table 2-5 listed existing PEUF studies for wastewater treatment. PEUF have been used to treat relatively low concentrations of cations (e.g.,  $\text{Cu}^{2+}$ ,  $\text{Ni}^{2+}$ ,  $\text{Zn}^{2+}$ ,  $\text{Co}^{2+}$ ,  $\text{Pb}^{2+}$ ,  $\text{Fe}^{3+}$ ,  $\text{Cd}^{2+}$ ,  $\text{Mn}^{2+}$ ,  $\text{Hg}^{2+}$ ) and less commonly anions (e.g.,  $\text{NO}_3^-$ ,  $\text{AsO}_4^{2-}$ ,  $\text{CrO}_4^{2-}$ ).

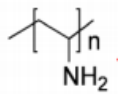
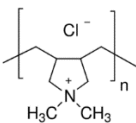
Although PEUF has been reported in some studies (Table 2-5), they have been rarely studied to remove anions from the aqueous streams. PEUF removal of sulfate has never been investigated. Only in two studies, sulfate ions present in PEUF systems as co-existed ions (i.e., interference) with low concentrations, but the sulfate removal efficiency or its behavior was not examined. The efficacy of sulfate removal using PEUF (as well as

MEUF) under different operational conditions, the sulfate-ligand interaction, and the underlying adsorption mechanism need investigation.

## **2.4. Ion Adsorption onto Surfactant Micelles/Polymers in MEUF/PEUF**

The binding mechanism of a MEUF or PEUF is the adsorption of dissolved pollutant ions onto the oppositely charged ligand (Roach and Zapien, 2009). To evaluate the efficacy and efficiency of an adsorbent (surfactant micelles or polymers) to remove the ions of interest (e.g., sulfate ions), it is crucial to establish a proper adsorption equilibrium correlation that describes the interaction between the pollutant (adsorbate) and the adsorbent. This equilibrium correlation, namely the adsorption isotherms, is essential to predict adsorption parameters, to compare the adsorption behavior among different adsorption systems or experimental conditions, and to design and optimize the adsorption systems (Foo and Hameed, 2010).

Table 2-4 Summary of commonly used water-soluble polymers in PEUF studies

Polymer	Ionic property	Repeating unit	Solute examples	Advantage	Example of studies used the polymer
Polyethylenimine (PEI)	Cationic	$-\text{CH}_2-\text{CH}_2-\text{NH}-$	Metal ions ( $\text{Hg}^{2+}$ ) and anionic species ( $\text{HAsO}_4^{2-}$ , $\text{HPO}_4^{2-}$ , $\text{SeO}_3^{2-}$ , $\text{CrO}_4^{2-}$ )	High content of functional groups, good water-solubility and chemical stability; strong chelating property owing to the presence of imine groups	(Volchek et al., 1993; Juang and Chen, 1996; Cojocaru et al., 2009a; Chakraborty et al., 2014; Huang et al., 2016a)
Polyvinylamine (PVAm)	Cationic		Heavy metals ( $\text{Co}^{2+}$ , $\text{Cu}^{2+}$ , $\text{Ni}^{2+}$ , $\text{Pb}^{2+}$ , $\text{Fe}^{3+}$ , $\text{Cd}^{2+}$ , $\text{Zn}^{2+}$ , $\text{Mn}^{2+}$ , $\text{Hg}^{2+}$ )	Large number of primary amino groups (up to 95%)	(Huang et al., 2015; Huang et al., 2016a; Huang et al., 2016b)
Poly(diallyldimethyl ammonium chloride) (PDADMAC)	Cationic		$\text{CrO}_4^{2-}$ , $\text{AsO}_4^{2-}$	Very low acute and chronic toxicity to environmental organisms; readily biodegradable	(Geckeler and Volchek, 1996; Sriratana et al., 1996; Pookrod et al., 2005)

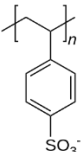
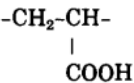
Polymer	Ionic property	Repeating unit	Solute examples	Advantage	Example of studies used the polymer
Sodium poly(styrene sulfonate) (PSS)	Anionic		$K^+$ , $Ca^{2+}$ , $Na^+$	Has sulfonate functional groups; can be used in water softening	(Scamehorn et al., 1990; Tabatabai et al., 1995)
Polyacrylic acid (PAA)	Anionic		$Hg^{2+}$	Commercially available chelating agents to heavy metals	(Volchek et al., 1993; Huang et al., 2016a)

Table 2-5 Summary of PEUF removal of dissolved ions from aqueous streams

Solute	Polymer	UF system	Membrane	Condition and parameters	Result	References
<b><u>Cations</u></b>						
Cu <sup>2+</sup> -EDTA chelate	PEI (PEI: Cu <sup>2+</sup> =2.0-20)	Batch stirred cell	RC (10 and 30 kDa)	pH (2-10), TMP (0.68-3.40 atm); effect of salt (NaCl, CaCl <sub>2</sub> , Na <sub>2</sub> SO <sub>4</sub> )	R > 97%	(Juang and Chen, 1996)
Cu <sup>2+</sup> and citrate (1mM)	PDADMAC (5, 10, 20 mM)	Centrifugal instead of dead-end		change pH	PDADMAC 5, 10 mM (R=90%) and 20 mM (R=98%)	(Yang et al., 2006)
Cu <sup>2+</sup>	PSS	Stirred cell	CA (1, 5, and 10 kDa)	30°C, 60 psi	R > 96%	(Scamehorn et al., 1990)
Cu <sup>2+</sup> , Ni <sup>2+</sup> , Zn <sup>2+</sup> , Co <sup>2+</sup>	PEI, PAA, MC, VBAC, VA-212	Batch stirred cell	CA or PA	TMP (0.02-0.4MPa), pH (2-9.5)		(Volchek et al., 1993)

Solute	Polymer	UF system	Membrane	Condition and parameters	Result	References
Hg <sup>2+</sup> (0-50 ppm); sulfate as interference (650 ppm)	PVAm	Dead-end and cross-flow	PES (10 kDa)	0.1-0.8 MPa; flow rate 20-100 L/h,	R = 99%	(Huang et al., 2015)
Heavy metals (Co <sup>2+</sup> , Cu <sup>2+</sup> , Ni <sup>2+</sup> , Pb <sup>2+</sup> , Fe <sup>3+</sup> , Cd <sup>2+</sup> , Zn <sup>2+</sup> , Mn <sup>2+</sup> ); sulfate interference	PVAm		PES (10 kDa)	200 kPa, 1000 rmp, TMP (40-800kpa), temperature (25-60°C)	R > 99%	(Huang et al., 2016b)
Hg <sup>2+</sup>	PEI, PVAm, PAA	Batch, cross-flow UF (tangential)	PES (10 kDa)	200 kPa, 65 L/h, room temperature	Flux (PVAm > PEI > PAA)	(Huang et al., 2016a)
Hardness (calcium, magnesium)	PSS	Stirred cell	Spiral wound UF membrane modules (10 kDa)	514.9 kPa; different temperature		(Tabatabai et al., 1995)

Solute	Polymer	UF system	Membrane	Condition and parameters	Result	References
Co <sup>2+</sup>	PEI	Dead-end cell	RC (5 kDa)	Room temperature, TMP=350 kPa; Effect of Co <sup>2+</sup> concentration, ratio, pH	R = 96.65%	(Cojocaru et al., 2009a)
Cu <sup>2+</sup> , Zn <sup>2+</sup> , Cr <sup>2+</sup> , Ni <sup>2+</sup> , Co <sup>2+</sup> , Cd <sup>2+</sup> (2-60 mg/L)	PEI	Stirred dead-end	PES (30 kDa)	Metal (2-60 mg/L); PEI 1g/L; pH 5.5		(Almutairi et al., 2011)
Cr <sup>6+</sup>	PEI	Cross flow	PES (6 kDa)			(Chakraborty et al., 2014)
<b><u>Anions</u></b>						
NO <sub>3</sub> <sup>-</sup> (groundwater)	poly(dimethyl-amine-co-epichlorohydrin-co-ethylenediamine); poly(dimethylamine-co-epichlorohydrin); PDADMAC	Lab made UF cell	RC (3, 10, 30, and 100 kDa)	1 bar; 300 rpm, ~25°C	R > 90%	(Zhu et al., 2006)

Solute	Polymer	UF system	Membrane	Condition and parameters	Result	References
AsO <sub>4</sub> <sup>2-</sup> (Cr <sup>5+</sup> ) (100 ppb); sulfate as salt (0-10 mM)	PDADMAC; initial polymer-to-arsenic ratio fixed (50, 100, and 150)	batch stirring cell	CA (10 kDa)	Effect of As, polymer concentration, pH (6.5-8.5); ionic strength; room temperature, 60 psi, 250 rpm	R = 99.95%	(Pookrod et al., 2005)
Cr <sup>5+</sup> (5.5-47.6mg/L) NaCl and Na <sub>2</sub> SO <sub>4</sub> interference (0.001-0.1M)	hydrophilic polymer: P(SAETA), P(CIAETA) (p:As=20:1)		10 kDa	pH adjusted to 8, 3.5 bar,	R=58% (high arsenate) to 100% (low arsenate)	(Sánchez and Rivas, 2011)
CrO <sub>4</sub> <sup>2-</sup>	PDADMAC					(Dunaway et al., 1998)
CrO <sub>4</sub> <sup>2-</sup>	PDADMAC	Stirred cell	CA (10 kDa)	NaCl interfere; fix 30°C, 250 rpm, 60psi		(Sriratana et al., 1996)



### **2.4.1. Adsorption isotherm models**

An adsorption isotherm is a curve that describes the mathematical relationship between the adsorbed and the residual adsorbate in the aqueous media at a constant temperature at solution equilibrium (Rangabhashiyam et al., 2014). After sufficient contact time, the adsorbed and residual amount is dynamically balanced, where the sorption and desorption rates are equal. The system hence reaches the adsorption equilibrium. The physicochemical parameters derived from adsorption isotherms provide crucial information such as the underlying adsorption mechanisms, surface properties, and the degree of affinity of the adsorbents (Rangabhashiyam et al., 2014).

A number of equilibrium isotherm models have been established, including two-parameters isotherm models (e.g., Langmuir, Freundlich, Dubinin–Radushkevich, Temkin) and three-parameter models (e.g., Redlich–Peterson, Sips, Toth) (Foo and Hameed, 2010). The Langmuir and Freundlich isotherms are the earliest isotherm models describing the adsorption process (equations listed in Chapter 5). Though many other isotherm models were built up on their basis, they remain to be the most frequently used models in current studies.

The Langmuir adsorption isotherm is an empirical model that assumes (1) structurally homogeneous adsorbent; (2) monolayer adsorption, where the thickness of the adsorbed layer is one molecule; (3) fixed number of identical adsorption sites, while each site having equal affinity to the adsorbate (all sites are energetically equivalent); and (4) no interaction between the molecules adsorbed on adjacent sites (Foo and Hameed, 2010; Lima et al., 2015). That is, the Langmuir isotherm describes homogeneous

adsorption, where a molecule being adsorbed to a site on the surface of the adsorbent no further adsorption takes place. When the solute molecules or available adsorption sites are saturated, the adsorption reaches an equilibrium.

The Freundlich adsorption isotherm describes heterogeneous system, assuming that multilayer adsorption could occur, and the adsorption heat and affinity on the surface of the adsorbent are not uniform (Rangabhashiyam et al., 2014). Sites with stronger binding energy will be occupied first. The adsorption energy is exponentially decreased until the adsorption process ends (Rangabhashiyam et al., 2014).

#### **2.4.2. Adsorption kinetic models**

The kinetic investigation is another important tool to discover the mechanism and reaction pathway of an adsorption process. The kinetics constants (such as the rate of adsorption, one of the criteria for the efficiency of the adsorbent) are directly associated with the residence time and provide crucial information to optimize the treatment of aqueous effluents (Lee and Shrestha, 2014; Aljeboree et al., 2017).

The most common adsorption kinetic models are the pseudo-first-order (Lagergren, 1898) and pseudo-second-order kinetic equations (Ho and McKay, 1999). Both are reaction-based models (equations listed in Chapter 5).

#### **2.4.3. Adsorption in MEUF and PEUF systems**

In MEUF and PEUF adsorption studies, the surfactant micelles and polymer ligands are considered to be the adsorbent, and ionic pollutants (such as copper, nickel, and sulfate ions) the adsorbate. It is assumed that the adsorbent and the adsorbed ions are all retained

by a UF membrane, while the unbound ions flow into the permeate (Huang et al., 2010; Almutairi et al., 2011).

Few studies reported the adsorption behaviors (commonly Langmuir and/or Freundlich models for isotherm fitness) in MEUF and PEUF systems, limited to a few metal ions. For example, Huang et al. (2010) reported better fitness of Langmuir isotherm ( $R^2 > 0.96$ ) than Freundlich isotherm ( $R^2 > 0.8$ ) to describe the adsorption of  $\text{Cd}^{2+}$  and  $\text{Zn}^{2+}$  on SDS micelles in their single metal systems. In contrast, Lee and Shrestha (2014) reported much better fitness of the Freundlich model ( $R^2 = 0.99$ ) than the Langmuir model ( $R^2 = 0.31$ ) to describe the adsorption of  $\text{Zn}^{2+}$  on SDS micelles, indicating a heterogenous surface of SDS micelles with adsorption sites of different affinities to zinc ions. The researchers suggested that the ratio of ion and surfactant concentration may play a role in the fitness of isotherms (Lee and Shrestha, 2014). While their study targeted on aqueous systems containing relatively high concentration of  $\text{Zn}^{2+}$  (approximately 1.8-9.2 mM) and low SDS (0.2 mM), in a similar study, Huang et al. (2010) examined low concentrations of  $\text{Zn}^{2+}$  (approximately 0.15-4.6 mM) and high concentration of SDS (7.5 mM). Despite the different result of adsorption isotherms, both studies reported good fitness ( $R^2 = 0.9999$ ) of the pseudo-second-order kinetic models. In another study, Almutairi et al. (2011) found good fitness of the Langmuir isotherm in the adsorption of metals ( $\text{Cu}^{2+}$ ,  $\text{Cr}^{6+}$ ,  $\text{Zn}^{2+}$ ,  $\text{Ni}^{2+}$ ,  $\text{Co}^{2+}$ , and  $\text{Cd}^{2+}$  in their individual systems) on the polymer PEI in a stirred dead-end PEUF system.

Most MEUF and PEUF studies of wastewater treatment aim at examining the system performance and the effect of operational parameters, though adsorption plays an important role in the process. The rare studies that discussed the intrinsic adsorption

mechanism focused on heavy metal removal. The behavior of sulfate ions (as the retained component) and the adsorption mechanism of sulfate to surfactant/polymer remains unknown. The adsorption studies can help to understand the knowledge such as the adsorption mechanism, the surface properties, the affinity of sulfate ions to the examined surfactant/polymer, and the rate of adsorption, hence providing important information to optimize the treatment of sulfate-containing effluents using MEUF/PEUF.

## **2.5. System Optimization and Modeling**

Traditionally, MEUF and PEUF were conducted using a one-factor-at-a-time method, whereas the system takes terms to examine the effect of one factor while fixing the others. Although easy to conduct, this method may require a large number of experimentations, often cannot observe the interactions between different variables, and is hard to find the true optimal condition of the system within reasonable experimental runs (Landaburu-Aguirre et al., 2010). As such, statistical methods such as a response surface methodology (RSM) are introduced to overcome these limitations. RSM is a statistical tool used for modeling and optimizing the process variables and revealing variable interactions. Commonly used models for system optimization include Box–Behnken designs (BBD), central composite design (CCD), and full factorial design (FFD).

Although some studies have developed RSM models in the MEUF/PEUF field in recent years, they are rare comparing to those using the one-factor-at-a-time method. Table 2-6 shows that the existing MEUF/PEUF-relevant RSM studies (commonly FFD and CCD methods) are limited to  $\text{Cu}^{2+}$ ,  $\text{Co}^{2+}$ ,  $\text{Zn}^{2+}$ , and  $\text{Cd}^{2+}$  ions. Relating to the context of this thesis, RSM modeling of  $\text{Ni}^{2+}$  is of interest. Also, previous studies mostly

examined parameters including the metal concentration, surfactant/polymer concentration, and pH. More parameters such as MWCO are to be investigated. In terms of system evaluation, metal ion rejection and permeate flux are common responses. They are also the most important indicators from an engineering viewpoint (Scamehorn et al., 1990).

Other mathematical tools have been combined with the RSM method for system optimization, such as fuzzy logic, artificial neural network (ANN), and adaptive neuro-fuzzy inference system (ANFIS), but these studies are even rarer (summarized in Table 2-7). The present study develops a BBD-based RSM model for the MEUF removal of  $\text{Ni}^{2+}$  and combines with an ANN model. It is to be investigated using dead-end MEUF, while examining the commonly studied parameters (metal and surfactant concentration, pH) the less studied parameter (MWCO).

Table 2-6 Summary of RSM studies in MEUF and PEUF

<b>Solute</b>	<b>UF system (surfactant/polymer) and mode</b>	<b>RSM method</b>	<b>Parameters examined</b>	<b>References</b>
$\text{Cu}^{2+}$	PEUF (PAA), dead-end and cross-flow	CCD	Feed PAA concentration, polymer/copper ratio, pH	(Cojocar and Zakrzewska-Trznadel, 2007)
$\text{Cu}^{2+}$	MEUF (SDS), dead-end	CCD	Feed SDS concentration, pH, S/M ratio	(Xiarchos et al., 2008)
$\text{Co}^{2+}$	PEUF (PEI), dead-end	CCD	Feed cobalt concentration, PEI/cobalt ratio, pH	(Cojocar et al., 2009a)
$\text{Co}^{2+}$	PEUF (PEI), cross-flow	FFD	Pressure, retentate flow rate, rotation frequency	(Cojocar et al., 2009b)
$\text{Zn}^{2+}$	MEUF (SDS), dead-end	FFD	Pressure, MWCO, feed zinc concentration, feed SDS concentration	(Landaburu-Aguirre et al., 2009)

<b>Solute</b>	<b>UF system (surfactant/polymer) and mode</b>	<b>RSM method</b>	<b>Parameters examined</b>	<b>References</b>
$\text{Cd}^{2+}$	MEUF (biosurfactant), dead-end	CCD	Feed biosurfactant concentration, pH, feed cadmium concentration	(Verma and Sarkar, 2017)
$\text{Pb}^{2+}$	MEUF (SDS), cross-flow	BBD	Feed SDS concentration, pH, S/M	(Rahmanian et al., 2012b)
$\text{Cd}^{2+}$ , $\text{Cu}^{2+}$ (mixed system)	MEUF (SDS), dead-end	CCD	pH, feed SDS concentration	(Landaburu-Aguirre et al., 2012)

CCD = central composite design

BBD = Box-Behnken Design

FFD = full factorial design

Table 2-7 Summary of studies using RSM combined with other mathematical models

<b>Solute</b>	<b>UF system (surfactant/polymer) and mode</b>	<b>RSM method</b>	<b>RSM parameters</b>	<b>Other optimization models</b>	<b>References</b>
Zn <sup>2+</sup>	MEUF (SDS), cross-flow	FFD	Pressure, pH, feed SDS concentration, S/M ratio, ligand-zinc ratio, electrolyte concentration, Brij35/SDS ratio	ANN	(Rahmanian et al., 2011b)
Pb <sup>2+</sup>	MEUF (SDS), cross-flow	BBD	Feed SDS concentration, S/M ratio, pH	Fuzzy logic	(Rahmanian et al., 2011a)
Pb <sup>2+</sup>	MEUF (SDS), cross-flow	BBD	Feed SDS concentration, S/M, pH	ANN and ANFIS	(Rahmanian et al., 2012a)
Cr <sup>6+</sup>	PEUF (PEI), cross-flow	CCD	Cross-flow rate, pressure, pH, polymer to metal ratio	ANN	(Chakraborty et al., 2014)
Pb <sup>2+</sup>	MEUF (SDS), cross-flow	BBD	Feed SDS concentration, S/M ratio, pH	Fuzzy logic	(Jana et al., 2018)

ANN = artificial neural network

ANFIS = adaptive neuro-fuzzy inference system



## **2.6. Summary**

The traditional treatment of wastewater containing dissolved ions (heavy metals or sulfate ions in the current study) consist of extraction, adsorption, precipitation, and ion exchange. Though these techniques have been successful, they can have disadvantages (e.g., longer operation times, a large volume of sludge generation, inadequate to reduce pollutant concentration to regulatory standards, and high chemical consumptions) especially when handling a large volume of wastewater containing relatively low concentrations of pollutants. In many cases, these techniques target on metal elimination rather than recovery. Membrane processes (e.g., RO and NF) are advanced technologies to treat dissolved pollutants, but the power consumption and maintenance requirement hinder them from wide applications. As such, MEUF and PEUF have emerged as promising options that can effectively treat the target pollutants and overcome some drawbacks of the above technologies. MEUF and PEUF make use of a surfactant or water-soluble polymer, respectively. The pollutant ions can be bound to the surfactant micelle or polymer ligands, generating an almost pollutant-free permeate. This thesis thus investigates MEUF and PEUF systems, aimed at filling research gaps identified based on the literature review in system operation and optimization, and understanding the adsorption mechanisms and the solute-adsorbent interactions in MEUF and PEUF systems.

## **Chapter 3.**

### **Removal of Heavy Metals from Mining Wastewater by Micellar-enhanced Ultrafiltration (MEUF): Experimental Investigation and Artificial Neural Network Modeling**

### 3.1. Introduction

Heavy metals are non-biodegradable, accumulative in living organisms, highly toxic, and sometimes carcinogenic (Fu and Wang, 2011). The removal of heavy metals has been a great concern for mining industries because of their persistence in the environment and toxicity even at low concentrations (Fu and Wang, 2011). Many technologies have been developed to meet the stringent environmental regulations. Micellar-enhanced ultrafiltration (MEUF) is an effective method for removing low-level metals from aqueous streams (Li et al., 2006; Samper et al., 2009; Tortora et al., 2016a; Tortora et al., 2016b). This technique makes use of a surfactant that can aggregate to form spherical micelles when the surfactant concentration is higher than its critical micellar concentration (CMC). The anionic micelles then bind with cationic metal ions to form a metal-micelle complex. The complex is large enough to be retained by a UF membrane, leaving the effluent with low concentrations of impurities (Xu et al., 2007b). Compared to the traditional separation methods (e.g., distillation and evaporation), MEUF generates concentrated retentate with about 10-30% of the original feed volume and is more cost-efficient than the direct treatment of the original feed (Tung et al., 2002; Karate and Marathe, 2008).

In exiting MEUF studies, a number of process parameters have been examined, including the molar concentration ratio of surfactant to metal (i.e., S/M ratio), pH, transmembrane pressure ( $\Delta P$ ), feed temperature, metal and surfactant concentration in the feed, and feed flow rate (Mungray et al., 2012). Among them, S/M ratio and pH are two crucial parameters most commonly investigated. Juang et al. (2003) used the surfactant

sodium dodecyl sulfate (SDS) to remove copper and cobalt ions from single metal systems, examining the effect of pH (2-12), S/M ratio (0.5-27), membrane molecular weight cut off (MWCO), and membrane material (polyamide, polyethersulfone). The authors reported that the increase in S/M ratio and feed pH led to significant changes in MEUF metal rejection rate. Landaburu-Aguirre et al. (2009) used SDS to remove zinc from synthetic wastewater and examined the effect of pressure, membrane MWCO, feed zinc concentration, and feed SDS concentration. They found zinc and SDS feed concentrations had a major influence on metal rejection rate, with up to 99% of the rejection was achieved with an S/M ratio above 5. Although the MEUF has been reported in the literature, research efforts are still desirable for a better understanding and prediction of the process, especially when multiple process parameters and responses are involved. Moreover, accurate knowledge of the relative importance of process parameters is also important in guiding policy, monitoring and sampling strategies, and formulation of scientific hypotheses. Therefore, mathematical models can serve as an effective tool for analysis and forecasting. However, different modeling approaches have only been recently introduced to study the simulation and optimization of MEUF and often limited to one or two metals, let alone the importance of parameters (Landaburu-Aguirre et al., 2010; Rahmanian et al., 2011a).

To tackle the above problems, artificial neural networks (ANNs) have been used as a statistical modeling tool to approximate complex functions, especially nonlinear ones between system inputs and outputs. A typical ANN comprises of an input layer with multiple inputs, an output layer with at least one output, and at least one hidden layer with multiple hidden neurons, which are all connected by weights and biases. Two general

types of ANNs are the multilayer feed-forward and the Kohonen self-organizing mapping (Kaltah et al., 2008; Jing et al., 2014). The application of ANNs in pollutant removal has been gaining increasing attention. Nevertheless, ANN has a “black box” nature such that the linearity or quadratic dependence of the transfer equations may not be well understood. In addition, the computational burden and the overfitting issue have also been identified (Elmolla et al., 2010). In terms of parameter importance, Garson (1991) proposed a measure to determine the contribution of independent input variables within an ANN. It partitions the hidden layer weights into components associated with each input, and then uses the percentage of all hidden nodes weights associated with a particular input to obtain the relative importance. However, the training of ANNs is considered to be a stochastic process, which means well-trained ANN models having the same modeling accuracy may have drastically different weights, biases, and hence inputs relative importance. Such a deficiency may be solved by using a resampling method to train a number of ANN models with acceptable accuracy and then to plot the relative importance of each input using probability density functions (Hattab et al., 2013).

In this study, a resampling-based ANN modeling approach is developed to examine the MEUF process for heavy metal removal. Copper, nickel, and cobalt are selected because they are the three most commonly mined metals in Newfoundland and Labrador (Environment Canada, 2011). In 2015, Voisey’s Bay mine reported production of 53,000 tonnes of nickel, 32,000 tonnes of copper, and 849 tonnes of cobalt (Government of NL, 2016). These metals are also characterized as persistent, bioaccumulative, and toxic by USEPA (Chhatre and Marathe, 2006). Therefore, the current study entails (1) removing copper, nickel, and cobalt ions from synthetic mining

wastewater samples using MEUF; (2) examining the effect of S/M ratio and feed pH on MEUF performance; (3) developing an ANN model to simulate the removal process and verify the applicability of ANN; (4) studying the relative importance of process parameters by coupling a resampling-based method; and (5) statistically discussing the effect of metal type on MEUF performance.

## **3.2. Material and Methods**

### **3.2.1. Materials**

The chemical surfactant sodium dodecyl sulfate (SDS, 20% in H<sub>2</sub>O) was purchased from Sigma-Aldrich, Canada. Cupric sulfate pentahydrate (CuSO<sub>4</sub>·5H<sub>2</sub>O, Fisher Scientific), nickel sulfate hexahydrate (NiSO<sub>4</sub>·6H<sub>2</sub>O, J.T. Baker), and cobalt chloride hexahydrate (CoCl<sub>2</sub>·6H<sub>2</sub>O, EMD) were used as sources of metal ions. All chemicals were of analytical grade and were used as received. The pH was adjusted using 1 M H<sub>2</sub>SO<sub>4</sub>, HCl, and NaOH. Copper, nickel, and cobalt reference standard solutions (1000 ppm  $\pm$  1%, certified) for Flame Atomic Absorption (FAA) tests were purchased from Fisher Scientific. Deionized water was used in all experimental procedures. Permeate samples were collected and stored using sorption-free materials.

### **3.2.2. Experimental set-up**

Figure 3-1 illustrates the MEUF mechanism and setup used in this study. UF experiments were carried out in an Amicon Stirred UF Cell Model 8400 (400-mL capacity; EMD Millipore). Regenerated cellulose membrane (EMD Millipore) was used, with 10 kDa MWCO and 76 mm filter diameter (effective area 0.00418 m<sup>2</sup>). A 300-mL feed solution

was filled and stirred at a constant rate in each experimental run. All experiments were conducted at room temperature ( $23 \pm 1$  °C). Transmembrane pressure was maintained at 40 psi (determined by pre-screening experiments) provided by nitrogen gas.

### **3.2.3. MEUF procedure**

The MEUF process was examined under different levels of S/M ratio (4-10) and pH (4-10) (Table 3-1). For each metal, nine scenarios were examined by using the one-factor-at-a-time method. A total of 27 experimental runs were conducted. Sampling cylinders and bottles were thoroughly cleaned to remove trace of residual metals. They were cleaned with detergent, acid-washed for 24 h, and thoroughly rinsed with deionized water. Before a UF test, water flux was measured by filtering 300-mL deionized water at 40 psi to check the membrane permeability. Water flux was estimated by collecting permeate of certain volumes during 30 s. Flux was measured at 2-min intervals until a constant value was found. For each UF run, 300 mL of feed solution was freshly prepared with designated metal and surfactant concentrations, and then adjusted to desired pH values as necessary. During the test, the first 10-mL sample was discarded; successive eight 25-mL samples were collected with each sampling time recorded, leaving 90 mL of feed (retentate) in the UF cell. Permeate samples were preserved with nitric acid (1% v/v) at 4 °C before measuring metal concentrations. Control experiments without the addition of SDS were conducted to examine the membrane effect. In each experimental run, the rejection rate and flux of eight permeate samples were determined; the values of the last sample identified the performance of that experimental run.

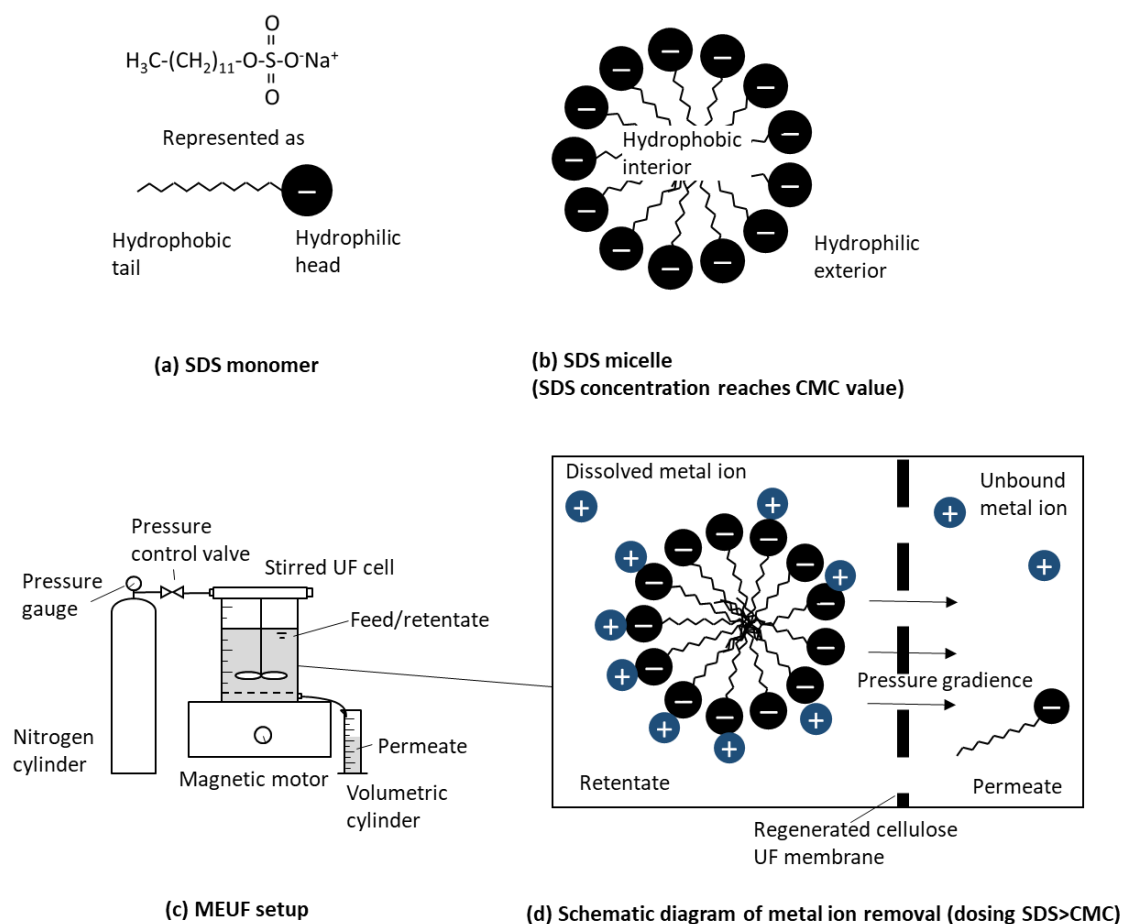


Figure 3-1 A Schematic diagram of (a) SDS monomer, (b) SDS micelle (when SDS concentration > CMC) (c) micellar-enhance ultrafiltration (MEUF) setup, and (d) mechanism of MEUF removal of metal ions



Table 3-1 Experimental runs of ultrafiltration tests

Metal <sup>a</sup>	Examine S/M ratio		Examine pH	
	S/M ratio	pH	S/M ratio	pH
CuSO <sub>4</sub> /NiSO <sub>4</sub> /CoCl <sub>2</sub>	0 (control)	Not adjusted	8.5	4
	4	Not adjusted	8.5	6
	6	Not adjusted	8.5	8
	8.5 <sup>b</sup>	Not adjusted	8.5	10
	10	Not adjusted		

<sup>a</sup> Metal concentration for all experiments is set at 1 mM

<sup>b</sup> SDS concentration is set at its critical micellar concentration

Membranes were used repeatedly. After each experiment, each membrane was thoroughly flushed with deionized water, rinsed with 0.5 N NaOH for 0.5 h, and flushed with deionized water again. Water flux was measured again at 40 psi to check membrane permeability. A water flux above 90% of that of the new membrane deemed the membrane reusable.

### 3.2.4. Sample analysis

The concentration of  $\text{Cu}^{2+}$ ,  $\text{Ni}^{2+}$ , and  $\text{Co}^{2+}$  in permeate samples were measured using a Varian Model 55B SpectrAA FAA Spectrophotometer. The average values of triplicate measurements for each permeate sample were calculated. FAA calibration curves were made before each set of measurements with  $R^2$  value of  $0.9984 \pm 0.0021$ . Diluted metal standards for making calibration curves were prepared every 4-6 months. The wavelengths used by AAS for Cu, Ni, and Co were set at 327.4, 232.0, and 240.7 nm, respectively.

The concentration of retentate was calculated using material balance:

$$C_r = \frac{(C_f V_f - C_p V_p)}{V_r} \quad (3-1)$$

where the subscripts  $r$ ,  $f$ , and  $p$  denote the retentate, feed, and permeate, respectively. As the permeate being continuously collected,  $C_f$  and  $V_f$  are continuously changing. Upon taking each sample, the  $C_f V_f$  was the calculated  $C_r V_r$  from the previous sample. Then, the rejection ratio (R) and permeate flux (J) of the metal were calculated as:

$$R(\%) = \left(1 - \frac{C_p}{C_r}\right) \times 100 \quad (3-2)$$

$$J(L/h/m^2) = \frac{V_p}{t \times A_m} \quad (3-3)$$

where  $V_p$  is the volume of the permeate sample;  $t$  is the time for collecting the sample (i.e., sampling time); and  $A_m$  is the membrane's effective area.

### 3.2.5. Artificial neural networks (ANN) modeling

Three multi-layer feed-forward ANN models, each with one hidden layer, were trained by the backpropagation algorithm to simulate the removal of  $\text{Cu}^{2+}$ ,  $\text{Ni}^{2+}$ , and  $\text{Co}^{2+}$ , respectively. The inputs were S/M ratio, pH, and cumulative sampling volume, whereas the two outputs were the rejection rate and permeate flux for each model (data shown in Appendix A). All inputs and outputs were normalized to [0, 1] range to avoid putting too much weight on variables with a large variance. The numbers of neurons in the hidden layers were optimized to be 12 for all three ANN models by following the procedures suggested by Jing et al. (2014). The transfer functions used at the hidden and output layers were log-sigmoid (logsig) and linear (purelin), respectively, based to literature recommendations (Elmolla et al., 2010; Jing et al., 2014). Neural network toolbox for MATLAB 2014b was used to develop the ANN models. Datasets obtained for each metal ( $n = 72$  for each metal) were randomly divided into training (60%), validation (20%), and testing (20%) subsets. The three models were trained by minimizing the mean squared error (MSE) while maximizing the correlation coefficients ( $R^2$ ) between the experimental and modeling outputs. The higher the correlation coefficient, the stronger the relationship. The two outputs, namely rejection rate and permeate flux, were given equal weight when

calculating  $R^2$  for each model. For comparison purposes, an inverse range scaling was performed on all modeling outputs to map them from [0, 1] to their original scales.

### 3.2.6. Resampling-based ANN modeling

Garson (1991) proposed an estimation of the relative importance of ANN model inputs:

$$I_j = \frac{\sum_{m=1}^{N_h} \left( \left( |W_{jm}^{ih}| / \sum_{k=1}^{N_i} |W_{km}^{ih}| \right) \times |W_{mn}^{ho}| \right)}{\sum_{k=1}^{N_i} \left\{ \sum_{m=1}^{N_h} \left( \left( |W_{jm}^{ih}| / \sum_{k=1}^{N_i} |W_{km}^{ih}| \right) \times |W_{mn}^{ho}| \right) \right\}} \quad (3-4)$$

where  $I_j$  is the relative significance of the  $j^{th}$  input variable on the output variable;  $N_i$  and  $N_h$  are the number of input and hidden neurons, respectively;  $W$  are the connection weights between layers;  $i$ ,  $h$ , and  $o$  refer to input, hidden, and output layers, respectively;  $k$ ,  $m$ , and  $n$  refer to input, hidden, and output neurons, respectively. Given the stochastic nature of ANN model training and the equifinality for different parameters,  $I_j$  could vary largely for multiple ANN models that would meet the same constraint for  $R$ . The ANN model was resampled to obtained 1000 ANN models (a random 60% of data was trained in each model) generating satisfactory  $R$  value. Each ANN model gives the relative contributions of three inputs (i.e., S/M, pH, and cumulative filtrate volume). For each metal, the relative contributions of each input to a output (i.e., rejection or flux) can be plotted using probability density functions.

### 3.2.7. Statistical analysis

Statistical analyses were performed to evaluate if the type of metal (factors) has a significant effect on metal rejection rate or permeate flux (responses). To examine each

factor, 27 data points were subjected to statistical analysis, including 9 data points of rejection/flux (under different S/M ratio and pH conditions, described in Table 3-1) for each metal. Data analysis was conducted using Minitab 17. The test procedure is illustrated in Figure 3-2 Flow chart of the statistical analysis method. Parametric (ANOVA) and nonparametric (ANOVA on rank transformation, Kruskal-Wallis test) tests were conducted to choose the one with more statistical power. If the assumptions of ANOVA (normality and equal variance of data groups) could not be met, the nonparametric method would proceed. The differences between measurements were considered significant at the level of  $p < 0.05$ .

### **3.3. Results and Discussion**

#### **3.3.1. MEUF performance in different conditions**

##### **3.3.1.1. Rejection change over S/M ratio and pH**

The effect of S/M ratio on UF rejection rate was examined (Table 3-1). The rejection of metals with the absence of SDS was checked to examine the membrane's effect. Figure 3-3a shows that the SDS-free system has a minimal 10-30% rejection rate of metals. The MEUF is effective typically when its surfactant concentration reaches its minimal effective concentration, namely its CMC value. Over 70% of the rejection rate was overserved when the SDS concentration was moderately below its CMC value (8.5 mM) (Figure 3-3a). When the SDS concentration reaches its CMC, MEUF obtained descent rejection rates of 91-97% for all metals. The S/M ratio was empirically optimized at the

value of 8.5, as there is only a marginal increase in the rejection when increasing the S/M ratio from 8.5 to 10. Therefore, an S/M ratio of 8.5 was set to examine the pH effect.

Figure 3-3b shows that MEUF performs more effectively in basic conditions. The rejection rate was increased from 92% to 99% when the pH value was increased from 4 to 10. High removal rates of  $\text{Ni}^{2+}$  and  $\text{Co}^{2+}$  were observed at pH of 10. In the Cu system, a pH of 8 seemed sufficient to achieve satisfactory rejection.

#### **3.3.1.2. Permeate flux change over S/M ratio and pH**

The effect of S/M ratio and pH on permeate flux was examined, as shown in Figure 3-3c and 3-3d, respectively. Generally, the flux trend is corresponding to the metal rejection, namely MEUF systems with high rejection rates generate low flux. Systems with higher S/M ratio (Figure 3-3c) and higher pH values (Figure 3-3d) tend to have lower fluxes.

#### **3.3.1.3. Effluent quality evaluation**

Figure 3-4 illustrates the metal concentrations in the permeate at the end of the UF test under different conditions. Metal Mining Effluent Regulations (MMER) listed the authorized limits of deleterious substances, where the maximum authorized concentrations for  $\text{Cu}^{2+}$  and  $\text{Ni}^{2+}$  are 0.6 and 1.0 mg/L, respectively (MMER, 2012). Discharge limit of  $\text{Co}^{2+}$  is not specified. Although the S/M ratio of 10 condition obtained a rejection rate of 97-98%, the effluent for three metals does not reach the MMER standard (Figure 3-4a). After pH adjustment, the metal concentrations in pH of 10 systems were well below the effluent limits. In systems with a pH of 8, only  $\text{Cu}^{2+}$  meets the standard.

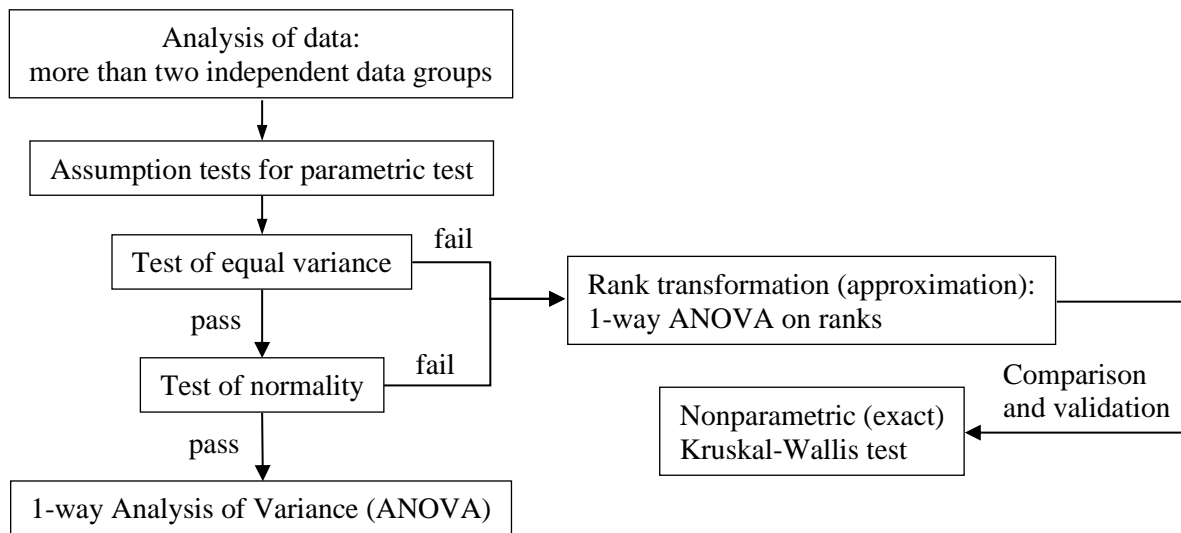


Figure 3-2 Flow chart of the statistical analysis method

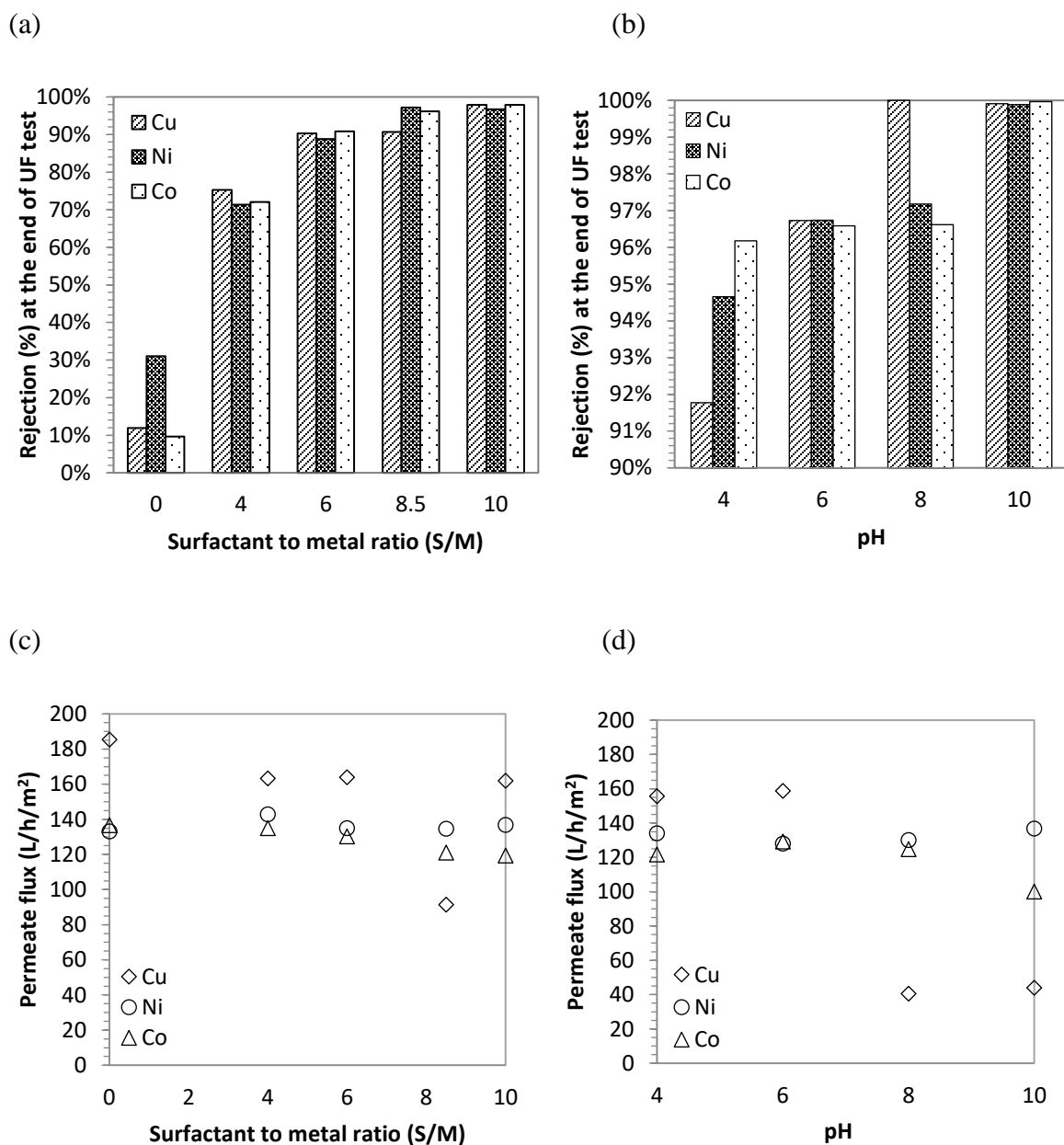
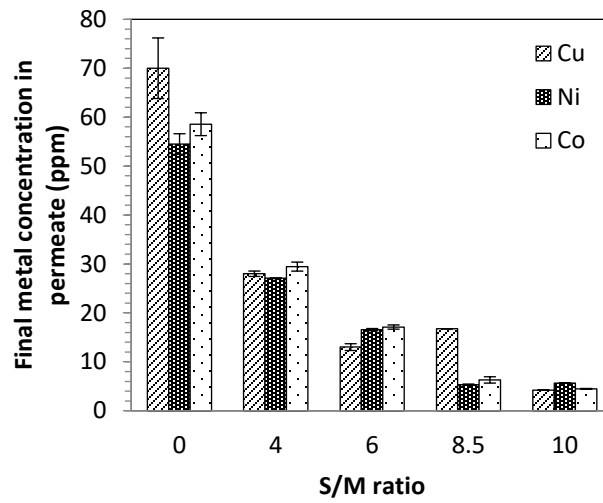


Figure 3-3 Effect of (a) S/M ratio (pH not adjusted) and (b) pH (S/M = 8.5) on metal rejection rate and effect of (c) S/M ratio (pH not adjusted) and (d) pH (S/M = 8.5) on permeate flux.  $[Cu^{2+}/Ni^{2+}/Co^{2+}]_f = 1$  mM,  $\Delta P = 40$  psi, and  $T =$  room temperature



(a)



(b)

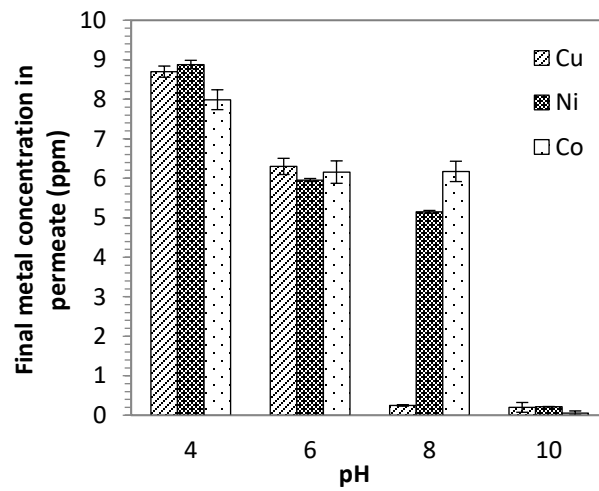


Figure 3-4 Metal concentrations in the permeate at the end of UF tests with the effect of (a) S/M ratio and (b) pH.  $[\text{Cu}^{2+}/\text{Ni}^{2+}/\text{Co}^{2+}]_f = 1 \text{ mM}$ ,  $\Delta P = 40 \text{ psi}$ , and  $T = \text{room temperature}$

### 3.3.2. Monitoring of parameter changes over time in MEUF runs

Figure 3-5 shows the dynamic behavior of MEUF in individual runs, taking the most effective condition (i.e., S/M ratio of 8.5 and pH of 10) as an example. Results for other conditions are showed in Figure 3-8 to Figure 3-13 in supplemental materials (section 3.5). In Figure 3-5a, high rejection rates are observed at the beginning of the UF test. Rejection of  $\text{Cu}^{2+}$  is the highest and relatively stable.  $\text{Ni}^{2+}$  and  $\text{Co}^{2+}$  have an only marginal increase in rejection. These observations indicated that high rejection of metal ions occurred in the early stage of the UF test. On the other hand, measured metal centration in the effluent was stable over the course of the UF test (partial data see Figure 3-5a). Also, the concentrations were all under the discharge limit since the start of the UF test (all concentrations < 0.3 ppm).

Flux variation was observed in all experiments. Before each experimental run, water flux was tested at the transmembrane pressure of 40 psi. A 140 to 180 L/h/m<sup>2</sup> flux was obtained. After adding SDS, the initial permeate fluxes were much lower than the water fluxes. In Figure 3-5b, permeate flux decreases with time, with a corresponding increase in sampling time. A non-linear decrease is apparent in the Cu system, while flux trends for Ni and Co systems seem to be linear.

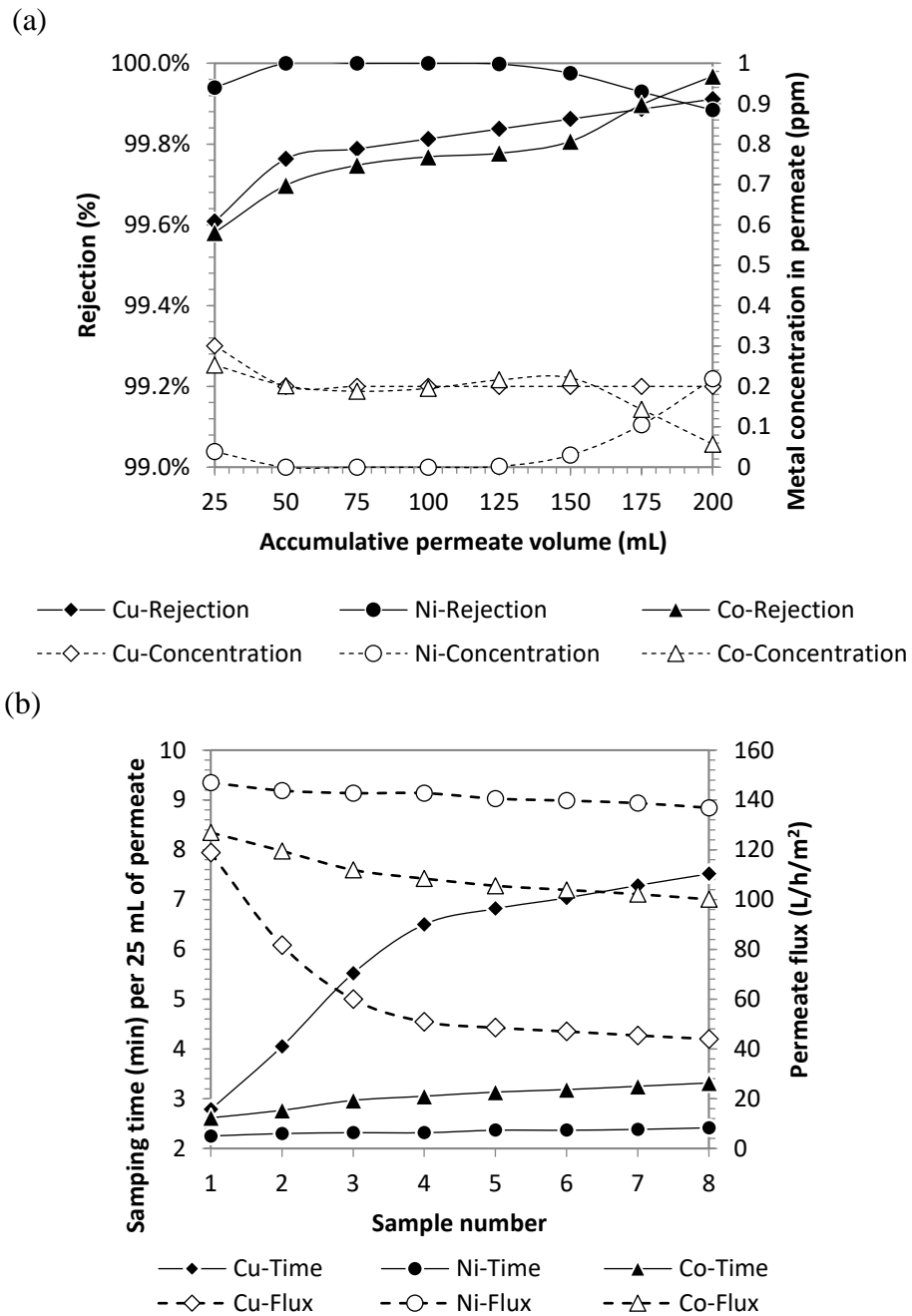


Figure 3-5 Change of (a) rejection rate and permeate concentrations of metal in single system and change of (b) sampling time and permeate flux during a UF run.  $[Cu^{2+}/Ni^{2+}/Co^{2+}]_f = 1 \text{ mM}$ ,  $[SDS]_f = 8.5 \text{ mM}$ ,  $pH = 10$ ,  $\Delta P = 40 \text{ psi}$ , and  $T = \text{room temperature}$

### 3.3.3. ANN modeling and parameter importance

The scatter regression plots of the ANN model predicted values against the experimental values for Cu system are shown in Figure 3-6. It should be noted that due to the inverse rescaling two outputs (rejection rate and permeate flux) were first converted from [0,1] and then plotted together within their original ranges. This would explain the gaps between different data clusters. The best linear fit equations for the training, validation, testing, and overall subsets all had a slope between 0.99 and 1, and the values of  $R^2$  were all higher than 0.99, indicating a close match between the experimental and modeling results. Therefore, the trained ANN model was able to accurately simulate the rejection rate and permeate flux for  $\text{Cu}^{2+}$  removal process. The modeling results for Ni and Co can be found in supplemental materials (Figure 3-14 to Figure 3-17, section 3.5).

By obtaining 1000 ANN models with acceptable accuracy were generated for each metal. According to the Garson Equation, the relative contributions of cumulative sampling volume, S/M ratio, and pH to the rejection rate and permeate flux for Cu are plotted in Figure 3-7. It can be seen that in terms of rejection rate, S/M ratio and pH had relatively close importance (45%) and were more influential than sampling volume (10%). However, pH had the most contribution (50%) to the permeate flux for Cu, which was higher than those from S/M ratio (40%) and sampling volume (10%). It also suggested that the removal performance did not change much as experiment-running time (i.e., sampling volume) increased, which can be confirmed by Figure 3-5.

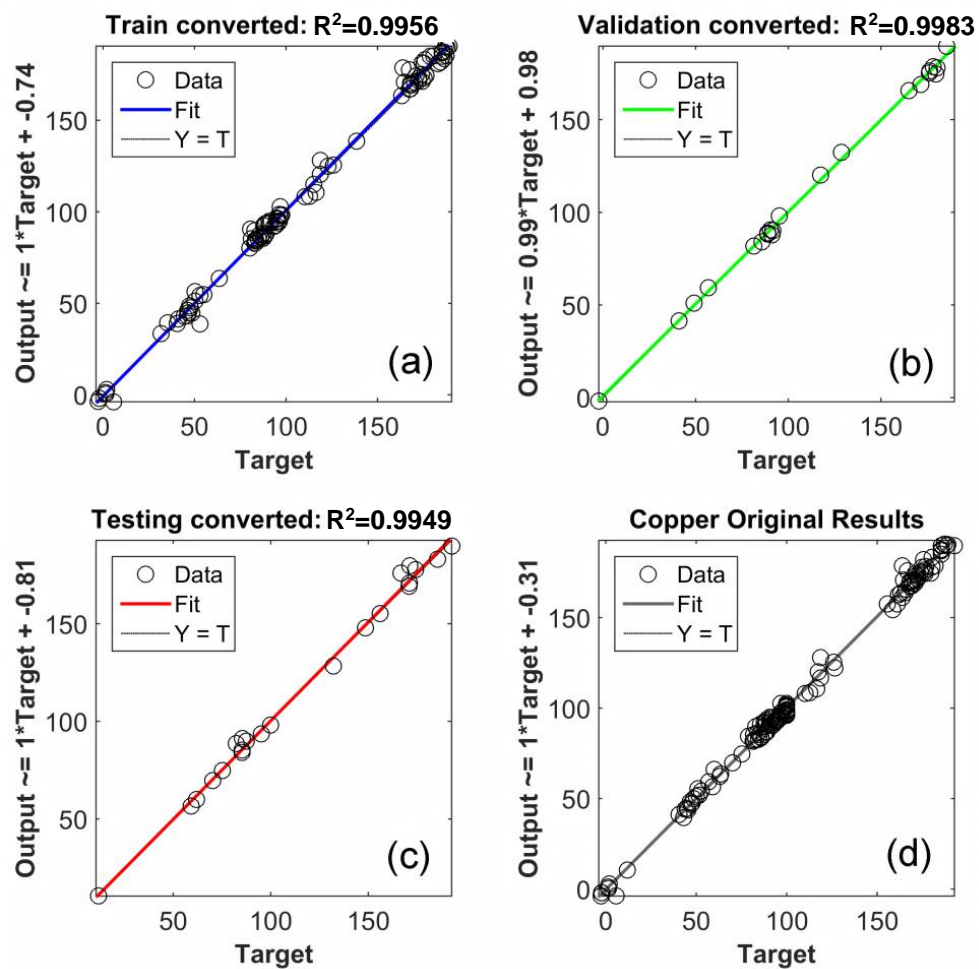
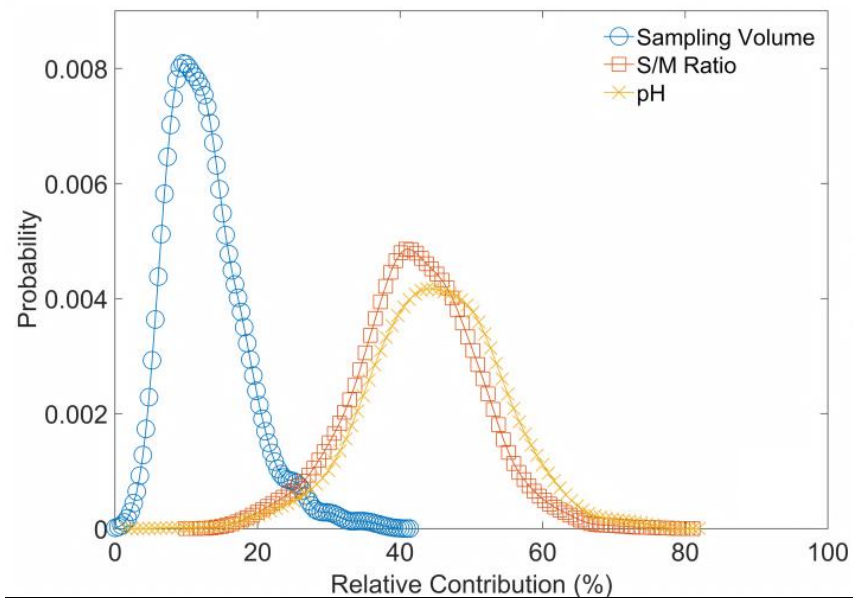


Figure 3-6 Comparison between ANN modeled (Output) and experimental (Target) results on the rejection rate and permeate flux for Cu system using (a) training, (b) validation, (c) testing, and (d) overall datasets

(a)



(b)

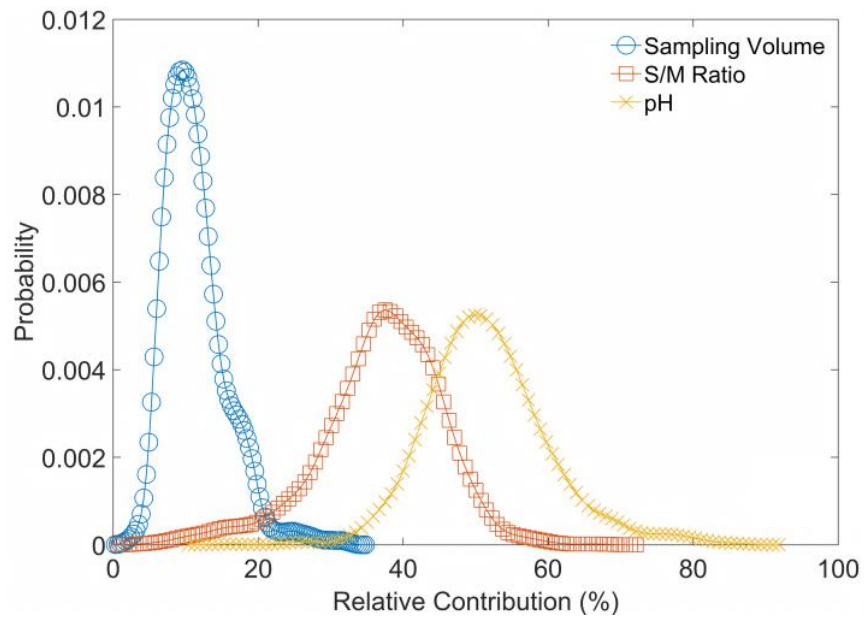


Figure 3-7 The relative contributions of sampling volume, S/M ratio, and pH to (a) rejection rate and (b) permeate flux for Cu system

### 3.3.4. Statistical analysis

Tests for equal variance and normality were conducted to examine the assumptions for ANOVA. Table 3-2 shows that the data group did not meet the ANOVA assumption, with all  $p$ -values less than 0.05. A rank-approximation or nonparametric method would therefore have more statistical power. The rank-approximation one-way ANOVA test was then conducted, its statistical parameters given in Table 3-3. No significant difference of rejection ( $p = 0.981$ ) or flux ( $p = 0.108$ ) was found between the different metal groups. The non-parametric Kruskal-Wallis test followed to compare and validate the results with the rank-approximation method. The two tests gave close  $p$ -values (Table 3-2), indicating that the MEUF performance removing different metals were not statistically different. This finding can be explained by the electrostatic nature of binding between metal ions and surfactant micelles. The removal efficiency of higher valence ions is higher than that of the lower valence ions, and the removal efficiency of the same valent ions are similar (Kim et al., 2008).

Table 3-2 Summary of statistical results

<b>Effect of A on B</b>	<b>Parametric test</b>		<b>Rank- approximation</b>	<b>Non- parametric test</b>
	<b>Test for equal variance</b>	<b>Test for normality</b>	<b>One-way ANOVA on ranks</b>	<b>Kruskal- Wallis test</b>
Metal type on rejection	0.982	<0.005	0.981	0.979
Metal type on flux	0.000	n/a	0.108	0.110

Listed data are p-values at 5% significance level

Failure in passing the test for equal variance does not proceed to the normality test



Table 3-3 Results of analysis of variance (rank-approximation method)

Source	DF	Adj SS	Adj MS	F-Value	P-Value
One-way ANOVA (response: rejection)					
Metal type	2	2.67	1.333	0.02	0.981
Error	24	1635.33	68.139		
Total	26	1638.00			
One-way ANOVA (response: flux)					
Metal type	2	277.6	138.78	2.45	0.108
Error	24	1358.9	56.62		
Total	26	1636.5			

DF = degree of freedom; SS = sum of squares; MS = mean of squares.

### **3.3.5. Discussion**

#### **3.3.5.1. Effect of S/M ratio on the metal rejection rate**

The SDS-free UF system showed small amount of metal rejection. The metal-containing salt in the feed solution dissociates into metal cations ( $\text{Cu}^{2+}$ ,  $\text{Ni}^{2+}$ , or  $\text{Co}^{2+}$ ) and sulfate/chloride anions. While most free metal ions pass through the membrane into the permeate stream, some can be adsorbed or trapped in the membrane pore due to membrane-solute interaction (associated with the charges, symmetry, and hydrophobicity of the membrane) (Kamble and Marathe, 2005). The RC membrane is hydrophilic and asymmetric in nature with no charges. The observed rejection of metal ions in the SDS-free systems may be due to the asymmetric membrane structure (non-uniform distribution of pore size), where smaller pores can trap some metal ions (Tortora et al., 2016b). Similar findings have been reported in other dead-end UF systems. Kamble and Marathe (2005) reported 29% rejection of chromate ions (chromate feed concentration at 1mM) in absence of the surfactant CTAB using a 20 kDa polysulfone membrane. Chhatre and Marathe (2006) reported approximately 13% of nickel removal (nickel feed concentration at 1 mM) in absence of SDS using a polysulfone membrane.

Figure 3-3a shows that the addition of SDS with a concentration below its CMC (when  $\text{S/M} = 4$  and  $6$ ) generated considerable metal rejection (approximately 70 and 90%, respectively). This could be explained by the fact that the long-chain SDS molecule can be rejected by the steric hindrance and adsorption of the membrane (Huang et al., 1994; Fillipi et al., 1999), forming higher concentrations of SDS near the membrane surface than in the feed (Kamble and Marathe, 2005). The accumulated SDS may reach or exceed

the CMC and start to form micelles and bind metal ions. The observation is similar to that of the study of Karate and Marathe (2008), in which  $\text{Ni}^{2+}$  and  $\text{Co}^{2+}$  rejection rates reached 94% at an SDS concentration of 6 mM. When the micelles are present in the solution, the randomly moving metal ions in the solution displace  $\text{Na}^+$  ions on the SDS micelle surface. Their ion exchange equilibrium is expressed in Equation 3-5:

$$2[\text{Na}^+]_{\text{micelle}} + [\text{M}^{2+}]_{\text{water}} = 2[\text{Na}^+]_{\text{water}} + [\text{M}^{2+}]_{\text{micelle}} \quad (3-5)$$

Figure 3-3a shows that when the S/M ratio further increases (dosing SDS with concentration of 1 CMC and more) metal rejections continue to increase and then level off. With a higher S/M ratio, the number of micelles formed in feed increases. Hence, metal ions have more available binding sites and the rejection rate is increased (Tung et al., 2002). Meanwhile, dynamic competition is taking place between metal ions and  $\text{Na}^+$  to bind themselves onto the micelle surfaces, associated with the electrical charge and concentration of these ions. The bivalent metal ions are preferred to bind the polar heads of micelles, but such preference can be compromised when  $\text{Na}^+$  concentration is large (Azoug et al., 1997; Lee and Shrestha, 2014). When the SDS concentration is low in the solution, the valence effect of metal ions prevails; hence more metal ions are bound to the micelle surface and an increase in rejection rates. When the SDS concentration is high, the concentration effect (which reduces rejection) can cancel out the valence effect (which increases rejection), thus the rejection rates remain stable. In the current study, the S/M ratio of 8.5 was selected for the following experiments. This conclusion is in agreement with reported literature. Fillipi et al. (1999) concluded that the surfactant

concentration had to be higher than its CMC to achieved maximum metal removal efficiency (>99% for most of the metals examined).

#### **3.3.5.2. Effect of pH on the metal rejection rate**

In acidic conditions, a large amount of  $H^+$  ions are present in the UF system. Despite the competition between  $Na^+$  and metal ions ( $Cu^{2+}$ ,  $Ni^{2+}$ , or  $Co^{2+}$ ) that previously discussed, cationic  $H^+$  and metal ions compete to bind with the anionic SDS micelles. With their size much smaller than metal ions,  $H^+$  ions tend to bind with micelles selectively, leaving metal ions in the feed (Karate and Marathe, 2008). The rejection rate of metals decreases accordingly. A similar trend was observed in other studies. Vibhandik and Marathe (2014) reported the  $Ni^{2+}$  rejection increased from 82% to 95% corresponding to an pH increase from 2 to 5. Juang et al. (2003) examined the removal of  $Co^{2+}$  and  $Cu^{2+}$  under a broad pH range of 2-12 (at 44 psi). Both metal ions observed sharp increases in rejection from pH 2 to 5. Further increase in pH seemed to have minimal effect on rejection rates, but a peak in rejection can be found at a pH of 9.

#### **3.3.5.3. Effect of S/M ratio and pH on the permeate flux**

The flux decline may be attributed to concentration polarization or the deposit of SDS micelles on the membrane surface. When the accumulative micelle concentration is adequately high, a gel layer starts to form and block the membrane (Xu et al., 2007b). A MEUF system with higher S/M ratio tends to form more micelles. Therefore, the concentration polarization effect would be more apparent, resulting in a smaller flux. Likewise, in basic conditions, more metal-micelle complex is formed and then deposit on the UF membrane, resulting in a smaller flux.

#### 3.3.5.4. Changes of operation parameters during MEUF runs

When dosing sufficient amount of SDS (i.e., feed concentration of 1 CMC and more), MEUF is effective upon its initiation, and the rejection rates remain stable during the MEUF runs (Figure 3-8, Figure 3-10, Figure 3-12 in Supplemental Materials). This observation indicates that the filtrate volume (or filtration time) does not play a crucial role in the MEUF efficiency, which agrees with the modeling findings. When the SDS dosage is below its CMC value (i.e., in experimental runs with 4 mM and 6 mM of SDS), an increment of rejection rate with the filtrate volume is observed in all metal systems. For example, at 4 mM SDS concentration, the rejection rate of copper increases from 48% when MEUF starts to 75% when it ends. This increment can be associated with many factors. With SDS concentration lower than its CMC value, the system is initially absent of SDS micelles. The UF process concentrates SDS in the retentate to concentrations higher than its CMC, thus forming micelle that can bind metal ions, resulting in higher removal rates. Also, due to concentration polarization the SDS concentration near the membrane surface is higher than those in the bulk solution (Juang et al., 2003), which may form micelles and contribute to the metal removal. Further, the membrane's effect also contributes to a small amount of metal rejection (discussed in 3.3.5.1).

In terms of permeate quality, metal concentrations in the permeate remain fairly constant throughout the MEUF runs under different S/M ratio and pH scenarios. Slight variations in the permeate metal concentration can be attributed to the dynamic mass action shifts to keep the ion exchange equilibrium (Equation 3-5) and the electrical

neutrality (Equations 3-6 and 3-7) in the retentate (denoted by  $r$  below) and permeate (denoted by  $p$  below) (Chhatre and Marathe, 2006):

$$2[M^{2+}]_r + [Na^+]_r = 2[SO_4^{2-}]_r + [DS^-]_r \quad (3-6)$$

$$2[M^{2+}]_p + [Na^+]_p = 2[SO_4^{2-}]_p + [DS^-]_p \quad (3-7)$$

In all MEUF experiments, initial fluxes were much lower than the pure water flux. This may be due to the adsorption of SDS micelles on the surface and in pores of the membrane (Xu et al., 2007b). Xu et al. (2007b) reported an initial drop of flux followed by an almost-constant flux. This behavior may be attributed to concentration polarization that could cause a resistance to flow. Therefore, the permeate flux decreases quickly at the beginning. When the micelles on the membrane do not increase, permeates flux becomes stable (Xu et al., 2007b). This non-linear decrease was found in the Cu system in the current study, whereas in the other two systems flux decline appeared to be linear.

### 3.4. Summary

In this work, MEUF was used to remove  $Cu^{2+}$ ,  $Ni^{2+}$ , or  $Co^{2+}$  in single metal systems from synthetic mining wastewater using chemical surfactant SDS. The UF performance under an S/M ratio of 4-10 and a pH range of 4-10 was examined. Predicted values from a resampling-based ANN modeling approach agreed well with the experimental data ( $R^2 > 0.99$ ). The model also found that the S/M ratio and pH were of greater importance (30-50%) than sampling volume (10%) to both rejection rate and permeate flux. Experimental observations reflect modeling results, and high removal efficiency was found in the early stage of MEUF process under optimal conditions. Maximum rejection rate ( $> 99\%$ ) for

$\text{Cu}^{2+}$ ,  $\text{Ni}^{2+}$ , and  $\text{Co}^{2+}$  were obtained under the optimal conditions (i.e., S/M ratio of 8.5, pH of 10), with all effluent qualities meeting the Canadian Metal Mining Effluent Regulations. Flux decrease and minimal concentration polarization effect were observed during experimental processes. Statistical analysis indicated that the technique worked equally well for all tested metals.

### 3.5. Supplemental Materials

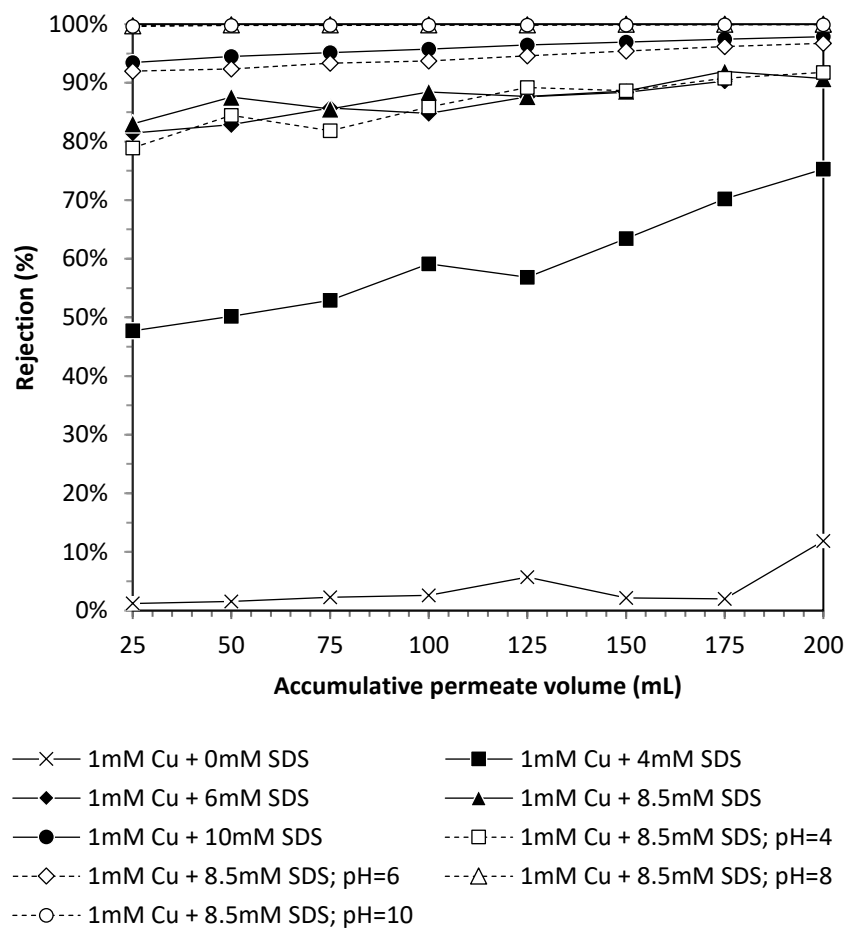


Figure 3-8 Change of rejection rate during UF runs (Cu system) examining the effect of S/M ratio (pH not adjusted) and pH value (S/M = 8.5).  $[Cu^{2+}]_f = 1 \text{ mM}$ ,  $\Delta P = 40 \text{ psi}$ ,  $T =$  room temperature



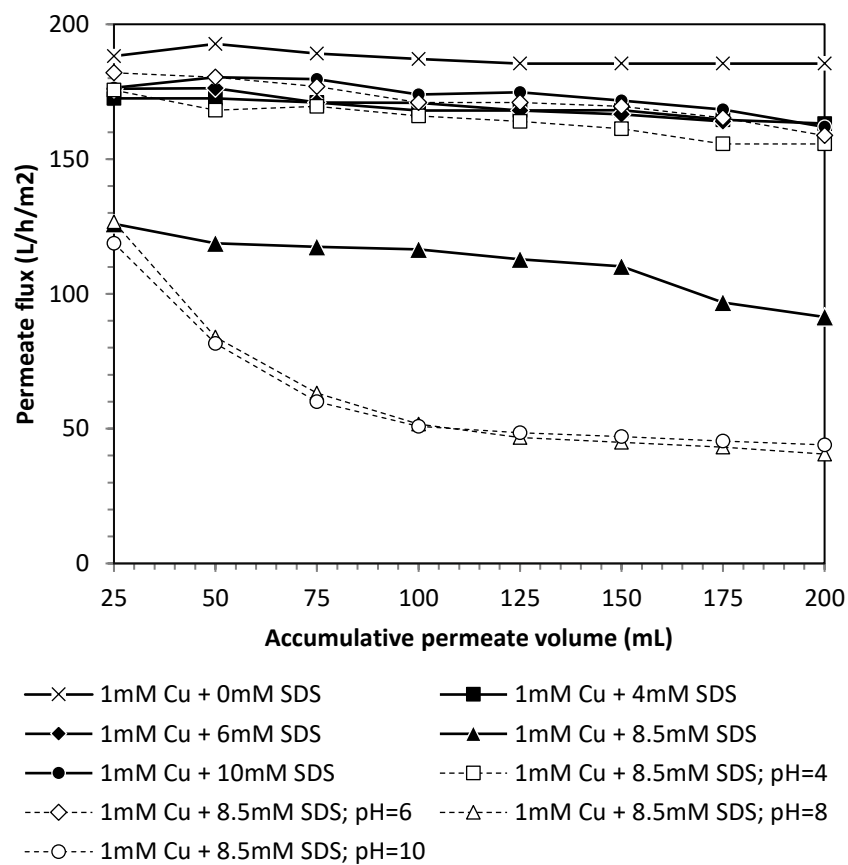


Figure 3-9 Change of permeate flux during UF runs (Cu system) examining the effect of S/M ratio (pH not adjusted) and pH value (S/M = 8.5).  $[Cu^{2+}]_f = 1 \text{ mM}$ ,  $\Delta P = 40 \text{ psi}$ ,  $T =$  room temperature

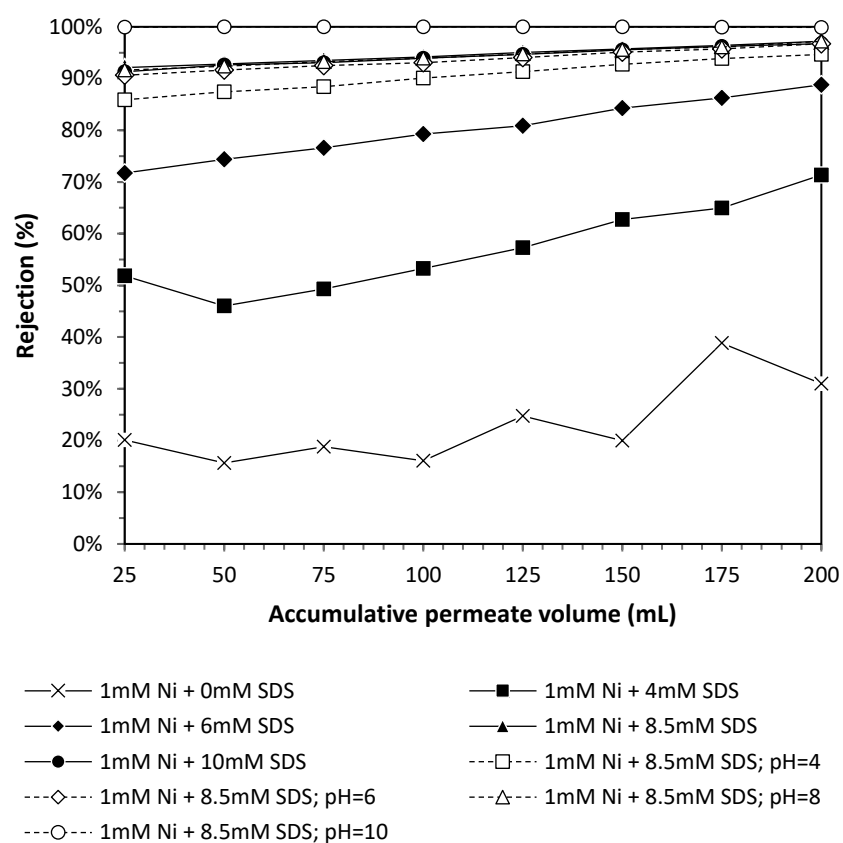


Figure 3-10 Change of rejection rate during UF runs (Ni system) examining the effect of S/M ratio (pH not adjusted) and pH value (S/M = 8.5).  $[\text{Ni}^{2+}]_f = 1 \text{ mM}$ ,  $\Delta P = 40 \text{ psi}$ ,  $T =$  room temperature

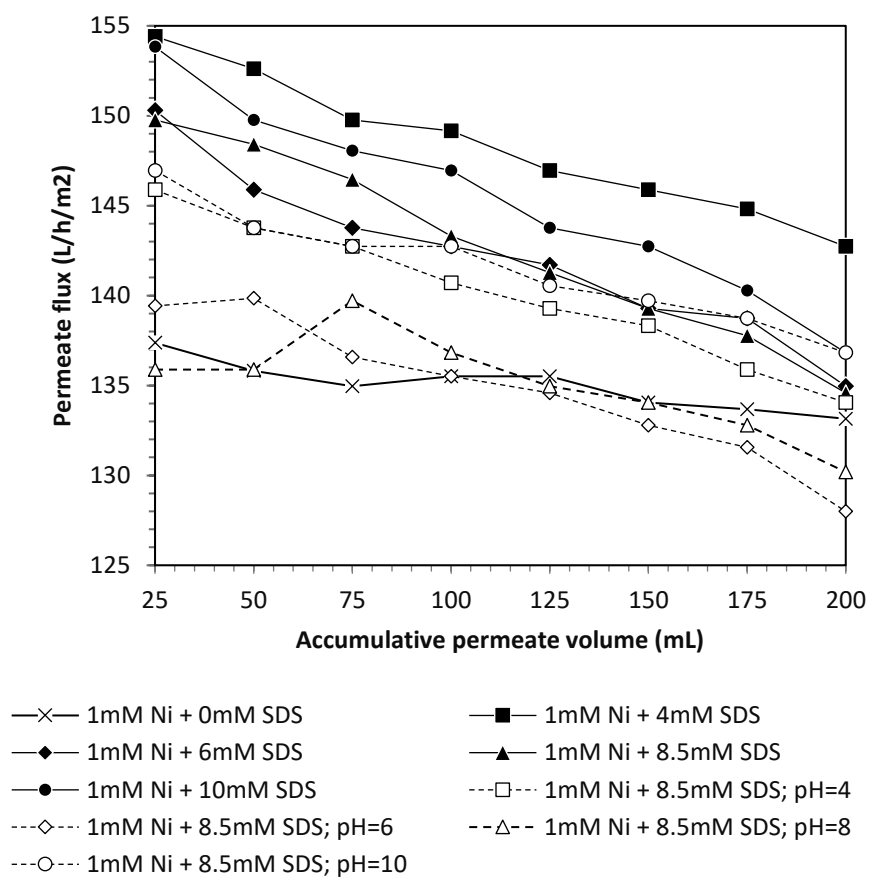


Figure 3-11 Change of permeate flux during UF runs (Ni system) examining the effect of S/M ratio (pH not adjusted) and pH value (S/M = 8.5).  $[\text{Ni}^{2+}]_f = 1 \text{ mM}$ ,  $\Delta P = 40 \text{ psi}$ ,  $T =$  room temperature

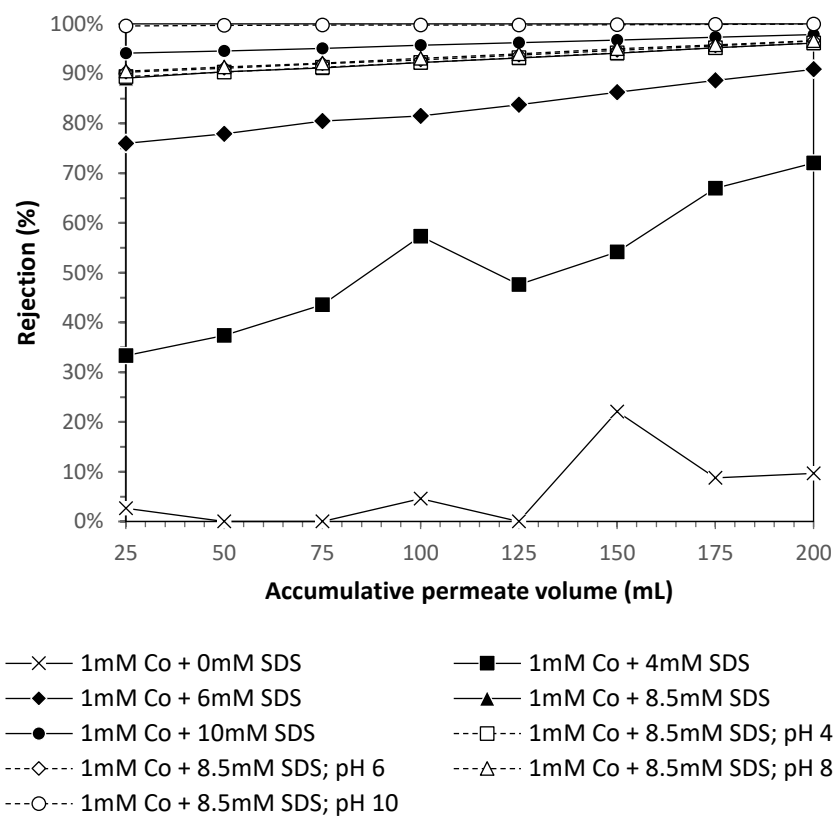


Figure 3-12 Change of rejection rate during UF runs (Co system) examining the effect of S/M ratio (pH not adjusted) and pH value (S/M = 8.5).  $[\text{Co}^{2+}]_f = 1 \text{ mM}$ ,  $\Delta P = 40 \text{ psi}$ ,  $T = \text{room temperature}$

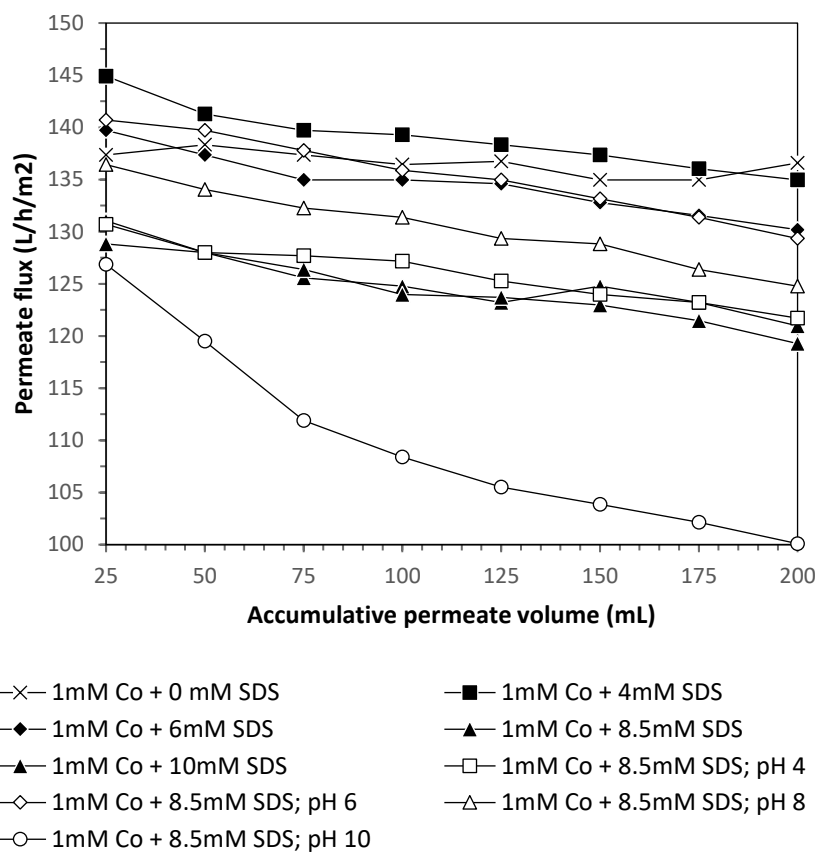


Figure 3-13 Change of permeate flux during UF runs (Co system) examining the effect of S/M ratio (pH not adjusted) and pH value (S/M = 8.5).  $[\text{Co}^{2+}]_f = 1 \text{ mM}$ ,  $\Delta P = 40 \text{ psi}$ ,  $T = \text{room temperature}$

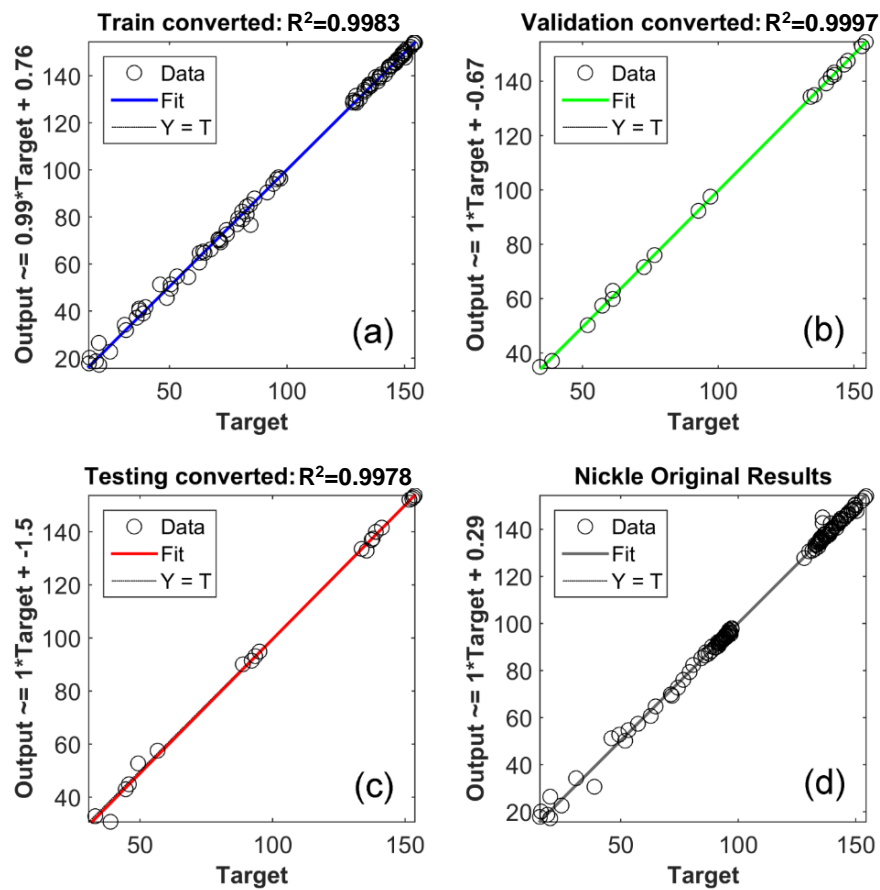


Figure 3-14 Comparison between ANN modeled (Output) and experimental (Target) results on the rejection rate and permeate flux for Ni system using (a) training, (b) validation, (c) testing, and (d) overall datasets

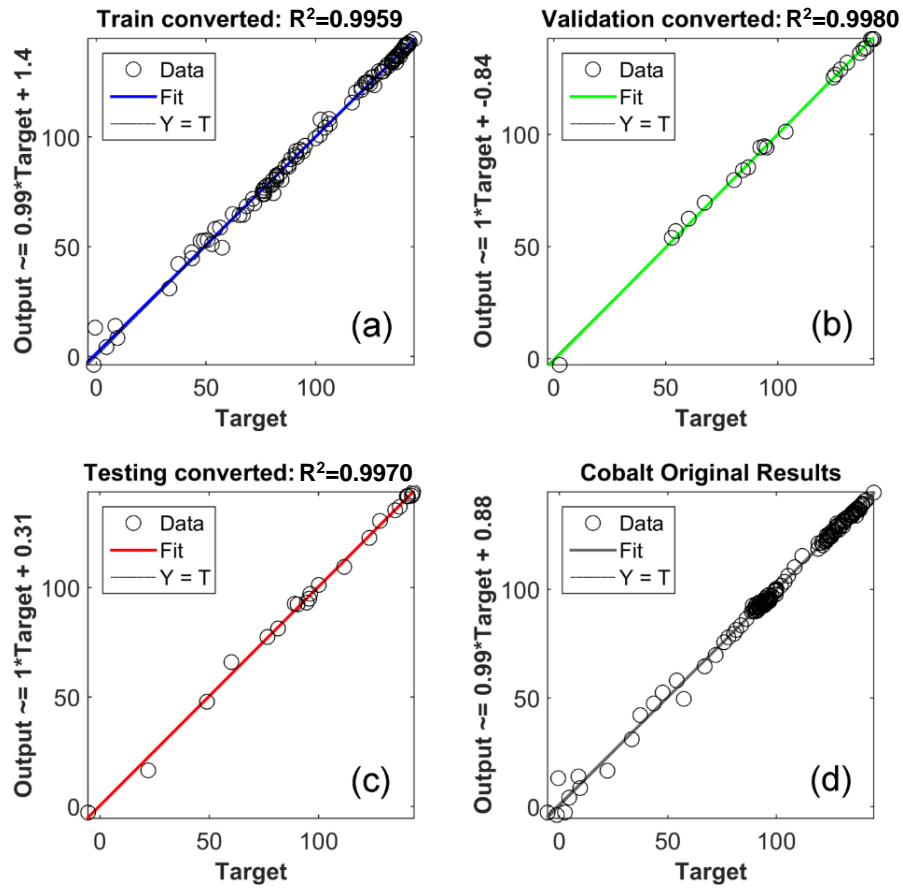
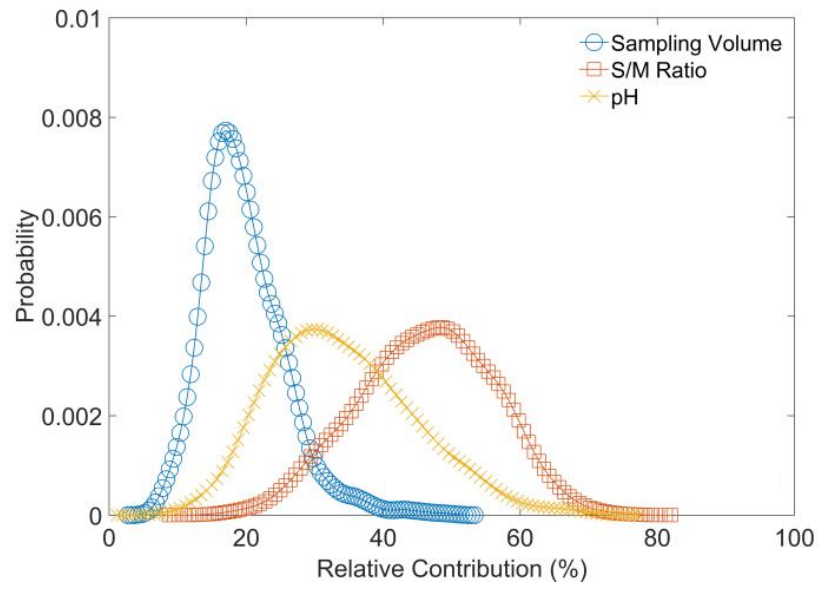


Figure 3-15 Comparison between ANN modeled (Output) and experimental (Target) results on the rejection rate and permeate flux for Co system using (a) training, (b) validation, (c) testing, and (d) overall datasets

(a)



(b)

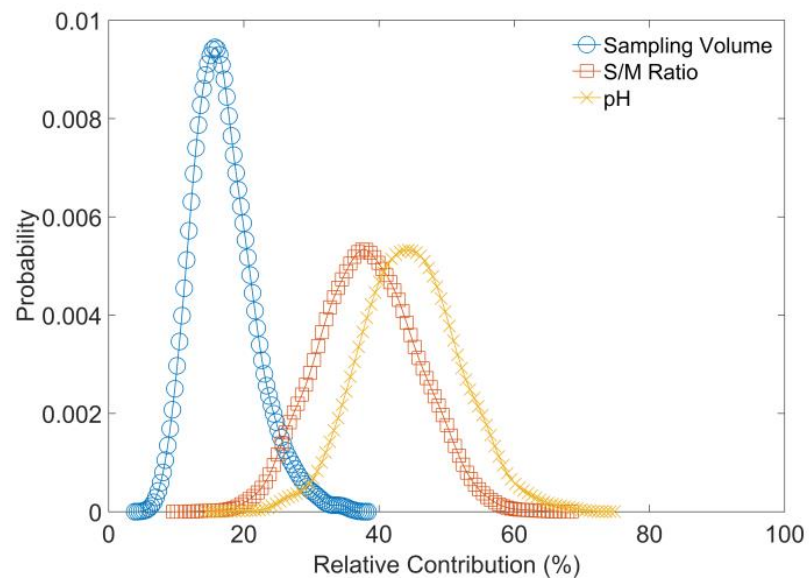
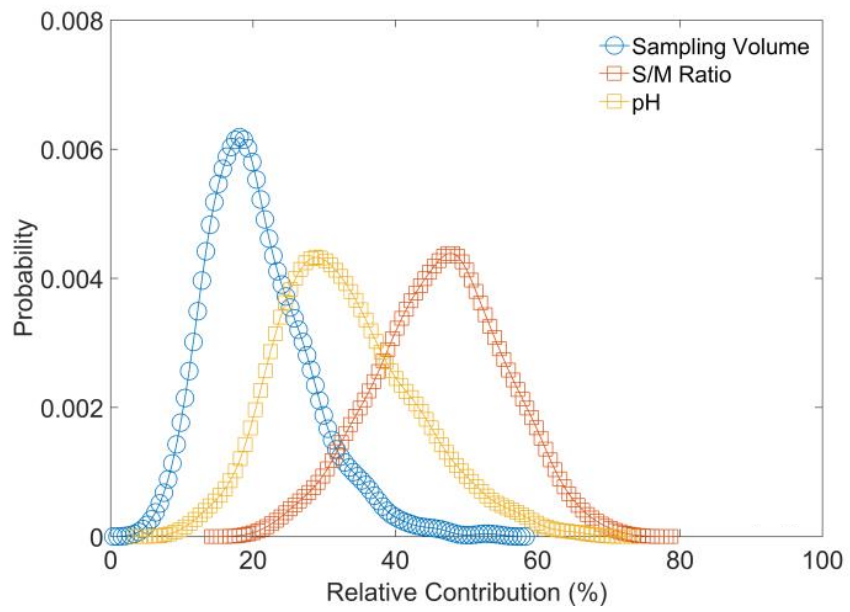


Figure 3-16 The relative contributions of sampling volume, S/M ratio, and pH to (a) rejection rate and (b) permeate flux for Ni system



(a)



(b)

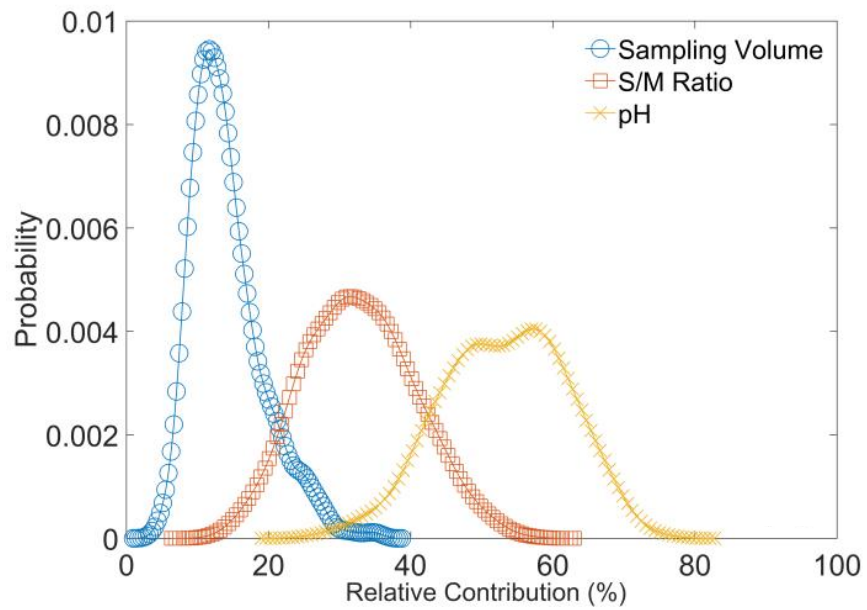


Figure 3-17 The relative contributions of sampling volume, S/M ratio, and pH to (a) rejection rate and (b) permeate flux for Co system

## **Chapter 4.**

### **Micellar-Enhanced Ultrafiltration to Remove Nickel: A Response Surface Method and Artificial Neural Network Optimization**

## 4.1. Introduction

Nickel is a common heavy metal generated from various industrial activities such as mining, electroplating, batteries manufacturing, metal finishing, and forging. It is carcinogenic, non-biodegradable, and could accumulate and persist in nature and living organisms (Fu and Wang, 2011; Tchounwou et al., 2012). Even at low concentrations, nickel can be toxic to the environment and humans. Conventional methods (e.g., chemical precipitation, adsorption, ion exchange, electrodialysis) when treating large-volume of aqueous solution containing low-concentration of heavy metals (e.g., nickel) can be challenged by secondary pollution of deposition, high cost, low selectivity, and difficulties of recycling metals (Xiarchos et al., 2008; Landaburu-Aguirre et al., 2010). Although membrane technologies such as reverse osmosis have been successfully used to remove metal ions from aqueous solution with high removal efficiency, their high operational and maintenance costs hinder their wider application. To overcome these drawbacks, micellar-enhanced ultrafiltration (MEUF) provides an alternative for heavy metal removal as it can achieve high removal rate and high permeate flux under mild conditions with lower energy costs (Tung et al., 2002). An MEUF integrates a surfactant, which with sufficient dose self-aggregates and forms micelles. The micelles then bind metal ions through electrostatic interactions and can be retained by a UF membrane (Huang et al., 2017).

Most MEUF studies for nickel removal used the conventional one-factor-at-a-time method, namely, to examine one operational variable while fixing the others. For example, Karate and Marathe (2008) examined the MEUF removal of nickel by testing a

series of factors individually: flow rate, surfactant to metal (S/M) ratio, pH, feed metal ion concentration, pressure, and presence of electrolytes. Tanhaei et al. (2014) investigated the MEUF removal of nickel using single and mixed surfactants. Similarly, they determined the optimum SDS and nickel concentrations by separately examining the effect of SDS concentration, nickel concentration, pressure, and pH. Danis and Aydiner (2009) examined the MEUF process performance in four stages, by changing surfactant concentrations, nickel concentrations, transmembrane pressure, and electrolyte content separately.

System optimization is important in engineering applications because it is directly related to costs. In MEUF studies, it is crucial to find an optimal operating condition that yields high rejection and high permeate flux simultaneously, with minimal dosages of surfactant and power consumption. Though easy to conduct, the one-factor-at-a-time method tend to involve much labor and resources (many experimental runs) for a multi-variable system, and does not provide adequate information on factor interactions or estimate the effects (Czitrom, 1999). Besides, the method is difficult to find a true optimal condition with a reasonable number of experimental runs. These limitations can be avoided by using a more systematic experimental method, such as a response surface methodology (RSM). RSM is an experiment- and statistic-based technique that involves multiple factors and their interactions to optimize a process (Montgomery, 2017). It has been increasingly used in environmental studies, such as to optimize the process condition for wastewater treatment (Ahmadi et al., 2005; Kiran et al., 2007; Körbahti et al., 2007; Wang et al., 2007; Chavalparit and Ongwandee, 2009; Sadri Moghaddam et al., 2010; Zhu et al., 2011). However, only a few attempts of MEUF have been made to

remove heavy metals using the RSM method, mostly focusing on copper, cadmium, and zinc (Xiarchos et al., 2008; Landaburu-Aguirre et al., 2009). Reports on RSM-based nickel removal using MEUF were rare.

Further, computer modeling can be integrated to describe a complex input-output relationship of a given system. Such approaches are suitable for uncertain or approximate reasoning when the systems are complex to describe with a mathematical model. Table 4-1 summarizes the MEUF studies integrating RSM and other optimization models. In recent years, artificial neural network (ANN) has been developed to understand non-linear multi-variable systems (Desai et al., 2005). ANN has been used in many fields of science and engineering (e.g., Kasiri et al., 2008; Yi et al., 2007; Zhang et al., 2016) but extremely limited in MEUF studies. The integration of ANN to RSM can provide additional information of the process behavior (Balkin and Lin, 2000), but research efforts in MEUF are scarce (Table 4-1). These studies examined the removal of lead and zinc from cross-flow UF systems, mostly conducted by the same researcher. Though the cross-flow operation could better scale-up to industrial application, most laboratory MEUF studies were carried out under batch operation. The removal of nickel ions from the common dead-end UF system is desired.

This chapter examines the process of MEUF to remove nickel ions from dilute aqueous streams. The objectives are to (1) optimize MEUF process conditions using RSM, (2) predict the maximum nickel removal and flux rate under optimal conditions, and (3) verify RSM results using ANN modeling.

Table 4-1 Summary of MEUF studies integrating RSM and other optimization models

<b>Solute</b>	<b>UF system (surfactant and flow</b>	<b>RSM design</b>	<b>Independent variables</b>	<b>Optimization model</b>	<b>References</b>
Pb <sup>2+</sup>	MEUF (SDS), cross-flow	BBD (3 factors and 3 levels)	C <sub>SDS</sub> , S/M, pH	ANN and ANFIS	(Rahmanian et al., 2012a)
Zn <sup>2+</sup>	MEUF (SDS and Brij-35), cross-flow	FFD (7 factors)	Pressure, pH, C <sub>SDS</sub> , S/M, L/M, C <sub>NaCl</sub> , Brij35/SDS ratio	ANN ( $R^2 >$ 0.91)	(Rahmanian et al., 2011b)
Pb <sup>2+</sup>	MEUF (SDS), cross-flow	BBD (3 factor, 3 levels)	C <sub>SDS</sub> , S/M, pH	Fuzzy logic models ( $R >$ 0.91)	(Rahmanian et al., 2011a)
Pb <sup>2+</sup>	MEUF (SDS), cross-flow	BBD (3 factors, 3 levels)	C <sub>SDS</sub> , S/M, pH	Fuzzy logic	(Jana et al., 2018)

ANFIS = adaptive neuro-fuzzy inference system; ANN = artificial neural network; BBD = Box-Behnken Design; CCD = central composite design; CCF = face centered composite design; FFD = full factorial design

## **4.2. Material and Methods**

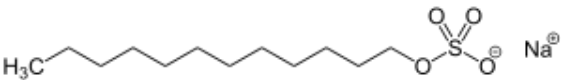
### **4.2.1. Materials**

All chemicals were of analytical grade and were used as received. The anionic surfactant sodium dodecyl sulfate (SDS, 20% in H<sub>2</sub>O) was purchased from Sigma-Aldrich, Canada. Its properties are listed in Table 4-2. Nickel sulfate hexahydrate (NiSO<sub>4</sub>·6H<sub>2</sub>O, J.T. Baker) were used as the source of nickel ions. The pH of feed solutions was adjusted to 8 ± 0.1. Nickel reference standard solution (1000 ppm ± 1%, certified) for Flame Atomic Absorption (FAA) tests was purchased from Fisher Scientific and diluted as needed. Distilled water was used in all experimental procedures. Permeate samples were collected and stored using sorption-free materials.

### **4.2.2. Dead-end ultrafiltration experiments**

The UF experiment setup follows the description in 3.2.2. Batch experiments were conducted in a stirred UF Cell (Amicon Model 8400, EMD Millipore) with a maximum volume uptake of 400 mL. Regenerated cellulose membrane (EMD Millipore, Canada) was used, with 3, 5, and 10 kDa MWCO (diameter of 76 mm and effective area of 0.00418 m<sup>2</sup>). An initial 250-mL feed solution was filled and continuously stirred (at a constant rate to get effective agitation and prevent membrane fouling) in each experimental run. All experiments were conducted at room temperature (23 ± 1 °C). The applied transmembrane pressure was controlled by pressurized nitrogen gas.

Table 4-2 Properties of the surfactant used in this study

Properties	Specifications
Name	Sodium dodecyl sulfate (SDS)
Chemical structure	 <chem>CCCCCCCCCCCCOS(=O)(=O)[O-].[Na+]</chem>
Ionic type	Anionic
Molecular weight	288.38 g/mol
Critical micellar concentration (CMC)	8.2-8.3 mM



In each UF run, 250 mL of feed solution was prepared with desired nickel and surfactant concentrations. When a UF run starts, the first 10-mL sample was discarded, then every 20-mL permeate was sampled. The run was terminated when successive five samples were collected and timed. Nickel concentrations of the permeate samples were measured, and their permeate fluxes and rejection rates were determined. For both rejection rate and permeate flux, the average values of five permeate samples for each experimental run were calculated and used as inputs for RSM and ANN modeling. The membrane was cleaned after each run to recover its permeability (indicated by the flux rate of distilled water measured at 40 psi) and can be repeatedly used if over 90% of the original water flux (i.e., flux of distilled water passing the clean membrane at 40 psi) was recovered. Pretreatment of sampling apparatus, storage of samples, and recovery of membranes followed the procedures described by Lin et al. (2017).

#### **4.2.3. Sample and data analysis**

The nickel concentration in permeate samples ( $C_p$ ) was measured using a Varian Model 55B SpectrAA FAA Spectrophotometer at 232.0 nm. The mean values of triplicate measurements for each permeate sample were calculated (%RSD  $\leq$  1.3%). FAA calibration curves were made before each set of measurement ( $R^2 > 0.999$ ).

To evaluate the efficiency of nickel removal using MEUF, the nickel rejection rate (R) and permeate flux (J) were calculated as follows:

$$R(\%) = \left(1 - \frac{C_p}{C_r}\right) \times 100 \quad (4-1)$$

where  $C_p$  and  $C_r$  denote the nickel concentration in the permeate and retentate, respectively.  $C_r$  was calculated using material balance.

$$J(L/h/m^2) = \frac{V_p}{t \times A_m} \quad (4-2)$$

where  $V_p$  is the volume of the permeate sample;  $t$  is the sampling time; and  $A_m$  is the effective area of the membrane.

#### **4.2.4. Response surface modeling**

The RSM modeling and optimization consist of the following steps: (1) statistically design the experiment, where all process variables vary simultaneously over experimental runs; (2) define coefficients of variables (and their interactions) in the mathematical model based on experimental results; (3) check the adequacy of the regressed model; and (4) predict the optimal experimental condition and response using the model.

##### **4.2.4.1. Design of experiments**

In this study, an RSM model based on Box-Behnken design (BBD) was used to optimize the four independent variables (factors) and to observe their effect on MEUF performance in terms of rejection rate and permeate flux. A BBD design entails factors at high (+1), basic (0), and low (-1) levels. The center points (coded level 0 or the basic level), which were the midpoints between the high and low levels, were repeated multiple times. Table 4-3 presents the factors and levels set by the BBD design. The design consists of 29 experimental runs, including 5 replicates of the central experiments to check the analysis repeatability and to estimate the experimental error. The responses (rejection rate and

permeate flux) were determined experimentally according to designed runs. Design-Expert (version 11.1) was used for RSM modeling.

#### 4.2.4.2. Response surface method (RSM) modeling

To determine the mathematical relationship between the responses and factors the following second-order polynomial equation was used to fit the experimental data obtained from the BBD experimental design. The response surface model includes the main, quadratic, and interactions terms:

$$Y = b_0 + \sum_{i=1}^n b_i X_i + \sum_{i=1}^n b_{ii} X_i^2 + \sum_{i=1}^{n-1} \sum_{j=i+1}^n b_{ij} X_i X_j \quad (4-3)$$

where Y is the predicted response;  $b_0$  the constant coefficient;  $b_i$  the linear coefficients;  $b_{ii}$  the quadratic coefficients;  $b_{ij}$  the interaction coefficients; n the number of design variables; and  $X_i, X_j$  the coded levels of design variables.

Table 4-3 Factors and levels set by Box-Behnken design (BBD)

<b>Factors</b>	<b>Levels</b>		
	<b>Minimum (-1)</b>	<b>Center (0)</b>	<b>Maximum (+1)</b>
(A) Pressure (psi)	30	40	50
(B) Feed Ni <sup>2+</sup> concentration (mM)	0.5	1.25	2
(C) Feed SDS concentration (mM)	8.3	16.6	24.9
(D) Molecular weight cut-off, or MWCO (kDa)	3	5*	10

\* the center point 5 kDa MWCO was used instead of 6.5k Da due to the size availability of commercial membranes

Stepwise regression procedure was performed using backward elimination method to exclude non-significant terms ( $p$ -values  $> 0.05$ ) from the initial response surface model. The regression coefficients of the reduced model are computed by the multiple linear regression (MLR) method to minimize the sum of square of the residuals. The validity of the empirical model was tested using analysis of variance (ANOVA) at the 95% confidence level. The fitted model was assessed by the R-squared ( $R^2$ ), the adjusted R-squared ( $R^2$ -adj), and the predicted R-squared ( $R^2$ -pre). The  $R^2$  value increases with the number of model terms, even when non-significant terms are added to the model. Therefore, the  $R^2$  value of a refined model is usually smaller than that of the full model. The  $R^2$ -adjusted coefficient is used to adjust to the number of model terms, where the addition of non-significant terms usually decreases the  $R^2$ -adjusted value. The predicted R-squared shows how well a model predicts responses for new observations. Based on the obtained response surface models, optimal conditions were determined by maximizing the nickel rejection and the permeate flux.

#### **4.2.5. Artificial neural network (ANN) modeling**

The BBD design (factors and levels) and the corresponding responses were used to develop the ANN model, using the neural network toolbox for MATLAB 2016b. An ANN model with one hidden layer was trained to simulate nickel removal by MEUF. The inputs were pressure, feed nickel concentration, feed SDS concentration, and MWCO, whereas the outputs were rejection rate and permeate flux. All inputs and outputs were normalized into the range of [0, 1] to avoid putting too much weight on variables with a large variance. Twelve neurons in the hidden layer were optimized for the ANN model

following Jing et al. (2014). Datasets were randomly divided into training (70%), validation (15%), and testing (15%) subsets. The model was trained by minimizing the mean squared error (MSE) while maximizing the correlation coefficients ( $R$ ) between the experimental and modeling outputs. The two outputs, i.e., rejection rate and permeate flux, were given equal weightings when calculating  $R^2$  for the ANN model. For comparison purposes, an inverse range scaling was performed on all modeling outputs to transfer them from  $[0, 1]$  to their original scales.

### **4.3. Results and Discussion**

#### **4.3.1. Ultrafiltration experimental results**

Experimental results (i.e., nickel rejection rates and permeate flux) of the BBD design are reported in Table 4-4. The maximum rejection rate of nickel is 98.70% (flux = 23.03 L/s·m<sup>2</sup>) in run 17, with a transmembrane pressure of 30 psi, nickel concentration of 1.25 mM, SDS concentration of 16.6 mM, and MWCO of 3 kDa. The maximum flux 178.28 L/s·m<sup>2</sup> ( $R = 91.83\%$ ) was found in run 26 with 50 psi pressure, 1.25 mM nickel, and 16.6 mM SDS using membrane MWCO of 10 kDa. It can be seen that higher rejection (or flux) tend to compromise on lower flux (or rejection), yet in practice high values of both rejection (indicates MEUF effectiveness) and flux (indicates efficiency) are desired. As such, an operating condition generating high rejection and flux is needed.

Table 4-4 Design layout and experimental results of the BBD design

Std.	Run	Factor input variables				Response variable	
		Factor A Pressure (psi)	Factor B Ni conc. (mM)	Factor C SDS conc. (mM)	Factor D MWCO (kDa)	Rejection <sup>a</sup> (%)	Flux <sup>a</sup> (L/s·m <sup>2</sup> )
13	1	40	0.5	8.3	5	94.86	37.93
18	2	50	1.25	8.3	5	92.98	45.15
25	3	40	1.25	16.6	5	98.13	36.83
7	4	40	1.25	8.3	10	94.30	158.67
29	5	40	1.25	16.6	5	97.09	37.43
20	6	50	1.25	24.9	5	98.13	43.31
6	7	40	1.25	24.9	3	97.15	29.96
19	8	30	1.25	24.9	5	98.17	28.74
22	9	40	2	16.6	3	97.98	31.03
23	10	40	0.5	16.6	10	97.76	148.64
14	11	40	2	8.3	5	88.06	37.41
10	12	50	1.25	16.6	3	98.67	38.25
3	13	30	2	16.6	5	96.15	29.27
28	14	40	1.25	16.6	5	96.59	39.51
11	15	30	1.25	16.6	10	97.84	115.56
27	16	40	1.25	16.6	5	96.32	37.78
9	17	30	1.25	16.6	3	98.70	23.03
26	18	40	1.25	16.6	5	96.47	36.45

Std.	Run	Factor input variables				Response variable	
		Factor A Pressure (psi)	Factor B Ni conc. (mM)	Factor C SDS conc. (mM)	Factor D MWCO (kDa)	Rejection <sup>a</sup> (%)	Flux <sup>a</sup> (L/s·m <sup>2</sup> )
8	19	40	1.25	24.9	10	80.53 <sup>b</sup>	149.23
4	20	50	2	16.6	5	95.70	45.36
2	21	50	0.5	16.6	5	95.08	46.16
17	22	30	1.25	8.3	5	91.31	28.78
16	23	40	2	24.9	5	98.20	35.00
21	24	40	0.5	16.6	3	98.40	29.10
1	25	30	0.5	16.6	5	90.43 <sup>b</sup>	30.19
12	26	50	1.25	16.6	10	91.83	178.28
15	27	40	0.5	24.9	5	96.94	35.67
24	28	40	2	16.6	10	93.53	138.17
5	29	40	1.25	8.3	3	92.61	28.96

<sup>a</sup> Rejection/flux values of a UF run are the mean values of rejection/flux of all permeate samples (n=5) in that UF run

<sup>b</sup> Observed outliers; eliminated from analysis



#### 4.3.2. RSM models

Goodness-of-fit of the regression model is evaluated using ANOVA by testing the significance of the regression model, significance of individual model coefficients, and lack-of-fit. For both rejection and flux models the assumptions for ANOVA are met, e.g., the residuals are normally and randomly distributed (figures not shown). Tables 4-5 and 4-6 summarize the ANOVA analysis for rejection and flux, respectively, showing the goodness-of-fit of the quadratic models. The regression models for nickel rejection and permeate flux are statistically significant at the 95% confidence level in the studied range.

The significance of the model on rejection rate was determined by Fisher test, indicated by the F-value. The model F-value of 12.61 indicates that the model is significant, with a 0.01% chance that an F-value could occur due to noise. The lack-of-fit F-value of 3.46 indicates that there is a 12% chance that an F-value could occur due to noise. The calculated  $R^2$  (0.8486) and adjusted  $R^2$  (0.7813) was reasonably close to 1, showing good fitness of the regressed model. The difference between predicted  $R^2$  and the adjusted  $R^2$  is over 0.02. This may due to the close values of the response (which can be sensitive to experimental and measurement errors).

The flux model shows great fitness. The model F-value of 2171.32 indicates that the model is highly significant, with only 0.01% chance that the value could occur due to noise. Non-significant lack-of-fit ( $p = 0.4387$ ) also indicates good fitness of the model. Both  $R^2$  (0.9972) and adjusted  $R^2$  (0.9968) show good fitness of the regressed model. High predicted  $R^2$  (0.9958) indicates that the model can well predict response for new observations.

Table 4-5 ANOVA for reduced quadratic model (response: rejection)

Source	Sum of Squares	df	Mean Square	F-value	p-value	
<b>Model</b>	158.79	8	19.85	12.61	< 0.0001	significant
A-Pressure	12.24	1	12.24	7.78	0.0121	
B-C-Ni	10.51	1	10.51	6.68	0.0187	
C-C-SDS	17.18	1	17.18	10.92	0.0039	
D-MWCO	13.18	1	13.18	8.37	0.0097	
AD	12.10	1	12.10	7.69	0.0125	
BC	16.26	1	16.26	10.33	0.0048	
CD	7.33	1	7.33	4.66	0.0447	
C <sup>2</sup>	27.39	1	27.39	17.40	0.0006	
<b>Residual</b>	28.33	18	1.57			
Lack of Fit	26.16	14	1.87	3.46	0.1200	not significant
Pure Error	2.16	4	0.5409			
<b>Cor Total</b>	187.12	26				

Fit statistics: R<sup>2</sup>=0.8486, Adjusted R<sup>2</sup>=0.7813, Predicted R<sup>2</sup> = 0.4481

df = degree of freedom

Table 4-6 ANOVA for reduced quadratic model (response: flux)

Source	Sum of Squares	df	Mean Square	F-value	p-value	
<b>Model</b>	10.68	4	2.67	2173.32	< 0.0001	significant
A-Pressure	0.5914	1	0.5914	481.41	< 0.0001	
C-C-SDS	0.0033	1	0.0033	2.67	0.1151	
D-MWCO	7.65	1	7.65	6229.95	< 0.0001	
D <sup>2</sup>	0.3832	1	0.3832	311.97	< 0.0001	
<b>Residual</b>	0.0295	24	0.0012			
Lack of Fit	0.0256	20	0.0013	1.31	0.4387	not significant
Pure Error	0.0039	4	0.0010			
<b>Cor Total</b>	10.71	28				

Data were transformed into natural log

$R^2 = 0.9972$ , Adjusted  $R^2 = 0.9968$ , Predicted  $R^2 = 0.9958$

### ***Regression model for nickel rejection***

Significant model terms ( $p < 0.05$ ) are coded factors A, B, C, D, AD, BC, CD, and  $C^2$ .

The reduced regression model (coded factors) for nickel rejection was determined as:

$$\begin{aligned} \text{Rejection} = & 96.48 - 1.15 A - 0.99 B + 1.77 C - 1.17 D \\ & - 1.65 AD + 2.02 BC - 1.84 CD - 2.17 C^2 \end{aligned} \quad (4-4)$$

where coded factor subject to the level of (-1,1)

The regressed model in terms of actual factors is:

$$\begin{aligned} \text{Rejection} = & 80.35 + 0.19 \text{ Pressure} - 6.69 C_{\text{Ni}} + 1.26 C_{\text{SDS}} + 2.60 \text{ MWCO} \\ & - 0.05 (\text{Pressure})(\text{MWCO}) + 0.32 C_{\text{Ni}} C_{\text{SDS}} - 0.06 (C_{\text{SDS}})(\text{MWCO}) \\ & - 0.03 (C_{\text{SDS}})^2 \end{aligned} \quad (4-5)$$

where factors subjected to:  $30 \leq \text{pressure} \leq 50$  psi,  $0.5 \leq C_{\text{Ni}} \leq 2$  mM,  $8.3 \leq C_{\text{SDS}} \leq 24.9$  mM,  $3 \leq \text{MWCO} \leq 10$  kDa. Equations 4-4 and 4-5 can be used to predict the nickel rejection for given levels of each factor.

The coefficients of coded factors indicate that the importance of the factor is in the order:  $BC > CD > C > AD > D \approx A > B$ , i.e., interaction of nickel concentration and SDS concentration  $>$  interaction of SDS concentration and MWCO  $>$  SDS concentration  $>$  interaction of pressure and MWCO  $>$  MWCO  $\approx$  pressure  $>$  nickel concentration.

### ***Regression model for permeate flux***

Table 4-6 shows that A, D, AD,  $A^2$ ,  $D^2$  are significant model terms. The final equation in terms of coded factors is:

$$\ln(\text{Flux}) = 3.89 + 0.22 A - 0.02 C + 0.80 D + 0.30 D^2 \quad (4-6)$$

where coded factor subject to the level of (-1,1)

Final equation in terms of actual factors is:

$$\ln(\text{Flux}) = 2.59 + 0.02 \text{ Pressure} - 0.002 C_{\text{SDS}} - 0.09 \text{ MWCO} + 0.024 (\text{MWCO})^2 \quad (4-7)$$

where factors subjected to:  $30 \leq \text{pressure} \leq 50$  psi,  $0.5 \leq C_{\text{Ni}} \leq 2$  mM,  $8.3 \leq C_{\text{SDS}} \leq 24.9$  mM,  $3 \leq \text{MWCO} \leq 10$  kDa

The importance of factors is:  $D > A > C$ , i.e.,  $\text{MWCO} > \text{pressure} > C_{\text{SDS}}$ .

#### **4.3.3. Effect of factors on rejection rate and permeate flux**

The response surface plots show the effect of pressure, nickel concentration, SDS concentration, and MWCO on rejection rate and permeate flux. The response surface and contour plot enable visualization of parameter interaction. Based on the ANOVA results, three interaction effect (i.e., pressure and MWCO, feed nickel and SDS concentration, feed SDS concentration and MWCO) on rejection rate and three individual effect (i.e., pressure, feed SDS concentration and MWCO) on flux will be discussed.

##### **4.3.3.1. Effect of factors on rejection**

ANOVA results indicate significant interaction effect between pressure and MWCO on rejection. Figure 4-1 shows the effect of pressure and MWCO on rejection, when feed nickel and SDS concentrations were fixed at their central levels. Pressure seems to affect the rejection rate more at higher MWCO than the lower end. The rejection rate was relatively stable with the increase of pressure at MWCO of 3 kDa but considerably dropped at MWCO of 10 kDa (Figure 4-1a). Previous one-factor-at-a-time studies showed that pressure alone had a small effect on the rejection rate. For example, Huang et al. (2016b) examined the rejection under a transmembrane pressure of 40 to 800 kPa and found that pressure did not significantly change the rejection rate. Mulligan et al.

(2011) reported similar conclusions for a pressure range from 30 to 140 kPa. This observation can be explained that because the pressure does not affect the interaction between metal ions and the surfactant but mainly provides a driving force for mass transport across the membrane.

In terms of MWCO, smaller MWCO tend to generate higher rejection (Figure 4-1 and Figure 4-3). The observation is in agreement with previous findings. For example, Baek and Yang (2004c) reported higher chromate rejection (>99%) using membrane MWCO of 3 kDa than that of 10 kDa (98%). Bade and Lee (2008) reported 98% rejection of chromate using CPC with 100 kDa membrane and 97% with 300 kDa membrane.

Figure 4-2 shows the predicted response under different metal and surfactant concentrations, when the pressure and MWCO were fixed as their central values. It can be seen that, at lower SDS concentration (1 CMC), low metal concentrations result in high rejection rate. At higher nickel concentration, the decrease in rejection might be attributed to a lack of available binding sites. To sum up, MEUF is more efficient to treat dilute (i.e., low concentration) nickel streams, showing an advantage to traditional techniques (e.g., precipitation) that are inefficient at dilute streams. Alternatively, MEUF could be used as a secondary treatment method.

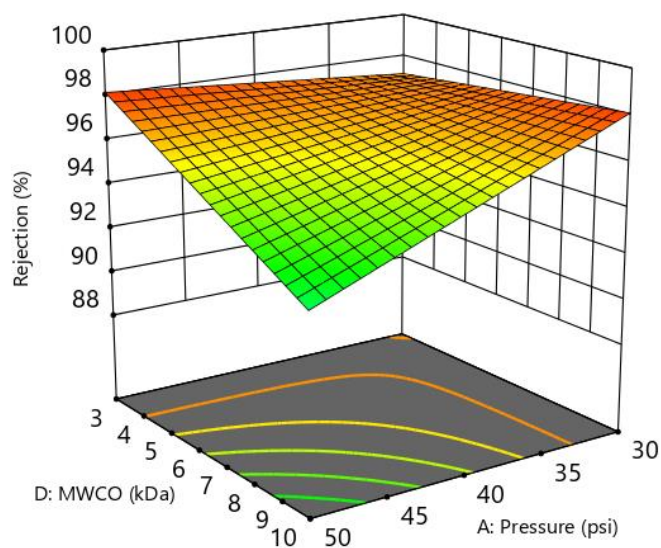
In the examined concentration range, higher SDS concentration resulted in higher rejection of nickel ions. When SDS concentration increased to approximately 20 mM no further increase in rejection is observed. Therefore, increasing the SDS feed concentration enhances the rejection of heavy metals until certain limits. The maximum rejection might be due to the competition between the surfactant sodium ions and nickel ions. The electrostatic interaction between the anionic micellar surface and nickel cations depends

on the ion charge and concentration. At first, when increasing the SDS feed concentration, a higher fraction of surfactants will be in the micellar form. This will increase the surface charge; hence more divalent nickel ions will be adsorbed on the micellar surface displacing the sodium ions. This ion exchange will consequently enhance heavy metal rejection. However, at low heavy metal feed concentration, when SDS concentration is further increased to concentration up to 20 mM, the sodium counter ion concentration might increase to an extent that the adsorption of sodium counter ions is favored. Therefore, no further increase in nickel rejection is achieved, as shown in Figure 4-2a and Figure 4-3a.

#### 4.3.3.2. Effect of factors on flux

Pressure, SDS concentration, and MWCO significantly contribute to the flux rate. When the pressure was increased from 30 to 50 psi, the permeate flux rate increased. The permeate flux follows the Darcy's law (Kamble and Marathe, 2005), i.e.,  $J = L_p \times \Delta P$ , where the membrane permeability  $L_p = 1/(\eta \cdot R_M)$ , where  $\eta$  is the viscosity of the solution and  $R_M$  is the membrane resistance. If the permeate flux linearly increases with pressure, the separation process is under the pressure controlled region, where the concentration polarization is negligible (Landaburu-Aguirre et al., 2010). This linear relationship was observed in the present study (figure not shown), indicating that concentration polarization was not obvious and the membranes performed well.

(a)



(b)

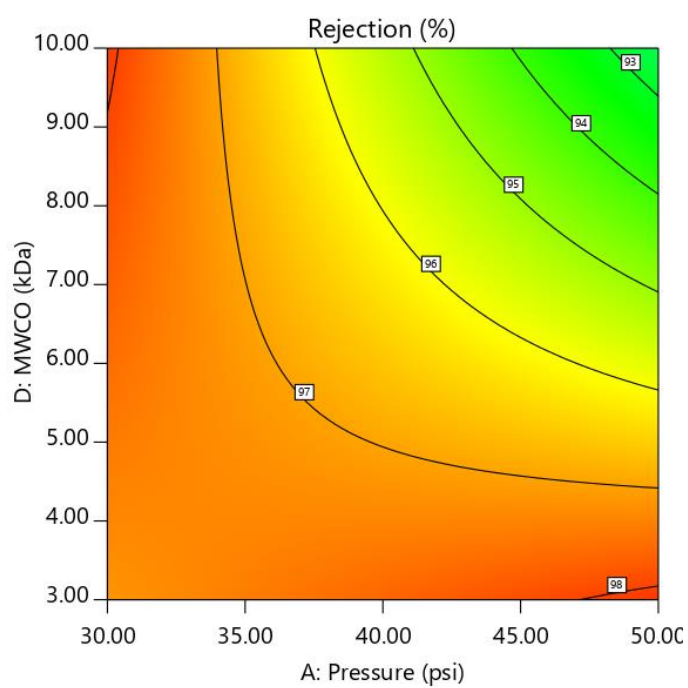
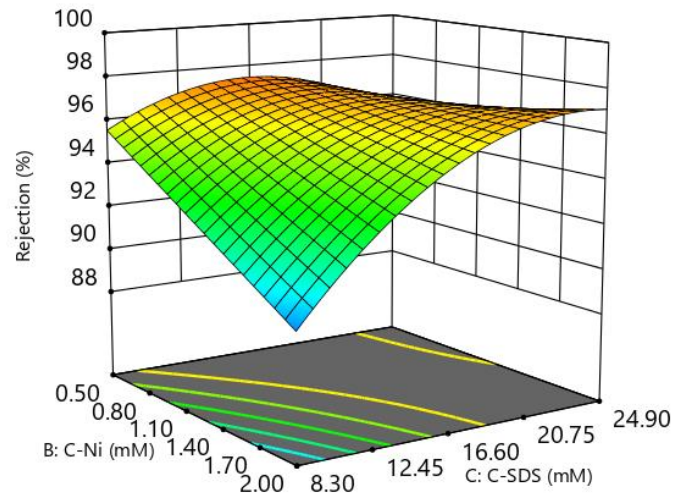


Figure 4-1 Response surface (a) and contour (b) showing the effect of pressure and MWCO on rejection rate.  $C_{Ni}=1.25\text{mM}$ ,  $C_{SDS}=16.6\text{mM}$



(a)



(b)

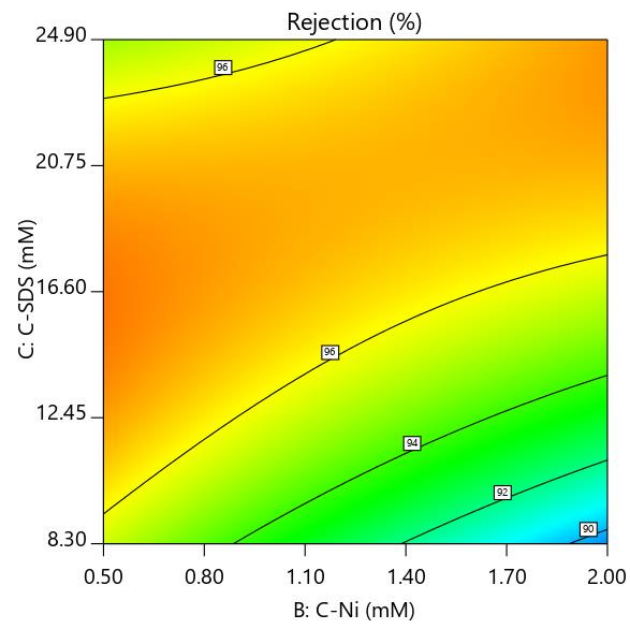
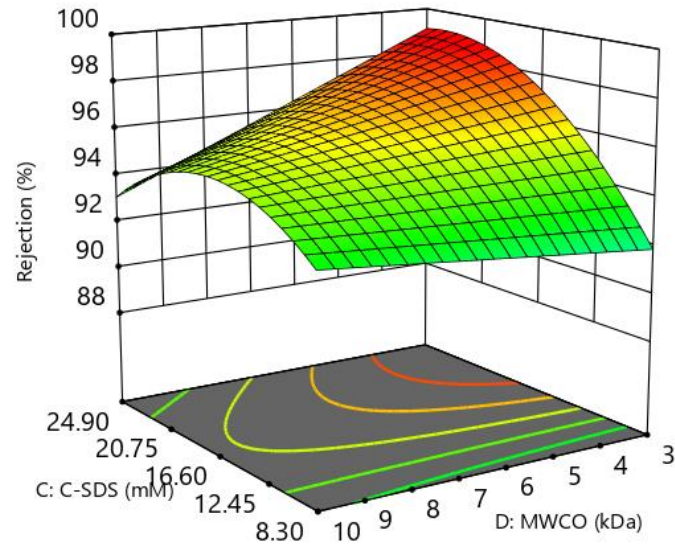


Figure 4-2 Response surface (a) and contour (b) showing the effect of nickel and SDS concentrations on rejection rate. Pressure = 40 psi, MWCO = 5 kDa.

(a)



(b)

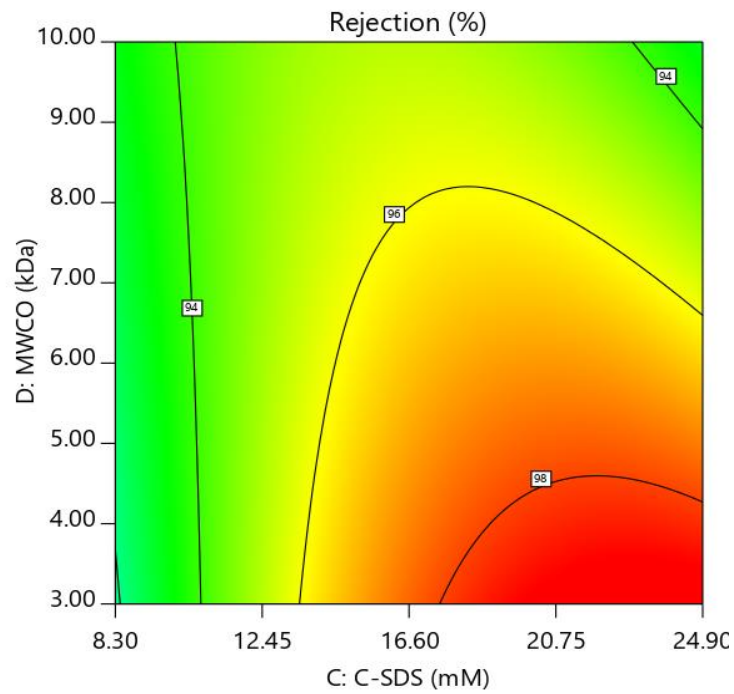


Figure 4-3 Response surface (a) and contour (b) showing the effect of SDS concentration and MWCO on rejection rate. Pressure = 40 psi,  $C_{Ni} = 1.25$  mM

SDS concentration was found negatively and linearly related to the flux rate. Increasing amount of SDS forms more SDS micelles which are retained by the membrane. The retained micelles may concentrate on the membrane surface or in its pores, hence reducing the permeate flux. The decrease of flux rate with the increase of surfactant concentration has been reported in literature (Kamble and Marathe, 2005). In addition, nickel concentration seems to have little effect on flux. This can be explained by the small size of nickel ions which can easily pass the ultrafiltration membrane.

Higher MWCO (i.e., bigger pore size) of the membrane increases the permeate flux. Nonlinear relationship between MWCO and flux was observed. Flux rate gradually increases with MWCO in its lower ranges (3-7 kDa) and quickly increase at higher ranges (7-10 kDa).

#### **4.3.4. RSM optimization**

The economic operation of the membrane processes draws attention to achieve lower costs in practice. As such, the use in lower transmembrane pressures (minimize pressure) of the selected membrane application, lower dosage of surfactant (minimize  $C_{SDS}$ ), and effective treatment of large volumes of water (maximize flux rate) is desired, as well as obtaining the high efficiency in removing nickel ions (maximize rejection).

Optimal conditions of the MEUF of nickel was obtained using the desirability function approach in Design Expert. The condition was found by maximizing rejection and flux (defined by equations 6 and 8, respectively) when setting minimum pressure,  $C_{Ni} = 1$  mM, minimum  $C_{SDS}$ , and  $3 \leq MWCO \leq 10$  kDa. The predicted maximum rejection rate (major response) and flux (secondary response) are 98.16% and 119.20 L/s·m<sup>2</sup>,

respectively, where pressure = 30 psi,  $C_{Ni} = 1.0$  mM,  $C_{SDS} = 10.05$  mM, and MWCO = 10 kDa.

#### **4.3.5. ANN modeling**

To predict the values of rejection rate and permeate flux using the ANN model, 75% of the data were randomly used for training purpose. The remainders were categorized as testing and validation data. In order to evaluate the ANN model, the model was presented with new values of rejection and flux that were not used during the training. The rejection and flux values estimated by ANN models were then compared with their corresponding actual values. The scatter regression plots of the ANN model predicted values against the experimental rejection and flux values for nickel removal are shown in Figure 4-4 and Figure 4-5, respectively. Due to the inverse rescaling, two outputs, i.e., rejection rate and permeate flux, were first converted from [0,1] and then plotted together within their original ranges. The best linear fit equations for the training, validation, testing, and overall subsets all had a slope between 0.99 and 1, and the values of  $R^2$  were all higher than 0.99 (except for the testing values for rejection model,  $R^2 = 0.719$ ), indicating a close match between the experimental and modeling results. Therefore, the trained ANN model was able to accurately simulate the rejection rate and permeate flux for nickel removal process.

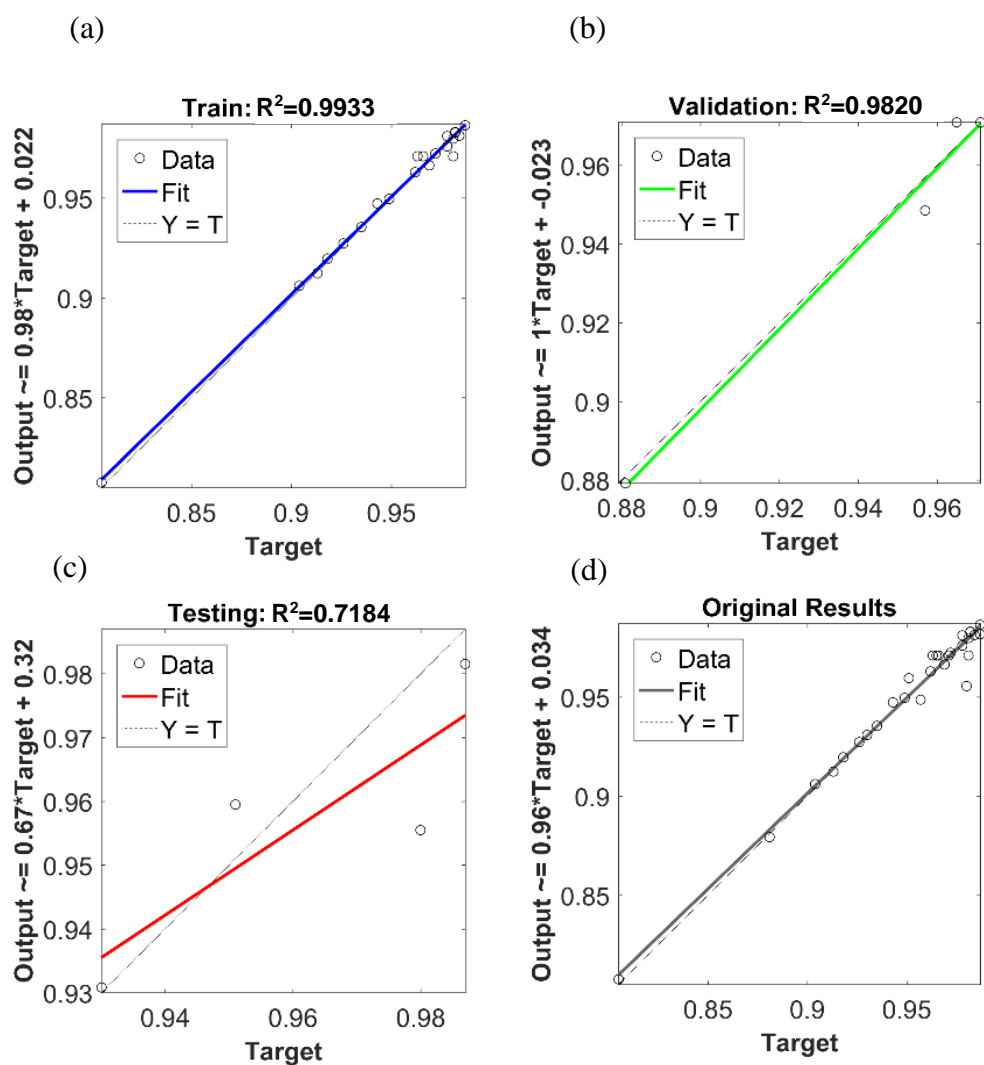


Figure 4-4 The scatter plots of ANN model predicted values (rejection rate of nickel ions) versus experimental values for (a) training, (b) validation, (c) testing, and (d) all data sets

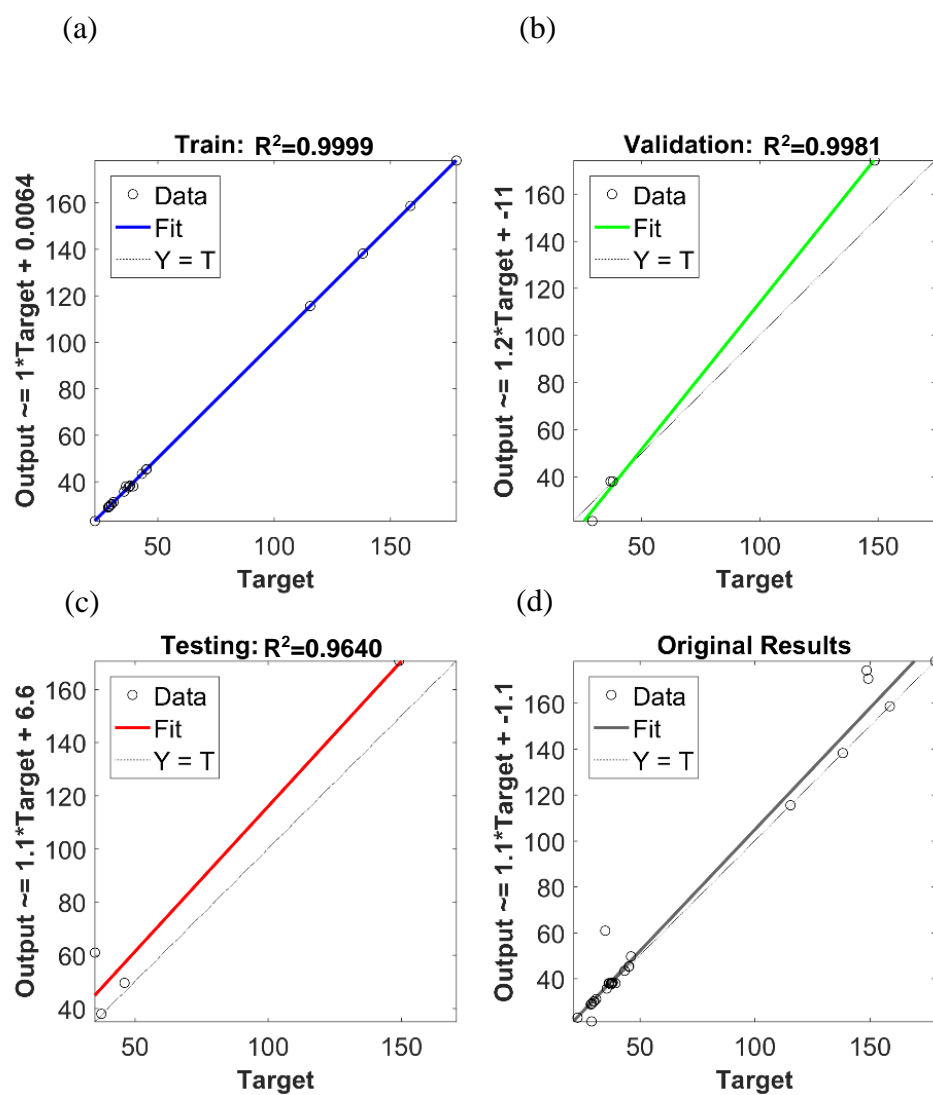


Figure 4-5 The scatter plots of ANN model predicted values (permeate flux) versus experimental values for (a) training, (b) validation, (c) testing, and (d) all data sets

#### **4.4. Summary**

This study demonstrated the feasibility of using BBD design of RSM to study the effect of process variables (pressure, nickel concentration, SDS concentration, and MWCO) on MEUF to remove nickel ions from aqueous solutions. RSM results showed that all factors are significantly contributing to the rejection rate, namely the effectiveness of a MEUF process. Pressure and MWCO are significant factors contributing to the permeate flux. Among the range of factors in the study, the optimal conditions to obtain highest rejection (98.16%) and flux (119.20 L/h·m<sup>2</sup>) are: pressure = 30 psi,  $C_{Ni} = 1.0$  mM,  $C_{SDS} = 10.05$  mM, and MWCO = 10 kDa. Optimization results from ANN modeling showed good model fitness. This study shows that RSM and ANN models could be used and provide information for the MEUF treatment of nickel-contaminated water.

## **Chapter 5.**

### **Sulfate Removal Using Colloid-Enhanced Ultrafiltration: Performance Evaluation and Adsorption Studies**



## 5.1. Introduction

Sulfate is present in effluents discharged from a wide range of industries including oil and gas, and mining. They can cause scaling and corrosion of equipment and acidification of soil and water. Sulfate that exists in nature also raises environmental problems. Seawater injection to enhance offshore oil production introduces high levels of sulfate to oil reservoirs, resulting in scaling problems and the growth of sulfate-reducing bacteria in oil reservoirs. These bacteria reduce sulfate to the extremely toxic and corrosive hydrogen sulfide and are referred to as one cause of reservoir souring. Sulfate removal from injection seawater is a method to control sulfate scaling and reservoir souring (Bader, 2007).

Membrane technology is an effective method to remove sulfate ions from water. While nanofiltration and reverse osmosis have been used, both require high operational and maintenance costs. Colloid-enhanced ultrafiltration (CEUF), such as micellar-enhanced ultrafiltration (MEUF) and polymer-enhanced ultrafiltration (PEUF), shows potential as a cost-efficient alternative. In these UF systems, water-soluble colloids such as surfactant micelles or polymers are added to the contaminated water to electrostatically bind the oppositely charged ions. The resulting colloid-solute complex can be retained by a UF membrane, generating clean permeate and higher permeate flux than that of nanofiltration and reverse osmosis. CEUF is most commonly used to remove cations from water (Scamehorn et al., 1994; Tung et al., 2002; Das et al., 2008b; Cojocaru et al., 2009a) and is rarely used to remove anions (Tangvijitsri et al., 2002; Kamble and Marathe, 2005; Zhu et al., 2006). Sulfate removal using CEUF is scarce in the existing

literature. Huang et al. (2015) examined mercury removal using MEUF in presence of sulfate ion (650 ppm, or ca. 4.6 mM). Pookrod et al. (2005) investigated the PEUF performance on arsenic removal with the influence of sulfate salts (0.5-10 mM). In both studies, sulfate was considered as co-existing or interference ions, while its own removal was not examined. When sulfate rejection is monitored, the sulfate concentration is often as low as 1 mM. For example, Chang et al. (2015) investigated the effect of anions (nitrate and sulfate) for chromate removal using MEUF and reported a sulfate removal efficiency of > 94%. Tangvijitsri et al. (2002) investigated chromate, sulfate, and nitrate removal in a PEUF system with a sulfate rejection rate > 98% under reasonable operating conditions. In fact, sulfate to be treated can reach concentrations of hundreds to several thousands of ppm (Maree et al., 2004; Bader, 2007; Agboola et al., 2017). Therefore, the feasibility of MEUF and PEUF to remove sulfate, especially in wider concentration ranges, are yet to be investigated.

Previous MEUF and PEUF studies of wastewater treatment focus on the control of operating conditions, system optimization, and membrane fouling (Schwarze, 2017). MEUF or PEUF processes are based on the adsorption of the solute to the oppositely charged colloid (Roach and Zapien, 2009). Thus, adsorption studies play an important role in understanding the mechanism, the surface properties, and the affinity of the adsorbent. Among the few adsorption studies in this area, Huang et al. (2010) reported adsorption isotherm and kinetics of cadmium and zinc ions on the surfactant sodium dodecyl sulfate in a MEUF system. Lee and Shrestha (2014) fitted the MEUF removal of zinc ions with adsorption kinetic and isotherm models. Almutairi et al. (2011) described the adsorption of metal ions onto polyethylenimine (PEI) using the Langmuir isotherm.

There is a research gap in the adsorption behavior between sulfate and surfactant/polymer, particularly at higher concentrations of sulfate, and in the underlying mechanisms and dynamics of the adsorption process.

This study aims to examine (1) the technical feasibility of MEUF and PEUF to remove sulfate from aqueous solutions, (2) the effect of initial sulfate and surfactant/polymer concentrations on UF performance, and (3) the associated adsorption behavior and the underlying mechanism.

## **5.2. Material and Methods**

### **5.2.1. Chemicals**

Potassium sulfate ( $\text{K}_2\text{SO}_4$ ,  $\geq 99\%$ , Sigma) was used as the source of sulfate ions. To remove anionic ions, the commonly used cationic surfactant, cetyltrimethylammonium bromide (CTAB,  $\geq 99\%$ , Sigma), was used. A water-soluble cationic polyelectrolyte, poly(diallyldimethylammonium chloride) (PDADMAC, 20 wt. % in  $\text{H}_2\text{O}$ , Aldrich) was chosen due to its low acute and chronic toxicity to environmental organisms and its biodegradability. Specifications of CTAB and PDADMAC are listed in Table 5-1. Deionized water (Milli Q water) was used in all experiments, produced by a Barnstead Nanopure water purification system (Thermo Scientific).

### **5.2.2. Ultrafiltration membranes**

The UF membrane was purchased from EMD Millipore (Canada). Its specifications are listed in

Table 5-2. Membranes were treated and washed following manufacturer instructions.

New membranes were soaked in deionized water for at least one hour, changing water at least three times to remove the manufacture residues. Water flux ( $J_{w\text{-new}}$ ) and membrane resistance ( $R_m$ ) of new membranes were determined. Membrane resistance is determined by the slope when plotting  $J_{w\text{-new}}$  ( $\text{m}^3/\text{m}^2\cdot\text{s}$ ) over transmembrane pressures (30–50 psi). After each UF experiment, used membranes were rinsed with deionized water, 0.1 mol/L NaOH, and again deionized water.

New and used membranes were observed using a scanning electron micrographs (SEM) (model FEI Quanta 400 and FEI MLA 650F) with 5 kV accelerating voltage and at a magnification of 500 to 1,000. Membranes were dried, coated with gold, and observed.

### **5.2.3. Experimental set-up**

Figure 5-1 illustrates the dead-end MEUF and PEUF setups used in this study.

Ultrafiltration experiments were carried out in an Amicon Stirred UF Cell (Model 8400, 400-mL capacity; EMD Millipore, Canada). A 240-mL feed solution was filled and continuously stirred in each experimental run. The initial pH of the feed solution was recorded for all runs ( $5.11 \pm 0.82$ ). All experiments were conducted at room temperature ( $24.3 \pm 1.1$  °C). High pressure nitrogen (Air Liquide, Canada) was used to maintain the transmembrane pressure (40 psi, unless specified otherwise).

Table 5-1 Specifications of the surfactant and polymer used in this study

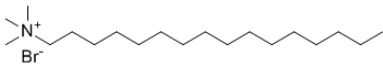
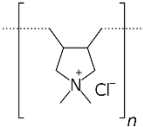
Surfactant/polymer	Molecular formula	Chemical structure	Molecular weight (g/mol)
cetyltrimethylammonium (CTAB)	$C_{19}H_{42}BrN$		364.45
poly(diallyldimethylammonium chloride) (PDADMAC)	$(C_8H_{16}NCl)_n$		Average 400k- 500k; 161.7 (monomer )

Table 5-2 Specifications of the membrane used in this study

<b>Material</b>	<b>MWCO</b>	<b>Diameter (mm)</b>	<b>Effective area (m<sup>2</sup>)</b>	<b>pH range</b>	<b>Operating pressure (psi)</b>	<b>Brand/series</b>
Regenerated cellulose	10,000	76	0.00418	3-13	<70	Amicon/Ultracel

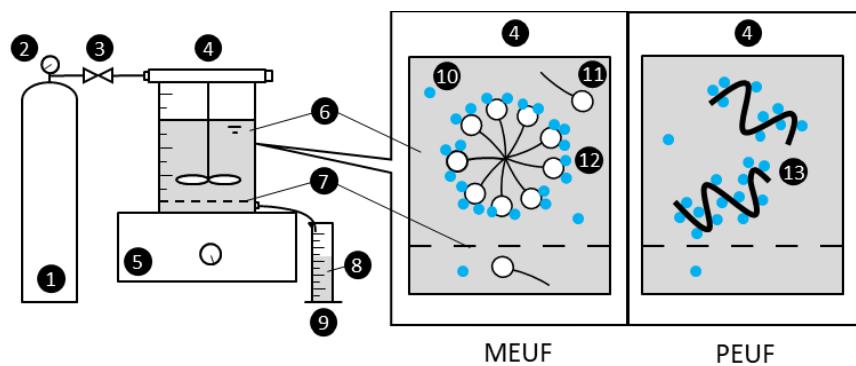


Figure 5-1 Schematic of micellar-enhanced ultrafiltration (MEUF) and polymer-enhanced ultrafiltration (PEUF) setups. 1, nitrogen gas; 2, regulator; 3, pressure control valve; 4, UF cell; 5, magnetic stirrer; 6, feed solution; 7, UF membrane; 8, permeate; 9, volumetric cylinder; 10, sulfate ions; 11, surfactant monomer; 12, surfactant micelle binding sulfate ions; 13, polymer binding sulfate ions.

## **5.2.4. Examination of ultrafiltration performance**

### **5.2.4.1. Experimental runs and procedures**

The UF performance was examined under different initial concentrations of sulfate and surfactant/polymer (Table 5-3) in 25 experimental runs using the one-factor-at-a-time method. The range of sulfate concentration was from relatively low at 1 mM to high 20 mM (reflecting sulfate in mining effluents and seawater). Surfactant/polymer concentrations were determined by preliminary experiments. Feed solutions were prepared dosing desired concentrations of sulfate, surfactant, or polymer (i.e.,  $K_2SO_4$ , CTAB, or PDADMAC) and allowed to sit overnight to reach the solution equilibrium. The molar concentration of PDADMAC solutions is expressed based on the monomer unit to permit comparison with surfactant performance under the same stoichiometric conditions.

Before a UF test, water flux was measured filtering 240-mL deionized water at 40 psi to measure the membrane permeability. Water flux was estimated by collecting permeate during 30s-intervals until a constant value was found. For each UF run, 240 mL of equilibrium feed solution was filled. The first 10-mL permeate was discarded. Seven 20-mL permeate samples were continuously collected with each sampling time recorded. Sampling the last 20-mL permeate marked the end of a run, leaving 90 mL of retentate in the UF cell. A constant stirring speed was maintained to minimize membrane fouling. The concentrations of sulfate, CTAB, and PDADMAC in feed and permeate samples were measured. Performance indicators were determined (described in 5.2.4.2).



Table 5-3 Experimental runs: effect of feed concentrations on ultrafiltration performance

<b>MEUF</b>		<b>PEUF</b>	
<b>Sulfate (mM)</b>	<b>Surfactant (mM)</b>	<b>Sulfate (mM)</b>	<b>Polymer (mM)</b>
<b>Effect of initial surfactant/polymer concentration</b>			
10	0 (blank)	10	0 (blank)
10	10	10	10
10	30	10	30
10	50	10	50
10*	80*	10	80
10	100	10	100
<b>Effect of initial sulfate concentration</b>			
0 (blank)	15	0 (blank)	15
1	15	1	15
5	15	5*	15*
10	15	10	15
15	15	15	15
20	15	20	15

\* duplicate experiments were conducted (randomly selected)

Sulfate concentrations were measured by ion chromatography (Dionex ICS 5000) using an AG23 guard column and AS23 analytical column. Carbonate/Bicarbonate eluent (4.5mM Na<sub>2</sub>CO<sub>3</sub>/0.8 mM NaHCO<sub>3</sub>) was used. The flow rate was 1 mL/min. The concentrations of CTAB and PDADMAC were determined by a total organic carbon analyzer (Shimadzu, Model TOC-L).

#### 5.2.4.2. Parameters for performance evaluation

Two major parameters, the rejection rate and permeate flux, evaluate the UF performance. Although the time-averaged values can be used to evaluate performance, parameters change over time and therefore the instantaneous flux and sulfate rejection at the end of the UF process indicate the performance.

**Rejection rate (R):** The ability of a UF membrane to retain sulfate ions in the solution is characterized by its rejection, R (%):

$$R = \left(1 - \frac{c_p}{c_r}\right) \times 100\% \quad (5-1)$$

where  $c_p$  and  $c_r$  (mg/L) represent sulfate concentrations in permeate and retentate, respectively. By measuring  $c_p$  values during a UF run, the instantaneous  $c_r$  can be calculated by mass balance.

**Flux (J):** Flux (L/m<sup>2</sup>·h) is defined as the flow per unit time per unit membrane effective area.

$$J = \frac{V_p}{t \cdot A_m} \quad (5-2)$$

where  $V_p$  (L) is the permeate volume,  $t$  (h) is the filtration time; and  $A_m$  (m<sup>2</sup>) is the effective membrane area. When deionized water is filtered, the water flux ( $J_w$ ) is obtained.

Three parameters evaluate the solute-colloid interaction: adsorption capacity, colloid loading, and amount of surfactant micelle/polymer. In MEUF/PEUF systems, It is assumed that the surfactant micelles, polymers, and adsorbed sulfate ions are completely retained by the UF membrane, while loose colloid and unbound sulfate ions flow into the permeate (Huang et al., 2010). The target species retained during the whole experimental run are of interest, and therefore the  $c_p$  and  $C_p$  values (outlined below) are the average concentration of all permeate in one experimental run.

**Adsorption amount ( $\Gamma_t$ ):** The solute mass adsorbed per unit adsorbent mass, i.e., the sulfate mass adsorbed per unit colloid mass in the retentate. By measuring sulfate and colloid concentration in the permeate, their mass in the retentate can be determined using mass balance.  $\Gamma_t$  can be expressed as:

$$\Gamma_t = \frac{c_{f,so_4^{2-}} - c_{p,so_4^{2-}}}{c_{f,colloid} - c_{p,colloid}} \quad (5-3)$$

where  $\Gamma_t$  (mg/g) is the amount of sulfate ions adsorbed per unit mass of colloid at time  $t$ ;  $c_{f,so_4^{2-}}$  (mg/L) and  $c_{f,colloid}$  (g/L) are the concentrations of sulfate ions and colloid in the feed, respectively;  $c_{p,so_4^{2-}}$  (mg/L) and  $c_{p,colloid}$  (g/L) are their corresponding concentrations in the permeate. When the solution reaches equilibrium,  $\Gamma_t$  reaches  $\Gamma_e$ .

**Colloid loading ( $L_c$ ):** The loading of surfactant micelles or polymers with sulfate ions is expressed as:

$$L_c = \frac{C_f - C_p}{S_f - S_p} \quad (5-4)$$

where  $L_c$  (mM/mM) is the colloid loading;  $C_f$  and  $C_p$  (mM) are the molar concentrations of sulfate ions in feed and permeate, respectively;  $S_f$  and  $S_p$  (mM) are the molar concentrations of surfactant/polymer in feed and permeate, respectively.

**Amount of surfactant micelle/polymer ( $S'$ ):** the amount of surfactant micelle or polymer that is formed can be expressed as:

$$S' = (c_{f,colloid} - c_{p,colloid}) \times V \quad (5-5)$$

where  $S'$  (g) is the amount of surfactant micelle formed per unit time;  $c_{f,colloid}$  (g/L) and  $c_{p,colloid}$  (g/L) are the concentrations of colloid in the feed and permeate, respectively;  $V$  (L) is the volume of the feed.

### 5.2.5. Adsorption studies

#### 5.2.5.1. Equilibrium isotherm models

Batch adsorption studies were carried out to evaluate the relationship between  $\Gamma_e$ , the amount of sulfate ions adsorbed by colloids, and  $C_e$ , the residual sulfate concentration in the solution (i.e., the average  $c_{p,so_4^{2-}}$  in one UF run). Isotherms studies were carried out with different initial sulfate concentrations (1-20 mM) and a fixed initial CTAB/PDADMAC concentration (15 mM). The equilibrium data were modeled with the frequently used two-parameter adsorption isotherms, i.e., the Langmuir and Freundlich isotherm.

The Langmuir isotherm proposes monolayer adsorption on a homogeneous adsorbent, where all sites are identical and energetically equivalent. No further adsorption

occurs when the monolayer sites are saturated with adsorbates. The Langmuir isotherm can be expressed as (Langmuir, 1918):

$$\Gamma_e = \frac{\Gamma_{max} \cdot K_L \cdot C_e}{K_L \cdot C_e + 1} \quad (5-6)$$

A linear form of this expression is given as:

$$\frac{C_e}{\Gamma_e} = \frac{1}{\Gamma_{max}} C_e + \frac{1}{\Gamma_{max} \cdot K_L} \quad (5-7)$$

where  $\Gamma_e$  and  $\Gamma_{max}$  (mg/g) are the equilibrium and the maximum amount of sulfate, respectively, adsorbed per unit mass of colloid;  $C_e$  (mg/L) is the equilibrium concentration of sulfate ions;  $K_L$  (L/mg) is the Langmuir equilibrium constant that is related to the energy of adsorption. The linear form of Langmuir equation (equation 5-7) plots experimental data  $C_e/\Gamma_e$  versus  $C_e$ . The intercept ( $1/\Gamma_{max}$ ) and slope ( $1/\Gamma_{max}K_L$ ) can be obtained using a linear least squares fitting. The Langmuir constant can then be back-calculated from the intercept and slope.

The Freundlich isotherm proposes that the adsorption occurs via multiple layers onto heterogeneous surfaces (Lima et al., 2015). It is expressed as (Kumar and Porkodi, 2006):

$$\Gamma_e = K_F C_e^{1/n_F} \quad (5-8)$$

A linear form of this expression is given as:

$$\ln \Gamma_e = \frac{1}{n_F} \ln C_e + \ln K_F \quad (5-9)$$

where  $K_F$  ( $\text{mg}^{1-1/n}\text{L}^{1/n}/\text{g}$ ) and  $n_F$  are Freundlich constants related to the adsorption capacity and adsorption intensity, respectively. By plotting  $\ln \Gamma_e$  over  $\ln C_e$  using experimental data, the slope  $1/n_F$  and intercept  $\ln K_F$  give Freundlich constants.

The experimental values of  $\Gamma_e$  and  $C_e$  are were used to plot the linearized equations (equations 5-7 and 5-9) to determine the equilibrium constants. Correlation coefficient ( $R^2$ ) evaluates the fit between experimental data and linear isotherm equations. The average percentage errors (APE) (equation 5-10) evaluates the fitness between experimental and calculated  $\Gamma_e$  (Hamdaoui and Naffrechoux, 2007).

$$\text{APE}(\%) = \frac{\sum_{i=1}^N |(\Gamma_{e,\text{experimental}} - \Gamma_{e,\text{calculated}}) / \Gamma_{e,\text{experimental}}|}{N} \times 100 \quad (5-10)$$

where  $N$  is the number of experimental data.

#### 5.2.5.2. Adsorption kinetics models

Batch kinetic experiments examined the effect of contact time ( $t_1$ - $t_8$ : 5 min, 15min, 30 min, 1h, 2h, 5h, 12h, 24 h) on adsorption. In each of the 16 experimental runs, 250-mL of aqueous solutions were prepared, containing 5 mM sulfate ions and 15 mM CTAB/PDADMAC. The solution was mixed for the designated contact time, then immediately followed by UF experiments at 40 psi. The first 10-mL permeate was discarded, and then 100 mL of permeate was collected and timed. After collecting the permeate sample, the UF was stopped. The concentrations of sulfate ions and CTAB/PDADMAC in the permeate were measured.

The pseudo-first-order (Lagergren, 1898) and pseudo-second-order (Ho and McKay, 1999) kinetic models were applied to fit the experimental data. Their original models (equations 5-11 and 5-13, respectively) and linearized forms (equations 5-12 and 5-14, respectively) are listed below.

$$\Gamma_t = \Gamma_e(1 - e^{-K_1 t}) \quad (5-11)$$

$$\ln(\Gamma_e - \Gamma_t) = \ln \Gamma_e - K_1 t \quad (5-12)$$

$$\Gamma_t = \frac{K_2 \Gamma_e^2 t}{1 + K_2 \Gamma_e t} \quad (5-13)$$

$$\frac{t}{\Gamma_t} = \frac{1}{\Gamma_e} t + \frac{1}{K_2 \Gamma_e^2} \quad (5-14)$$

where  $\Gamma_t$  and  $\Gamma_e$  (mg/g) are the adsorption amount of sulfate ions per unit mass of CTAB/PDADMAC at the adsorption time  $t$  (min) and at equilibrium, respectively;  $K_1$  and  $K_2$  are the pseudo-first-order rate constant ( $\text{min}^{-1}$ ) and pseudo-second-order rate constant ( $\text{g/mg} \cdot \text{min}$ ), respectively.

The initial sorption rate  $h_0$  ( $\text{mg/g} \cdot \text{min}$ ) in pseudo-second-order kinetics can be determined when  $t$  approaches to 0, expressed as

$$h_0 = K_2 \Gamma_e^2 \quad (5-15)$$

Regression analysis was carried out to fit experimental data to linearized kinetic models. Preliminary experiments were conducted to determine  $\Gamma_{e, \text{experiment}}$ . The experimental values of  $\ln(\Gamma_e - \Gamma_t)$  and  $t/\Gamma_t$  are plotted at times  $t_1, t_2, \dots, t_8$ . The slopes

and intercepts of their linear fit give the regressed values of  $\Gamma_{e,calculated}$  and kinetic constants. The coefficient of determination ( $R^2$ ) assesses the goodness of fit of the data by the model.  $\Gamma_{e,experiment}$  were compared with  $\Gamma_{e,calculated}$  to determine error (%).

#### 5.2.6. Quality Assurance/quality control (QA/QC)

**Membrane permeability and reuse:** The reported membrane resistance ( $R_m$ ) was the averaged  $R_m$  values of five new membranes, each measured with water flux over a range of transmembrane pressure (30-50 psi). Triplicate  $J_{w-new}$  was measured under the desired pressure. The fitness of the five flux-pressure relationships gives  $R^2$  of  $0.9951 \pm 0.0048$ . Used membranes were washed with deionized water and dilute solutions as appropriate to regain  $\geq 90\%$  of the original  $J_{w-new}$ . The membrane will be replaced otherwise.

**Ultrafiltration experiment:** Control experiments were conducted to examine the UF performance in absence of sulfate ions or colloids. Two random experimental runs were repeated: an MEUF run ( $[SO_4^{2-}]_f = 10\text{ mM}$ ,  $[CTAB]_f = 80\text{ mM}$ ) yielded a rejection rate of  $90.9 \pm 0.8\%$  and a PEUF run ( $[SO_4^{2-}]_f = 5\text{ mM}$ ,  $[CTAB]_f = 15\text{ mM}$ )  $87.1 \pm 0.1\%$ .

**Sulfate measurement:** Standard curves were prepared daily as appropriate. An internal standard of 5 mg/L was remeasured upon every 10 sample measurements (error < 5%). The detection limit was approximately 0.035 mg  $SO_4^{2-}$ /L. Duplicate tests were performed for each sample with an analytical error <  $\pm 5\%$ .

**TOC measurement:** All TOC bottles and handling glassware were acid washed for 24 h and thoroughly rinsed with deionized water. Standard solutions (20 ppm TOC) were prepared on the day of TOC measurement, diluted from stock standard of 1,000 ppm TOC. The fitness of standard curves gives  $R^2 \geq 0.9993$ . Samples of known



concentrations, deionized water, auto and manual dilution were tested to guarantee accurate results. Standard solution was remeasured after 10 measurement of samples (experimental error < 5%). For each sample, triplicate measurements were conducted (standard error < 5%) and mean values were reported.

**Adsorption experiment:** In equilibrium isotherm studies, the calculated average percentage errors are 8.6% (MEUF) and 5.9% (PEUF). In kinetic studies, the error between  $\Gamma_{e,experiment}$  and  $\Gamma_{e,calculated}$  are 1.12% (MEUF) and 1.25% (PEUF). The models can well describe the adsorption process.

## 5.3. Results and Discussion

### 5.3.1. Performance of ultrafiltration

#### 5.3.1.1. Effect of initial concentrations on rejection and flux

In absence of CTAB/PDADMAC, most sulfate ions in the feed (10 mM) go through the UF membrane (Figure 5-2a), showing that the RC membrane had little effect on sulfate removal. When both sulfate ions and aggregates are present in the solution, exchange takes place between  $SO_4^{2-}$  and  $Br^-$  (in case of CTAB) and between  $SO_4^{2-}$  and  $Cl^-$  (in case of PDADMAC) in the neighbourhood of the polar heads. Figure 5-2 shows that the initial CTAB/PDADMAC concentration, and therefore the quantity of surfactant micelles or polymer ligands in the feed solutions, affect sulfate rejection. At a fixed sulfate concentration of 10 mM, higher CTAB/PDADMAC concentration result in higher rejection (Figure 5-2a). This is because, at higher CTAB/PDADMAC concentrations, the available surfactant micelle or polymer ligand that provide binding sites for sulfate ion

are more abundant (Figure 5-3), therefore removing more sulfate ions. In Figure 5-2a, an initial concentration of 50 mM CTAB/PDADMAC yields a sulfate rejection of approximately 87-90%. Further increase in colloid concentration leads to a minimal increase in rejection, i.e., approximately 90-94% when CTAB/PDADMAC was dosed up to 100 mM. A similar trend of rejection increase was found in other studies when removing metal ions, such as using PEI to remove copper from wastewater (Juang and Chen, 1996).

Though an excess amount of CTAB/PDADMAC could enable highest retention, the process could reduce the permeate flux (i.e., treatment capacity). In Figure 5-2a, the addition of 10 mM CTAB/PDADMAC to the sulfate solution reduced the permeate flux from 154 to 84 and 37 L/m<sup>2</sup>·h for MEUF and PEUF, respectively. The flux further declines with the increasing initial concentration of CTAB/PDADMAC. After dosing 100 mM CTAB/PDADMAC, the permeate flux dropped to 10-20 L/m<sup>2</sup>·h. The increase in surfactant micelle or polymer ligands in the feed increased its viscosity and produced an additional hydrodynamic resistance, thus resulting in a declined permeate flux. Meanwhile, concentration polarization and membrane fouling are more likely to occur at higher colloid concentrations.

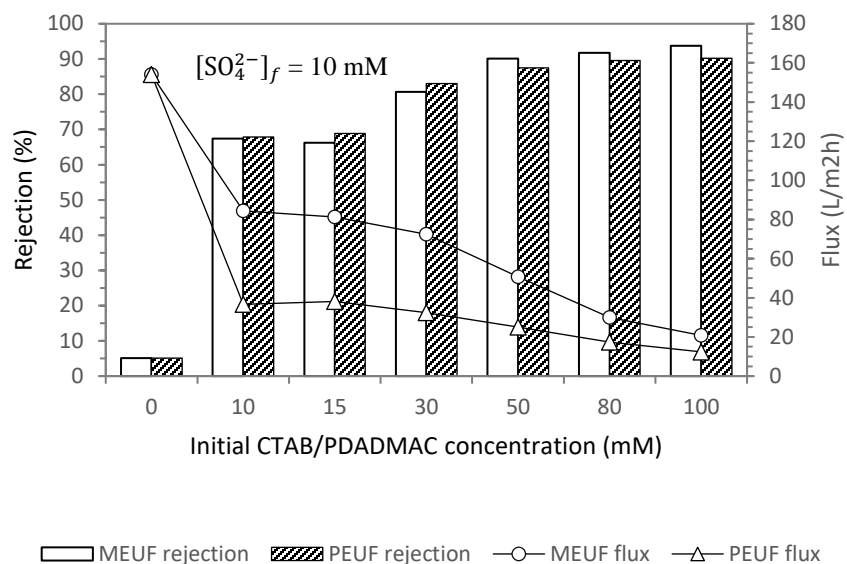
In practice, high rejection rate and high flux are both desired to enable effective removal of sulfate from large volumes of water. Yet a higher CTAB/PDADMAC dose resulted in a higher rejection rate but a lower flux. A trade-off exists between obtaining high rejection and efficiently treating a large volume of wastewater. A low CTAB/PDADMAC dose is desired as long as it yields sufficiently a high rejection. In this

study, a CTAB/PDADMAC dose of 50 mM, i.e., a colloid-to-sulfate ratio of 5:1 seemed sufficient to yield satisfactory results.

When the initial concentration of CTAB/PDADMAC is fixed, sulfate rejection decreases with the increase in initial sulfate concentration (Figure 5-2b). With a fixed adsorbent amount, the number of surfactant micelles or polymer ligands, and therefore the available binding sites for sulfate, were fixed. At low initial sulfate concentrations, sulfate ions bind to the most favorable sites, which are gradually saturated with increasing sulfate dosages (Huang et al., 2016b).

In MEUF systems for removing metal ions, despite the feed concentrations, the surfactant to metal ratio (S/M ratio) is often considered a crucial parameter (Schwarze, 2017). Effect of colloid-to-sulfate ratios (C/S ratio, i.e., the molar ratio of the colloid to sulfate ions in the feed solution) on sulfate rejection was thus considered. From Figure 5-2, it may appear that a higher C/S ratio results in higher rejection. However, comparing the two figures, UF runs with 10 mM sulfate and 10 mM CTAB/PDADMAC and runs with 15 mM sulfate and 15 mM CTAB/PDADMAC both give a C/S ratio of 1:1. The former run yields a rejection of approximately 68%, and the latter with a rejection of 57-61%. In another two runs, i.e., the run dosing 5mM sulfate and 15 mM colloid and another dosing 10mM sulfate and 30 mM colloid, both have a C/S ratio of 3, resulting in approximately 88% and 83% sulfate rejection, respectively. These results indicate that the colloid-enhanced ultrafiltration under the examined conditions was effective to remove sulfate ions from low to relatively high concentrations, showing potential to treat sulfate-rich wastewater.

(a)



(b)

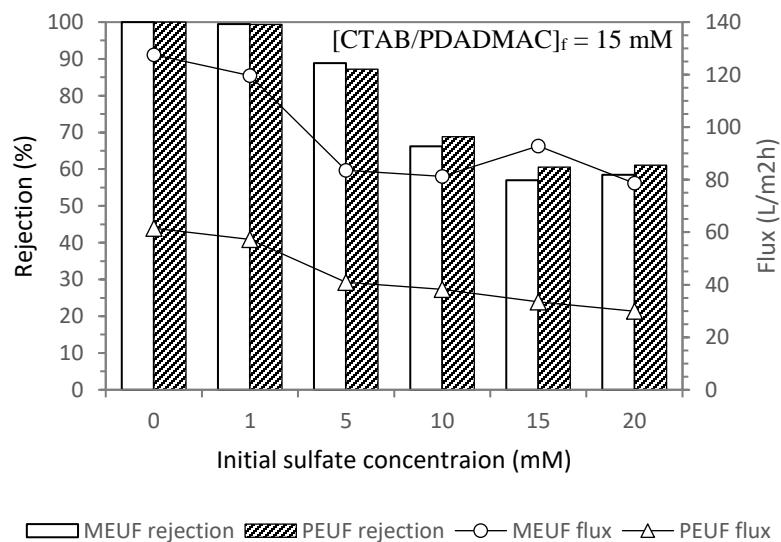


Figure 5-2 Sulfate rejection and permeate flux at different (a) initial CTAB/PDADMAC concentration ( $[\text{SO}_4^{2-}]_f = 10 \text{ mM}$ , and (b) initial sulfate concentration ( $[\text{CTAB/PDADMAC}]_f = 15 \text{ mM}$ ).  $\Delta P = 40 \text{ psi}$ .

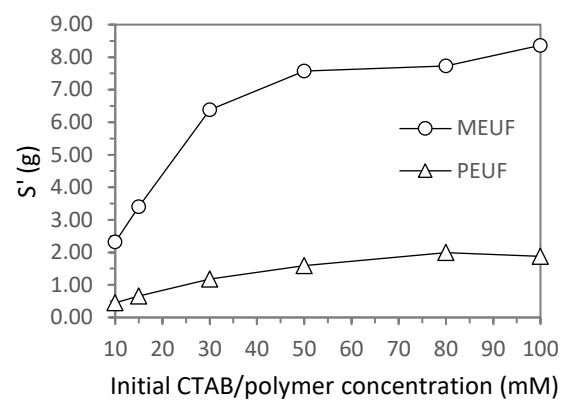


Figure 5-3 Effect of initial CTAB/PDADMAC concentration on the quantity of surfactant micelles/polymer ligands formed.  $[\text{SO}_4^{2-}]_f = 10 \text{ mM}$ .  $\Delta P = 40 \text{ psi}$

#### 5.3.1.2. Effect of initial concentrations on permeate quality

The sulfate concentration in the permeate decreased with increasing CTAB/PDADMAC dosage (Figure 5-4a). When the CTAB dosage was in the range of 10-100 mM, the sulfate concentration decreased from 5.74 to 1.50 mM. At lower CTAB/PDADMAC dosages, the binding sites accessible to sulfate ions are limited and adsorptive sites of the micelles and polymer gradually became saturated. The unbonded sulfate ions will pass through the membrane, resulting in increased sulfate concentration in the permeate.

Figure 5-4b shows the change of sulfate concentration in the permeate when dosing 15 mM of CTAB/PDADMAC in the feed solutions. When sulfate dosage is low, sulfate ions were almost completely adsorbed by the CTAB micelles and PDADMAC, resulting in clean permeates. As the feed sulfate concentration increased, so as the unbounded sulfate ions, therefore an increase of sulfate concentration in the permeate.

To assess the CTAB/PDADMAC passing into the permeate, a control experiment was performed (Figure 5-4b) where only the surfactant or polymer only was dosed. The CTAB/PDADMAC in permeate are minimal ( $< 5\%$  of the initial concentration), indicating that the selected membrane can effectively retain micelles and polymer ligands in the UF system. Low concentrations (0.3-5.3% of the feed concentration) of CTAB/PDADMAC were detected in permeate in all experimental runs (Figure 5-4). Though it was assumed that the critical micellar concentration (i.e., the concentration that surfactant molecules start to aggregate to form micelles) of the surfactant (i.e., 0.9 mM CTAB) would appear in the permeate (Schwarze, 2017), the permeate concentrations of CTAB in this study were less than 0.9 mM. The partial rejection of surfactant was

observed in previous studies and can be attributed to the surfactant-membrane effect (Azong et al., 1997). In terms of polymer, although it could be retained by the UF membrane under optimal conditions, incomplete rejection is often observed (Scamehorn et al., 1990). Such behavior may be due to the chain flexibility, the presence of small molecular weight chains of the polymer, or the existence of large-size pores of the membrane (Juang and Chen, 1996). Leakage of these compounds into the permeate can be mitigated by pre-treatment of the target polymer using UF to remove small molecular weight chains (Huang et al., 2016b). For example, Pookrod et al. (2005) purified PDADMAC using a 10 kDa UF membrane and obtained almost 0% leakage of PDADMAC in the subsequent PEUF experiments. Similar pre-treatment method was employed in other studies to purify other polymers such as Polyvinylamine (PVAm) (Huang et al., 2016b) and poly (styrene sulfonate) (PSS) (Tabatabai et al., 1995). As such, the examined MEUF and PEUF systems can effectively treat sulfate-rich water and generate clean effluent with minimal secondary pollution.

#### **5.3.1.3. Effect of initial concentrations on adsorption**

Both colloid loading and adsorption amount indicate the adsorption density on the adsorbent. Figure 5-5a shows that an increase in colloid dose lowers the adsorption density. This can be understood that higher colloid dose creates more available adsorption sites, where these sites remained unsaturated since the amount of sulfate ions is constant. Under fixed sulfate concentration, colloid loadings are highest at an initial surfactant concentration of 10 mM, generating approximately 0.5 mM/mM loading (i.e., 1 mM CTAB/PDADMAC can adsorb 0.5 mM sulfate ions). A similar trend of micelle loading

was observed in metal (e.g., zinc) removal in MEUF (Lee and Shrestha, 2014). The adsorption amount shows the same trend as that of micelle loading. Stoichiometrically, MEUF and PEUF show similar adsorption amount in terms of colloid loading. Considering colloid mass, PDADMAC can adsorb approximately double amount of sulfate than CTAB does.

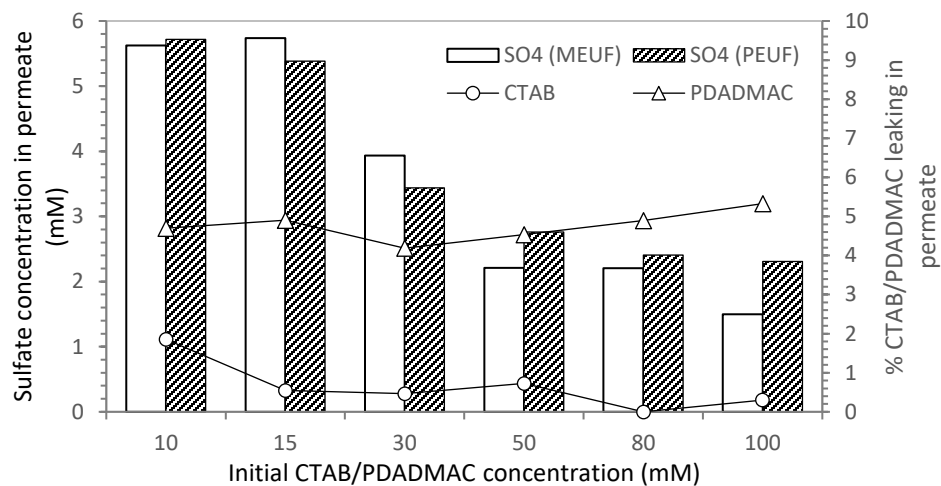
#### **5.3.1.4. Regression analysis of major parameters**

Stepwise regression analysis was conducted using Minitab 17 to investigate the relationship between major system inputs (i.e., initial concentrations of sulfate, surfactant, and polymer) and responses (i.e., sulfate rejection rate, permeate flux, and sulfate concentration in the permeate) (data see Appendix B). Data sets were transformed into natural logarithm as appropriate to obtain the best-fitted models, indicated by highest regression coefficient values (Adjusted  $R^2$ ). Results are summarized in Table 5-4. For three scenarios, the run dosing 1 mM of sulfate ions was eliminated to improve the fitness of regression models. These resulting equations would be more appropriate to describe UF systems with medium to high concentration of sulfate (i.e., 5-20 mM).

Regression results numerically explained the laboratory observations described above. Under the examined conditions, sulfate rejection is positively related to the CTAB/PDADMAC dosage and negatively related to the sulfate dosage, and sulfate dosage seems to play a more important role. Permeate flux is more affected by colloid concentrations than sulfate concentrations. In correspondence, sulfate concentration in permeate is positively related to sulfate dosage and negatively related to CTAB/PDADMAC dosage, while sulfate dosage affecting the effluent quality more.



(a)



(b)

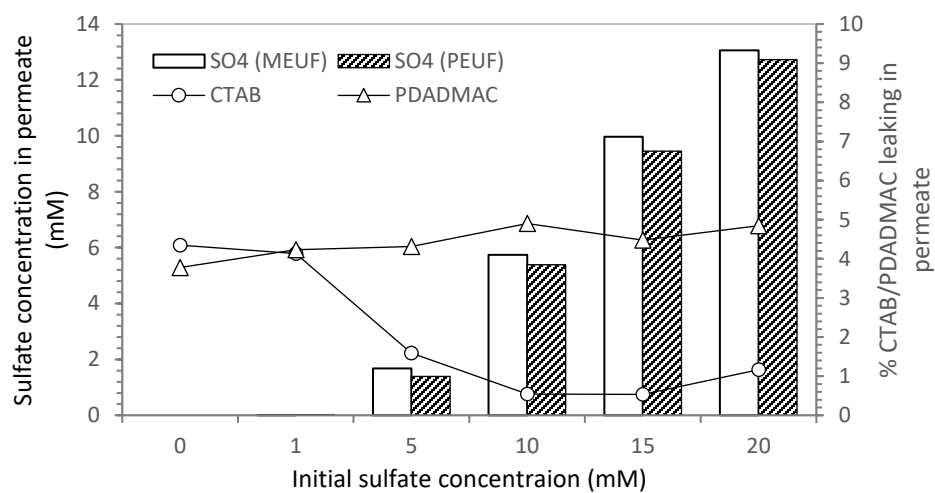
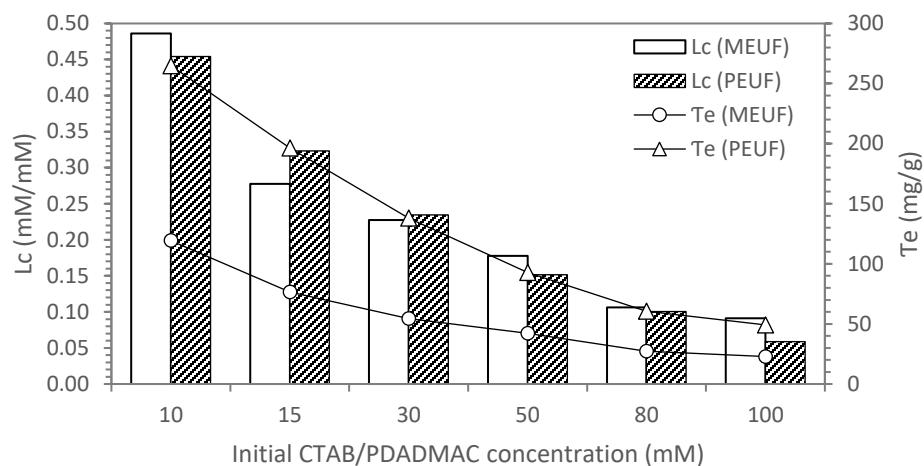


Figure 5-4 Effect of (a) initial CTAB/PDADMAC concentration ( $[\text{SO}_4^{2-}]_f = 10 \text{ mM}$ ) and (b) initial sulfate concentration ( $[\text{CTAB/PDADMAC}]_f = 15 \text{ mM}$ ) on permeate quality

(a)



(b)

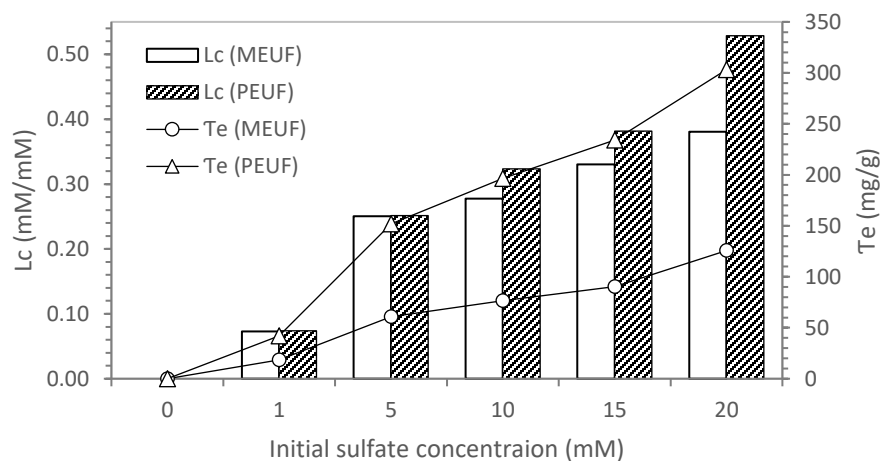


Figure 5-5 (a) Effect of CTAB/PDADMAC concentration on micelle loading ( $L_c$ ) and adsorption amount ( $T_e$ ),  $[SO_4^{2-}]_f = 10$  mM, (b) Effect of sulfate concentration on micelle loading and adsorption capacity  $[CTAB/PDADMAC]_f = 15$  mM

Table 5-4 Summary of results for regression analysis

	<b>Best fitted regression equations</b>	<b><i>Adjusted R<sup>2</sup></i></b>
Rejection– MEUF*	Rejection = 0.9172 - 0.2372 ln[SO <sub>4</sub> <sup>2-</sup> ] <sub>f</sub> + 0.1251 ln[CTAB] <sub>f</sub>	0.9439
Rejection– PEUF*	Rejection = 0.9083 - 0.2058 ln[SO <sub>4</sub> <sup>2-</sup> ] <sub>f</sub> + 0.1065 ln[PDADMAC] <sub>f</sub>	0.9461
Flux–MEUF	ln(Flux) = 4.751 - 0.0087 [SO <sub>4</sub> <sup>2-</sup> ] <sub>f</sub> - 0.01437 [CTAB] <sub>f</sub>	0.8211
Flux–PEUF	Flux = 87.55 – 9.05 ln[SO <sub>4</sub> <sup>2-</sup> ] <sub>f</sub> - 11.15 ln[PDADMAC] <sub>f</sub>	0.9553
Effluent quality– MEUF*	[SO <sub>4</sub> <sup>2-</sup> ] <sub>p</sub> = -2.2350 + 0.8218 [SO <sub>4</sub> <sup>2-</sup> ] <sub>f</sub> - 0.0496 [CTAB] <sub>f</sub>	0.9721
Effluent quality– PEUF*	ln[SO <sub>4</sub> <sup>2-</sup> ] <sub>p</sub> = -1.1360 + 1.6290 ln[SO <sub>4</sub> <sup>2-</sup> ] <sub>f</sub> - 0.3992 ln[PDADMAC] <sub>f</sub> *	0.9840

\* Experimental run with initial [SO<sub>4</sub><sup>2-</sup>]<sub>f</sub>= 1 mM was eliminated from regression analysis.

n=11

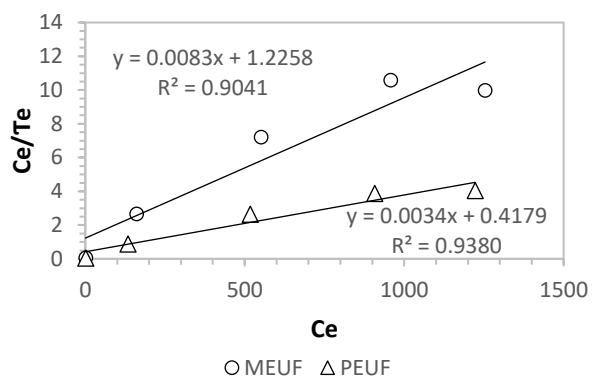
### 5.3.2. Adsorption studies

#### 5.3.2.1. Adsorption equilibrium isotherms

At a constant temperature, an adsorption isotherm describes the equilibrium relationship between  $\Gamma_e$  and  $C_e$ . In this study, batch experiments were conducted dosing fixed CTAB/PDADMAC concentration of 15 mM and varied sulfate concentrations ranging from 1 to 20 mM at room temperature. Regression analysis then fit the experimental data of  $\Gamma_e$  and  $C_e$  to the isotherm models (equations 5-7 and 5-9). Figure 5-6 shows that the Freundlich isotherm shows better linearity ( $R^2 = 0.9741$  and  $0.9896$  in MEUF and PEUF systems, respectively) than the Langmuir isotherm. The Freundlich equation, therefore, could better describe the adsorption process, expressed as  $\Gamma_e = 18.65C_e^{1/4.16}$  (MEUF) and  $\Gamma_e = 37.78C_e^{1/3.61}$  (PEUF).

To further check the validity of the Freundlich isotherm,  $\Gamma_e$  values were calculated from the regressed equations. The average percentage errors between experimental and calculated  $\Gamma_e$  are 8.6% (MEUF) and 5.9% (PEUF), mostly contributed from the higher end of equilibrium concentration (i.e., when  $[SO_4^{2-}]_f = 20$  mM) (Figure 5-7). This finding indicates that the obtained Freundlich equations could overall describe the adsorption process in the examined concentration range ( $[SO_4^{2-}]_f = 1-20$  mM) under experimental conditions and could better describe the 1-15 mM range.

(a)



(b)

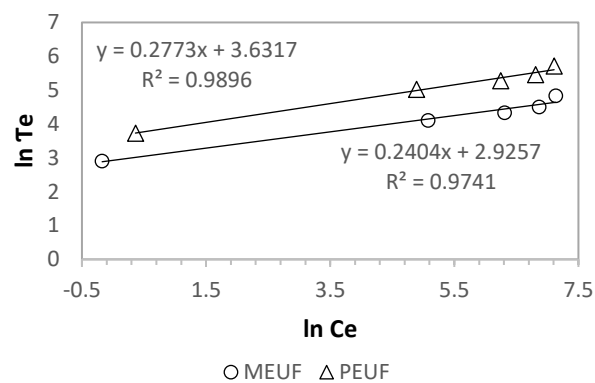


Figure 5-6 Regression analysis fitting experimental data to linearized (a) Langmuir and (b) Freundlich equilibrium isotherms in MEUF and PEUF systems.  $[SO_4^{2-}]_f = 1\text{-}20\text{ mM}$ ,  $[CTAB/PDADMAC]_f = 15\text{ mM}$ .

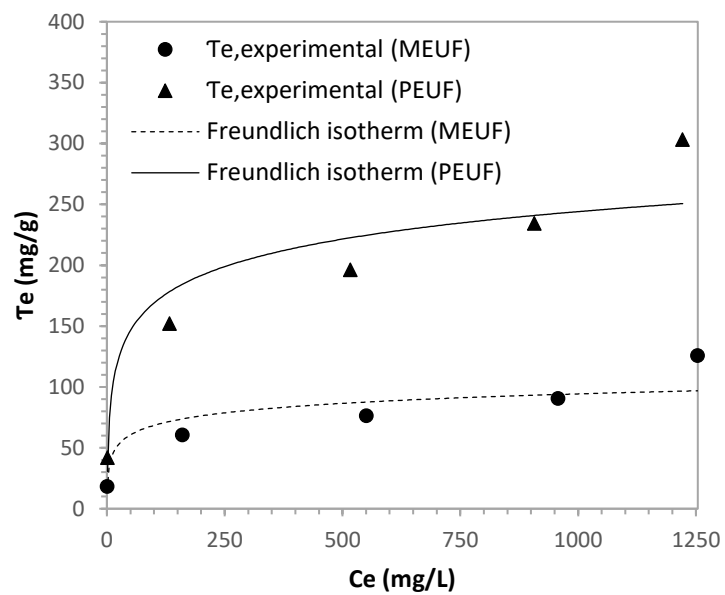


Figure 5-7 Comparison of experimental and calculated Freundlich isotherms of sulfate ions onto colloid.  $[SO_4^{2-}]_f = 1\text{-}20$  mM,  $[CTAB/PDADMAC]_f = 15$  mM.

The fitness of the Freundlich isotherm indicates that the surface of CTAB micelles and PDADMAC ligands are heterogeneous, with adsorption sites of varied affinities (Lima et al., 2015). Previous MEUF studies reported that the Langmuir model could be better to describe metal ions adsorption to the SDS micelle in a cross-flow UF process (Zhang et al., 2007; Huang et al., 2010) when high concentrations of SDS and relatively low metal concentrations were used. In contrast, in another cross-flow system, Lee and Shrestha (2014) reported that the Freundlich isotherm could describe a system containing higher metal concentration and relatively low SDS concentration, where multilayer metal ions adsorbed on SDS micelles. Among the few PEUF studies, adsorption isotherms were tracked in dilute systems containing low concentrations of polymers (Zhu et al., 2006). In this study, where relatively high sulfate concentrations were examined, multilayer sulfate ion adsorption is likely to occur.

The Freundlich constant  $n_F$  indicates the favorability of adsorption: a value of 2-10 shows good adsorption, 1-2 moderately difficult, and less than 1 poor adsorption (Hamdaoui and Naffrechoux, 2007). Under the experimental conditions, both CTAB ( $n_F = 4.16$ ) and PDADMAC ( $n_F = 3.61$ ) are good adsorbent to remove sulfate ions.

#### 5.3.2.2. Adsorption kinetic models

Adsorption kinetics of sulfate ions onto CTAB/PDADMAC have been evaluated by reaction-based models to understand the adsorption mechanism and rate controlling step of this process. The effect of contact time on sulfate adsorption was examined. Experimental data showed better compliance with the pseudo-second-order ( $R^2 > 0.9995$ ) than the pseudo-first-order kinetics ( $R^2 > 0.8808$ ). Calculated kinetics constants for the

pseudo-second-order model are listed in Table 5-5. Within 5 min, the adsorption has reached equilibrium capacity, i.e., 61.35 mg  $SO_4^{2-}$ /g CTAB in MEUF and 153.85 mg  $SO_4^{2-}$ /g PDADMAC in PEUF, indicating high adsorption rates in addition to capacity. No desorption was observed within 24 h.

Fitting of the pseudo-second-order model also indicated that the rate-controlling step in sulfate adsorption onto CTAB/PDADMAC was chemisorption interaction. This means that the concentration of the adsorbate (sulfate ions) and the number of active sites of adsorbents surface (CTAB micelle and PDADMAC ligands) could both affect the adsorption mechanism and the rate of adsorption.

### **5.3.3. Ultrafiltration performance during experimental runs**

Figure 5-8 shows that in one experimental run, instantaneous sulfate rejection was achieved upon initiating the UF process. This rejection value gradually increases during the process, most likely to be caused by concentration polarization. The traditional concentration polarization behavior was also observed in flux decline (Figure 5-9). Similar rejection and flux trend were observed in other systems (Scamehorn et al., 1990). The concentration polarization effect is not severe in the examined conditions, showing the great potential of MEUF and PEUF for sulfate removal in the field.

In Figure 5-10, concentration polarization behavior was also observed by a linear relationship between the permeate flux and the logarithm of colloid concentration in retentate (Scamehorn et al., 1990). In the extreme case of concentration polarization where the permeate flux approaches zero, the colloid concentration in the retentate reaches its maximum value, namely the gel layer concentration (Kamble and Marathe,



2005). From Figure 5-10, gel layer concentration of colloids can be estimated when the flux approaches zero. High gel layer concentrations (as high as approximately 429 mM) were observed. Under fixed initial CTAB/PDADMAC concentration, the UF system can concentrate the feed concentration to over 10 times higher (data not shown). Hence, PEUF and MEUF systems can potentially form concentrated and small-volume waste streams, which eases the further recycle or disposal process.

### **5.3.4. Membrane characteristics**

#### **5.3.4.1. Membrane permeability**

Membrane permeability is tested on five new membranes, yielding a membrane resistance of  $1006 \pm 52 \text{ m}^{-1}$ . Figure 5-11a shows that the water flux is proportional to the transmembrane pressure. When adding colloids, the permeate flux in the MEUF increased with an increase in the transmembrane pressure and it began to level off when the transmembrane pressure was sufficiently high (Figure 5-11b). This can be explained by concentration polarization and gel layer formation. At low pressures, the permeate flux is low and the boundary layer effect on mass transport is insignificant, and thus the water flux increases almost linearly with the transmembrane pressure. However, when the permeate flux becomes large enough that the concentration polarization is no longer negligible, the external mass transfer resistance will be increasingly important. The water flux will continue to increase with the transmembrane pressure but the increase in the flux is less than proportional.

Table 5-5 Pseudo-second-order kinetic constants for adsorption of sulfate ion in MEUF and PEUF systems

Parameters	MEUF	PEUF
$K_2$ (g/mg·min)	0.011	0.001
$h_0$ (mg/g·min)	40.82	20.04
$\Gamma_{e, \text{calculated}}$ (mg/g)	61.35	153.85
Percentage error between $\Gamma_{e, \text{experimental}}$ vs $\Gamma_{e, \text{calculated}}$ (%)	1.13	1.27
$R^2$	1.000	0.9995

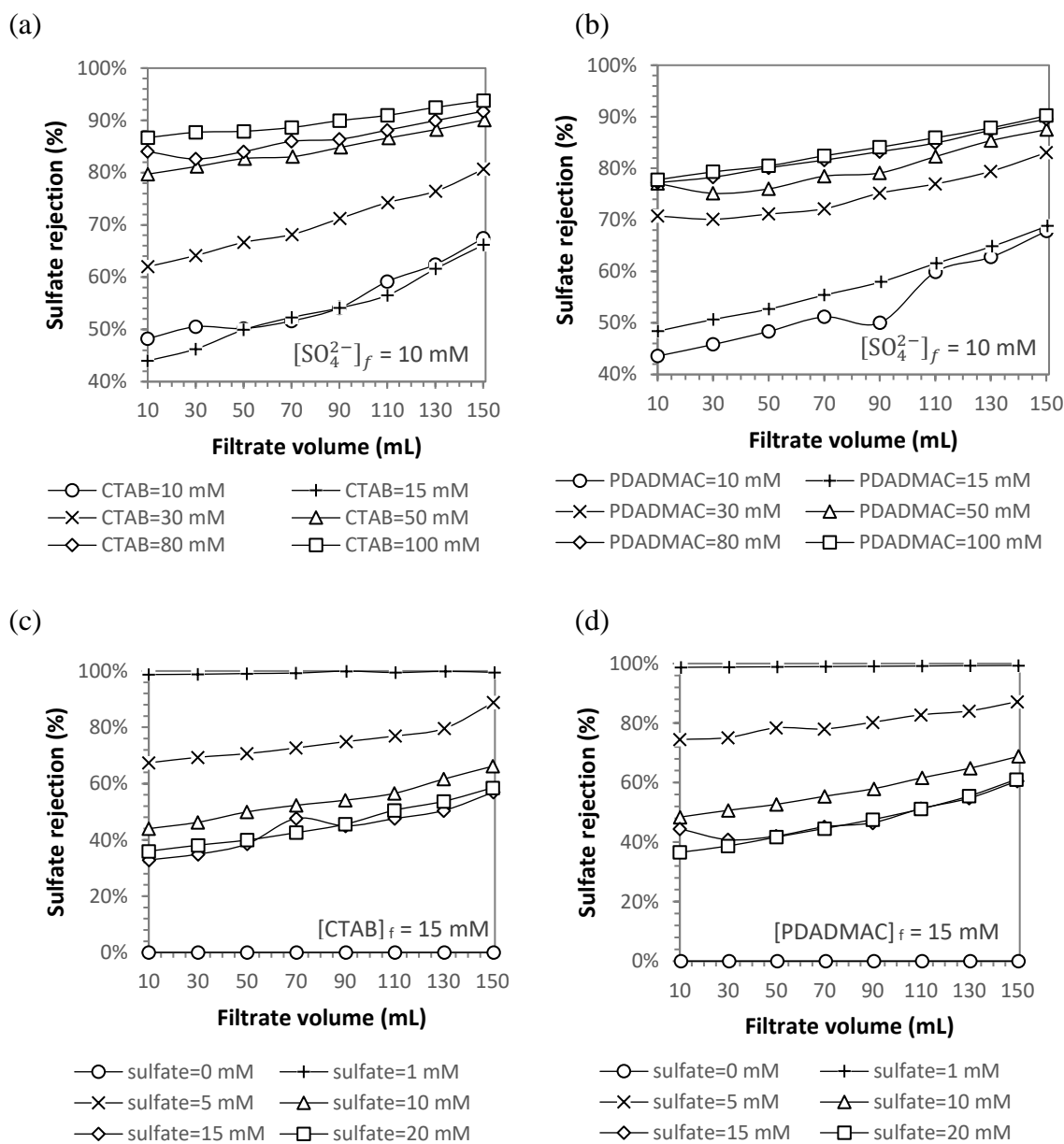


Figure 5-8 Sulfate rejection as a function of the accumulative amount of filtrate at different initial sulfate and colloid concentrations. (a)  $[SO_4^{2-}]_f = 10 \text{ mM}$ ,  $[CTAB]_f = 10\text{-}100 \text{ mM}$ ; (b)  $[SO_4^{2-}]_f = 10 \text{ mM}$ ,  $[PDADMAC]_f = 10\text{-}100 \text{ mM}$ ; (c)  $[SO_4^{2-}]_f = 0\text{-}20 \text{ mM}$ ,  $[CTAB]_f = 15 \text{ mM}$ ; (d)  $[SO_4^{2-}]_f = 0\text{-}20 \text{ mM}$ ,  $[PDADMAC]_f = 15 \text{ mM}$ .  $\Delta P = 40 \text{ psi}$ .

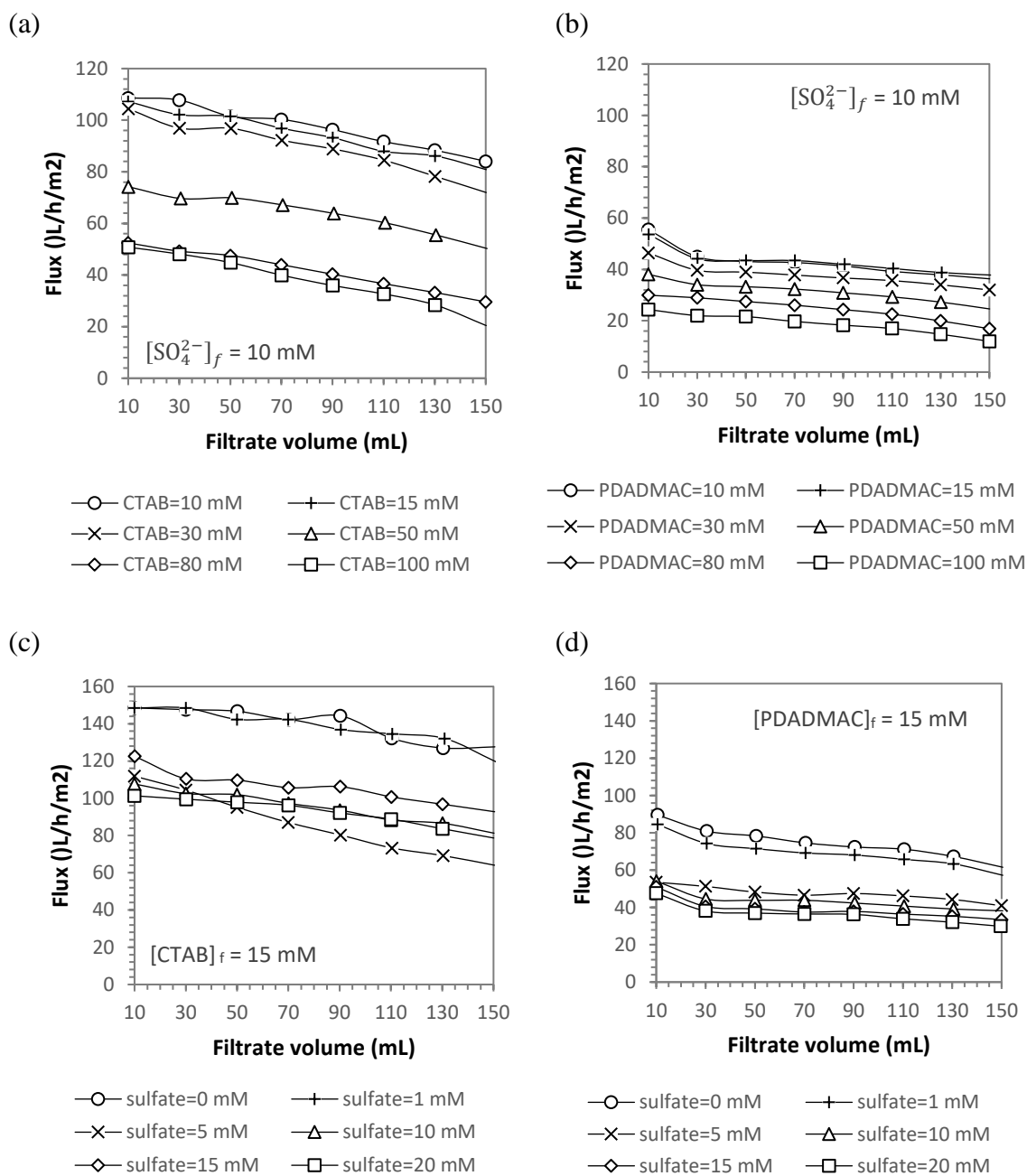


Figure 5-9 Permeate fluxes as a function of the accumulative amount of filtrate at different initial sulfate and colloid concentration. a)  $[SO_4^{2-}]_f = 10$  mM,  $[CTAB]_f = 10-100$  mM; (b)  $[SO_4^{2-}]_f = 10$  mM,  $[PDADMAC]_f = 10-100$  mM; (c)  $[SO_4^{2-}]_f = 0-20$  mM,  $[CTAB]_f = 15$  mM; (d)  $[SO_4^{2-}]_f = 0-20$  mM,  $[PDADMAC]_f = 15$  mM.  $\Delta P=40$  psi.

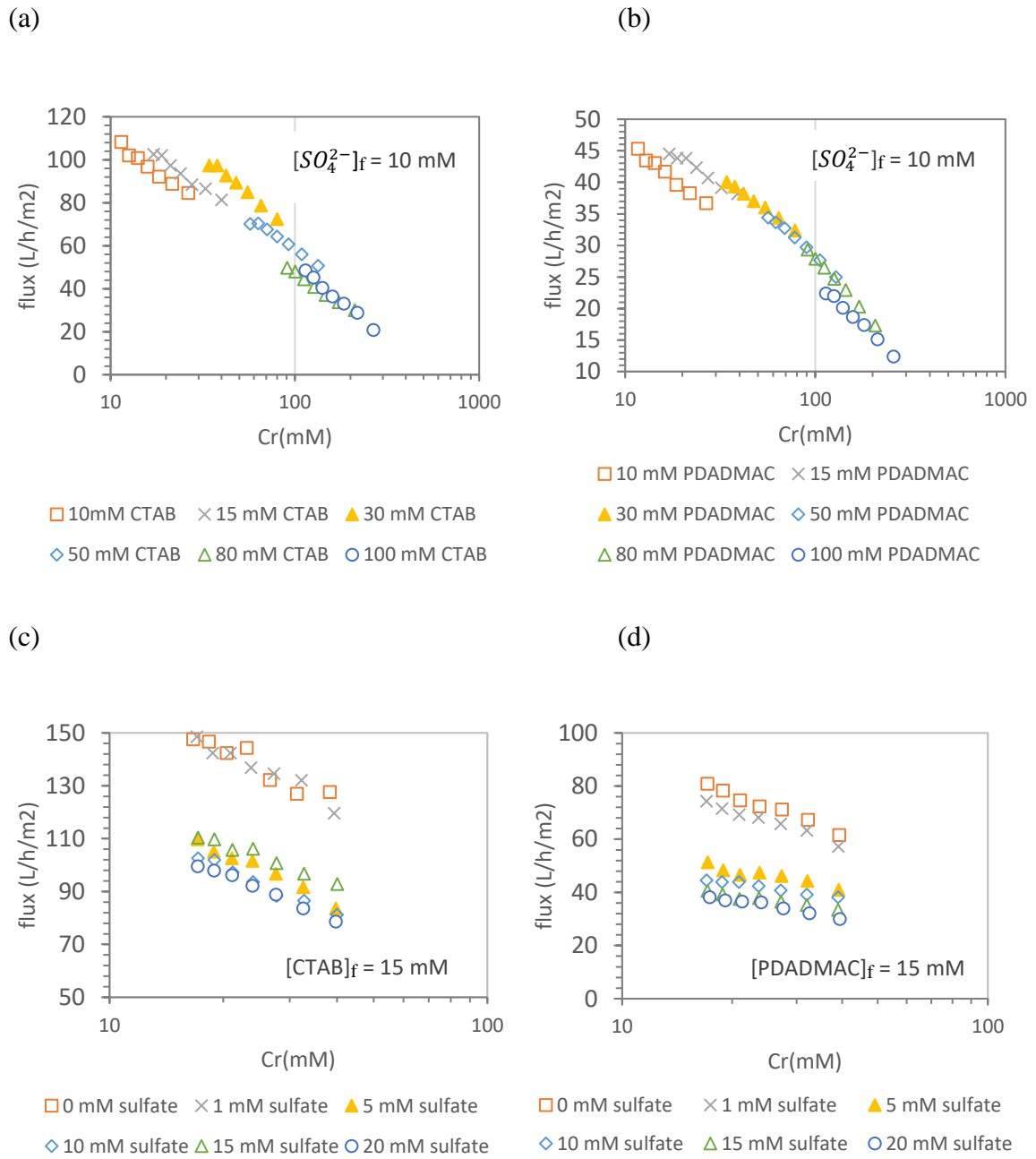


Figure 5-10 Logarithm plot of permeate flux over (a) CTAB and (b) PDADMAC concentrations in retentate

#### 5.3.4.2. Membrane cleaning and reuse

Membrane cleaning using deionized water and cleaning solutions was conducted between UF intervals to reduce membrane fouling. Used membranes were washed to recover at least 90% of the original water flux ( $J_{w\text{-new}}$ ). Figure 5-12 shows the  $J_w$  of a membrane after 10 MEUF runs and another membrane after 13 PEUF runs. Water flux was recovered, indicating that the flux decline during UF runs was associated to reversible fouling. SEM observation (Figure 5-13) compares new and used membranes and shows similar results: few particles were observed in the membrane pores (Figure 5-13 d and f), indicating membranes are feasible to reuse.

#### 5.3.5. MEUF and PEUF comparison

From Figure 5-2a, comparing MEUF and PEUF, when sulfate concentration is fixed, at lower colloid-to-sulfate ratios (i.e., C/S ratio=1 and 3), rejection of PEUF was slightly higher than the rejection of MEUF. On the other hand, at higher ratios (i.e., C/S ratio=5 to 10), the rejection in MEUF was higher than that of in PEUF. That is, considering rejection rate only, PEUF is more effective in systems with low concentrations of sulfate, while MEUF is more effective at higher sulfate concentration. At fixed initial surfactant/polymer concentration (Figure 5-2b), with lower sulfate concentrations (e.g., sulfate 1-5 mM, corresponding to feed ratios of 15 and 3, respectively), rejection of MEUF was higher than that of PEUF. In higher sulfate systems (e.g., sulfate 10-20 mM, C/S ratio=1.5, 1, and 0.75), the rejection of PEUF was higher than that of MEUF. In summary, in terms of rejection rate, at higher C/S ratio, MEUF is more efficient; while at lower ratios, PEUF is more efficient.

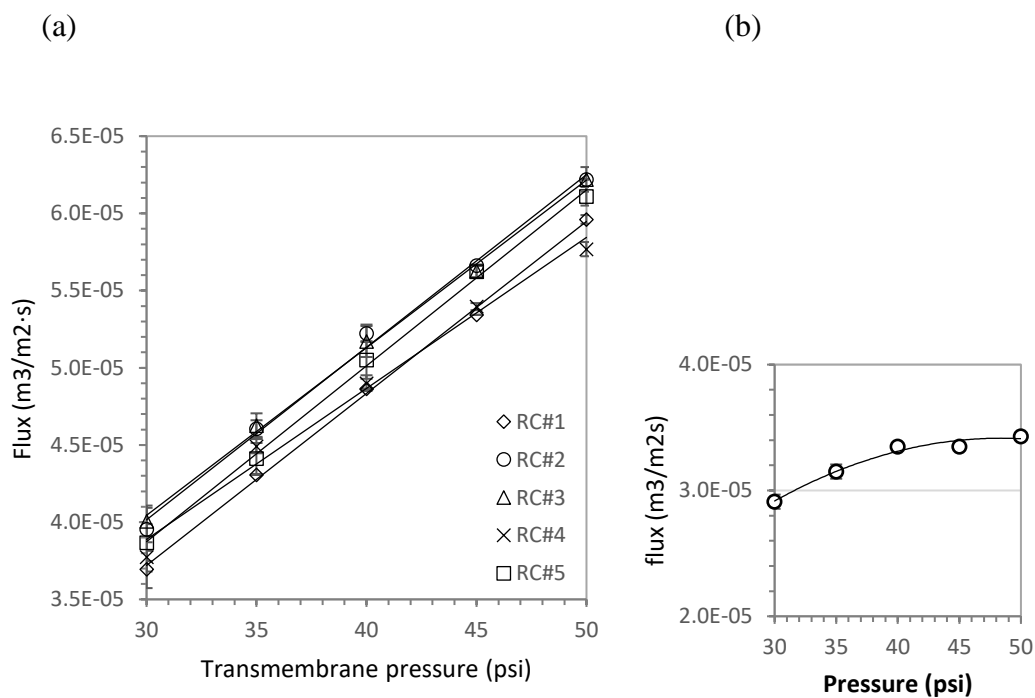


Figure 5-11 Summary of membrane permeability test (a) water flux on new membranes (b) feed solution containing 5 mM  $\text{SO}_4^{2-}$  and 15 mM CTAB. All values are the average of triplicate measurements.

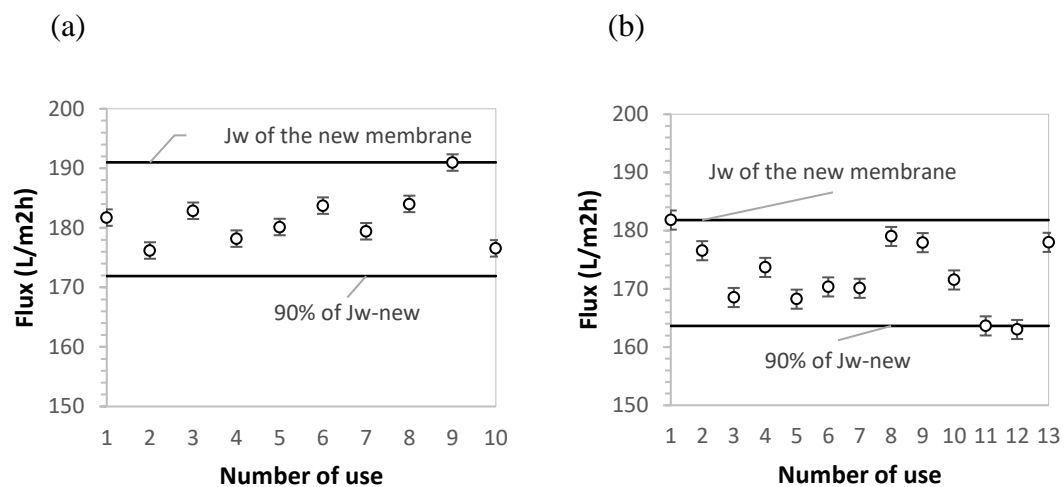


Figure 5-12 Change of water flux: membrane for (a) MEUF use and (b) PEUF use. Values are the mean and standard deviations of triplicate tests. Retaining 90% of  $J_{w\text{-new}}$  deems membrane reusable.



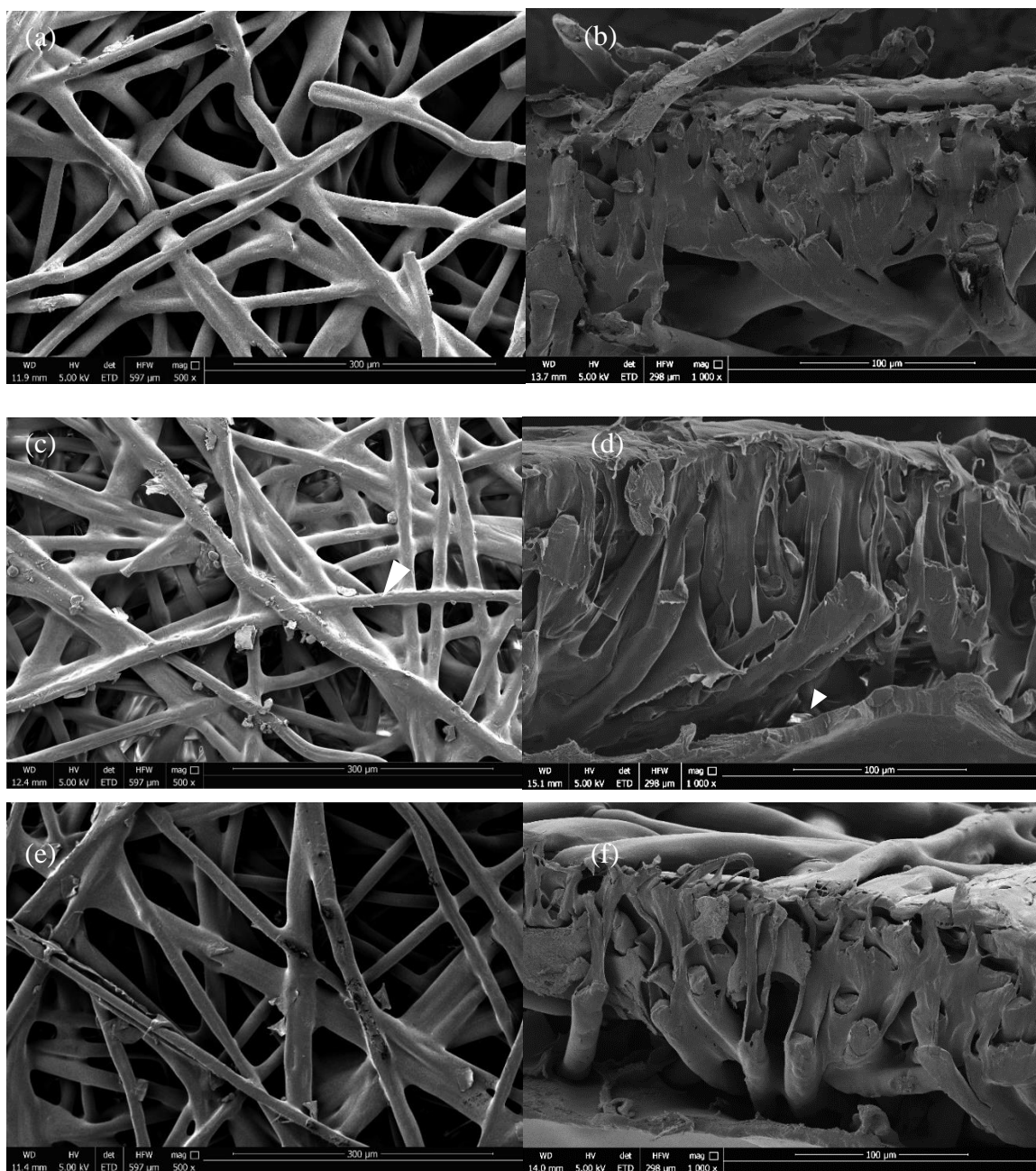


Figure 5-13 Scanning electron micrographs (SEM) of (a) back and (b) cross-section views of a new regenerated cellulose membrane; (c) back and (d) cross-section view of a membrane after 9 MEUF runs; (e) back and (f) cross-section view of membrane after 14 PEUF runs. ( $\blacktriangle$ ) trapped micelle-sulfate complex.

A summary of MEUF and PEUF performance based on findings of this study is listed in Table 5-6, giving a preliminary comparison between the two systems under the same laboratory conditions. Both MEUF and PEUF performed satisfactory sulfate removal. As a whole, PEUF seems preferable than MEUF in the current study, given its low breakthrough in permeate, its potential to be completely retained in UF cells, and lower costs. Due to the large molecular weight, the permeate fluxes in PEUF were much smaller than that in MEUF. One can expect that the intertwining polymer chains, with much bigger molecular weight, may cause a polymer solution to have a higher viscosity and smaller flux than a micellar solution does. The smaller flux directly links to a smaller treatment capacity of sulfate-containing wastewater. This advantage may be mitigated replacing the 10 kDa UF membrane with larger MWCO. In addition, due to the minimal concentration polarization and fouling in the experimental runs, the frequency of membrane replacement is unsure. Additional fouling experiments will be needed to estimate membrane life.

## **5.4. Summary**

In this study, MEUF and PEUF are both effective in removing low-to-high concentrations of sulfate from the water. Under the examined conditions, sulfate removal is more effective with higher surfactant/polymer dosage and/or lower sulfate dosage in the feed. That is, the PEUF/MEUF system is more effective to treat a dilute sulfate system with sufficient surfactant/polymer dosage. In the examined concentration range, an initial 50 mM CTAB or PDADMAC seemed suffice to remove 10 mM of sulfate ions, resulting in approximately 90% sulfate rejection with relatively small flux decline. Both MEUF and

PEUF were more effective in treating dilute sulfate systems, where over 99% rejection rates were achieved. In comparison, PEUF seems preferable than MEUF given its low leakage in permeate, its potential to be completely retained in UF cells, though MEUF is more efficient under higher colloid-to-sulfate ratio.

Equilibrium studies showed that the UF fits Freundlich adsorption isotherm and Lagergren second-order kinetics. The equilibrium adsorption capacity was 61.35 mg  $SO_4^{2-}$ /g CTAB in MEUF and 153.85 mg  $SO_4^{2-}$ /g PDADMAC in PEUF, reached within 5 minutes of the adsorption process, indicating high efficiency of the adsorption process. Traditional concentration polarization behavior (irreversible fouling) was observed in both MEUF and PEUF systems, resulting in flux decline and increased rejection rate during the UF process. Up to 429 mM gel layer concentrations were obtained. Due to the minimal concentration polarization effect, membranes can be reused without much losing the initial flux. To further understand the membrane's resistant to fouling, additional fouling experiments will be needed.

The colloid-enhanced ultrafiltration showed potential as a promising separation technique in treating water containing low to relatively high concentrations of sulfate ions. This study provides information to reservoir souring control and mining wastewater treatment in treating sulfate-containing waters.

Table 5-6 Summary of MEUF vs PEUF performance in this study

	<b>MEUF</b>	<b>PEUF</b>
Sulfate rejection	MEUF higher than PEUF at large surfactant-to-sulfate ratio	PEUF higher than MEUF at low polymer-to-sulfate ratio
Permeate flux	Higher	Lower
UF time	Faster	Slower
Leakage of colloid	Higher percentage	Lower percentage
Fouling tendency	Lower	Higher

## **Chapter 6.**

### **Conclusions, Research Contributions, and Future work**

## 6.1. Conclusions

This thesis investigated MEUF and/or PEUF techniques to treat wastewater containing heavy metal and sulfate ions:

(1) The removal of copper, nickel, and cobalt ions from aqueous solution was investigated using SDS with different surfactant-to-metal (S/M) ratio and pH values. An S/M ratio of 8.5 with a pH of 8-10 was found optimal in the examined range, where the rejection rates of all three metals exceeded 99% and were below Canadian environmental standards. Flux decrease and concentration polarization effect were observed during the experimental procedure. A resampling-based ANN predicted values showing good agreement with experimental data ( $R > 0.99$ ). S/M ratio and pH had relatively greater contributions (30-50%) to the metal rejection rate and permeate flux, whereas sampling time contributed less (10%). High removal rates were achieved quickly after the initiation of the MEUF process, indicating high MEUF efficiency. Also, statistical analysis showed that the type of metal examined in this study did not affect MEUF performance.

(2) An RSM methodology was used to optimize system performance of MEUF for nickel removal, using a BBD design. The generated quadratic models described the relationship between a performance indicator (nickel rejection rate or permeate flux) and process variables (pressure, nickel concentration, SDS concentration, and molecular weight cut-off (MWCO)). The analysis of variance (ANOVA) showed that models are statistically significant. To remove 1 mM of nickel ions, the optimal condition for maximum nickel removal and flux were: pressure = 38.79 psi,  $C_{\text{SDS}} = 12.89$  mM, and MWCO = 10 kDa, resulting in a rejection rate of 97.38% and flux of 118.22 L/h·m<sup>2</sup>.

Further, an ANN model was simulated to predict MEUF performance and validate the RSM results. The model showed good fitness to experimental data ( $R^2 > 0.99$  in most tests). Both RSM and ANN methods could adequately describe the performance indicators within the examined ranges of the process variables.

(3) The technical viability of MEUF and PEUF to sulfate ions were proved, using CTAB and PDADMAC, respectively, as binding ligands. The UF performance was evaluated under different initial concentrations of sulfate (0-20 mM) and CTAB/PDADMAC (0-100 mM). The removal rate was found highest in dilute sulfate solutions (rejection rate  $> 99\%$ ). At higher sulfate concentrations (e.g.,  $> 10$  mM), 50 mM CTAB or PDADMAC can retain approximately 90% of sulfate ions. The observed concentration polarization did not affect membranes reuse. Further, adsorption equilibrium and kinetics studies show that Freundlich isotherm and pseudo-second-order kinetics can describe the adsorption process, indicating that the surface of absorbents are heterogeneous and the rate-controlling step is chemisorption. Both MEUF and PEUF show potential as an effective separation technique in removing sulfate from aqueous solutions. Under the same examined conditions, PEUF shows advantages over MEUF in its higher rejection at lower polymer-to-sulfate ratios, cleaner effluent, and higher adsorption capacity, but compromises on severer flux decline and a tendency of membrane fouling. To overcome this disadvantage, membranes with higher molecular weight cut-off can be used.

## **6.2. Contribution to Knowledge**

(1) The study shows that MEUF is a promising technique and potential treatment method for metal-containing wastewater. The MEUF removal of copper, nickel, and cobalt ions improves the understanding of system parameters' effect and the relative importance between these parameters using a resampling-based ANN tool.

(2) This study is the first report using an BBD based RSM methodology for system optimization of nickel ions removal using MEUF, combined with ANN modeling. The optimization results further enhance the understanding of examined parameters and their interactions in a MEUF system.

(3) The study reported the first investigation for the removal of sulfate as the target solute (from low to high concentrations) under different system conditions in MEUF and PEUF systems. It is also the first report of sulfate-colloid interaction (including adsorption isotherm and kinetic equations) in these systems.

## **6.3. Recommendations and Future Work**

Based on the research findings, further investigations can be extended in following aspects:

- (1) Recovery of metal, surfactant, and polymer: the current study aims at removing the target components by retaining (i.e., concentrating) metal ions, surfactant, and/or polymers in the UF cell. These components either show economic values (i.e., heavy metals) or could be reused for further MEUF runs (i.e., surfactant and polymers). Their recovery and/or reuse could reduce the



costs of MEUF/PEUF process so as to make the technique a more economical alternative.

- (2) Scale-up of MEUF and PEUF system: the current studies used the common dead-end UF cell. In order to bridge the industrial application, the system could be scaled up to use a cross-flow filtration mode with the addition of a feed tank to enable longer filtration time.
- (3) Enhancement of complexity of solute: the current study tackles single-solute systems. In the real case, many ions exist in the effluents. Further investigations could target on MEUF/PEUF systems for the removal and competition effect of co-existing ions. Studies could also test on real industrial wastewater.
- (4) Validation of RSM and regression models: further experiments will be conducted to validate the prediction equations of RSM and regression models.

## Appendix A

Input and output data for Artificial neural networks (ANN) modeling in Chapter 3 (all metal concentration set at 1mM) are listed in Table A-1 below. Inputs include surfactant-to-metal ratio (S/M ratio), pH, and cumulative sampling volume. Outputs are the rejection rate and permeate flux. Each model contents 72 data points.

Table A-0-1 Input and output data for ANN models (Chapter 3)

<b>Input 1</b> <b>S/M ratio</b>	<b>Input 2</b> <b>pH</b>	<b>Input 3</b> <b>cumulative sampling</b> <b>volume (mL)</b>	<b>Output 1</b> <b>Rejection</b>	<b>Output 2</b> <b>Flux (L/h/m2)</b>
<b><u>Cu model</u></b>				
0	Not adjusted	25	1.21%	188.19
0	Not adjusted	50	1.54%	192.72
0	Not adjusted	75	2.28%	189.12
0	Not adjusted	100	2.59%	187.16
0	Not adjusted	125	5.73%	185.41
0	Not adjusted	150	2.14%	185.41
0	Not adjusted	175	2.00%	185.41
0	Not adjusted	200	11.89%	185.41
4	Not adjusted	25	47.70%	172.52
4	Not adjusted	50	50.18%	172.52
4	Not adjusted	75	52.93%	171.03
4	Not adjusted	100	59.14%	168.05
4	Not adjusted	125	56.86%	168.05
4	Not adjusted	150	63.47%	168.13
4	Not adjusted	175	70.23%	164.62
4	Not adjusted	200	75.28%	163.19
6	Not adjusted	25	81.43%	176.12
6	Not adjusted	50	82.89%	176.27
6	Not adjusted	75	85.72%	171.03
6	Not adjusted	100	84.80%	170.92
6	Not adjusted	125	87.61%	168.05
6	Not adjusted	150	88.40%	166.65

<b>Input 1</b> <b>S/M ratio</b>	<b>Input 2</b> <b>pH</b>	<b>Input 3</b> <b>cumulative sampling</b> <b>volume (mL)</b>	<b>Output 1</b> <b>Rejection</b>	<b>Output 2</b> <b>Flux (L/h/m2)</b>
6	Not adjusted	175	90.29%	163.96
6	Not adjusted	200	n/a	n/a
8.5	Not adjusted	25	83.00%	125.98
8.5	Not adjusted	50	87.57%	118.80
8.5	Not adjusted	75	85.57%	117.39
8.5	Not adjusted	100	88.42%	116.51
8.5	Not adjusted	125	87.68%	112.79
8.5	Not adjusted	150	88.62%	110.22
8.5	Not adjusted	175	91.95%	96.78
8.5	Not adjusted	200	90.70%	91.43
10	Not adjusted	25	93.46%	176.43
10	Not adjusted	50	94.52%	180.36
10	Not adjusted	75	95.15%	179.64
10	Not adjusted	100	95.77%	173.90
10	Not adjusted	125	96.46%	174.72
10	Not adjusted	150	96.95%	171.71
10	Not adjusted	175	97.45%	168.38
10	Not adjusted	200	97.86%	161.91
8.5	4	25	78.91%	175.57
8.5	4	50	84.43%	168.13
8.5	4	75	81.83%	169.57
8.5	4	100	85.89%	165.99
8.5	4	125	89.19%	163.96
8.5	4	150	88.67%	161.27
8.5	4	175	90.76%	155.61
8.5	4	200	91.77%	155.61
8.5	6	25	91.99%	182.01
8.5	6	50	92.36%	180.36
8.5	6	75	93.35%	176.97
8.5	6	100	93.75%	171.03
8.5	6	125	94.62%	171.03
8.5	6	150	95.40%	169.57
8.5	6	175	96.19%	165.33
8.5	6	200	96.73%	158.71
8.5	8	25	99.74%	126.67
8.5	8	50	99.88%	84.03

<b>Input 1</b> <b>S/M ratio</b>	<b>Input 2</b> <b>pH</b>	<b>Input 3</b> <b>cumulative sampling</b> <b>volume (mL)</b>	<b>Output 1</b> <b>Rejection</b>	<b>Output 2</b> <b>Flux (L/h/m2)</b>
8.5	8	75	99.89%	63.18
8.5	8	100	99.91%	51.67
8.5	8	125	99.92%	46.68
8.5	8	150	100.00%	44.89
8.5	8	175	100.00%	43.13
8.5	8	200	100.00%	40.57
8.5	10	25	99.61%	118.80
8.5	10	50	99.76%	81.64
8.5	10	75	99.79%	59.94
8.5	10	100	99.81%	50.87
8.5	10	125	99.84%	48.51
8.5	10	150	99.86%	47.01
8.5	10	175	99.89%	45.40
8.5	10	200	99.91%	43.99

#### **Ni model**

0	Not adjusted	25	20.09%	137.37
0	Not adjusted	50	15.66%	135.81
0	Not adjusted	75	18.81%	134.96
0	Not adjusted	100	16.07%	135.50
0	Not adjusted	125	24.77%	135.50
0	Not adjusted	150	19.99%	134.05
0	Not adjusted	175	38.83%	133.68
0	Not adjusted	200	30.99%	133.15
4	Not adjusted	25	51.87%	154.41
4	Not adjusted	50	46.02%	152.61
4	Not adjusted	75	49.32%	149.76
4	Not adjusted	100	53.28%	149.17
4	Not adjusted	125	57.30%	146.96
4	Not adjusted	150	62.76%	145.88
4	Not adjusted	175	64.93%	144.81
4	Not adjusted	200	71.35%	142.73
6	Not adjusted	25	71.72%	150.30
6	Not adjusted	50	74.39%	145.88
6	Not adjusted	75	76.60%	143.76
6	Not adjusted	100	79.28%	142.73

<b>Input 1</b> <b>S/M ratio</b>	<b>Input 2</b> <b>pH</b>	<b>Input 3</b> <b>cumulative sampling</b> <b>volume (mL)</b>	<b>Output 1</b> <b>Rejection</b>	<b>Output 2</b> <b>Flux (L/h/m2)</b>
6	Not adjusted	125	80.84%	141.71
6	Not adjusted	150	84.25%	139.29
6	Not adjusted	175	86.23%	138.74
6	Not adjusted	200	88.80%	134.96
8.5	Not adjusted	25	92.11%	149.76
8.5	Not adjusted	50	92.79%	148.42
8.5	Not adjusted	75	93.47%	146.46
8.5	Not adjusted	100	94.15%	143.30
8.5	Not adjusted	125	95.01%	141.27
8.5	Not adjusted	150	95.69%	139.29
8.5	Not adjusted	175	96.42%	137.77
8.5	Not adjusted	200	97.21%	134.59
10	Not adjusted	25	91.30%	153.83
10	Not adjusted	50	92.64%	149.76
10	Not adjusted	75	93.04%	148.05
10	Not adjusted	100	93.93%	146.96
10	Not adjusted	125	94.69%	143.76
10	Not adjusted	150	95.52%	142.73
10	Not adjusted	175	96.21%	140.27
10	Not adjusted	200	96.74%	136.82
8.5	4	25	85.88%	145.88
8.5	4	50	87.42%	143.76
8.5	4	75	88.44%	142.73
8.5	4	100	90.07%	140.70
8.5	4	125	91.34%	139.29
8.5	4	150	92.73%	138.32
8.5	4	175	93.84%	135.89
8.5	4	200	94.65%	134.05
8.5	6	25	90.63%	139.43
8.5	6	50	91.64%	139.85
8.5	6	75	92.47%	136.58
8.5	6	100	93.08%	135.50
8.5	6	125	94.02%	134.59
8.5	6	150	95.11%	132.79
8.5	6	175	95.70%	131.57
8.5	6	200	96.74%	128.00

Input 1 S/M ratio	Input 2 pH	Input 3 cumulative sampling volume (mL)	Output 1 Rejection	Output 2 Flux (L/h/m2)
8.5	8	25	91.62%	135.89
8.5	8	50	92.39%	135.89
8.5	8	75	93.25%	139.71
8.5	8	100	93.92%	136.82
8.5	8	125	94.72%	134.96
8.5	8	150	95.57%	134.05
8.5	8	175	96.10%	132.79
8.5	8	200	97.18%	130.19
8.5	10	25	99.94%	146.96
8.5	10	50	100.00%	143.76
8.5	10	75	100.00%	142.73
8.5	10	100	100.00%	142.73
8.5	10	125	100.00%	140.55
8.5	10	150	99.98%	139.71
8.5	10	175	99.93%	138.74
8.5	10	200	99.88%	136.82
<b><u>Co model</u></b>				
0	Not adjusted	25	2.64%	137.37
0	Not adjusted	50	0.20%	138.32
0	Not adjusted	75	0.42%	137.37
0	Not adjusted	100	4.60%	136.43
0	Not adjusted	125	0.45%	136.73
0	Not adjusted	150	22.10%	134.96
0	Not adjusted	175	8.74%	134.96
0	Not adjusted	200	9.64%	136.58
4	Not adjusted	25	33.32%	144.91
4	Not adjusted	50	37.38%	141.27
4	Not adjusted	75	43.57%	139.71
4	Not adjusted	100	57.33%	139.29
4	Not adjusted	125	47.61%	138.32
4	Not adjusted	150	54.15%	137.37
4	Not adjusted	175	66.96%	136.04
4	Not adjusted	200	72.04%	134.96
6	Not adjusted	25	75.98%	139.71
6	Not adjusted	50	77.89%	137.37

<b>Input 1</b> <b>S/M ratio</b>	<b>Input 2</b> <b>pH</b>	<b>Input 3</b> <b>cumulative sampling</b> <b>volume (mL)</b>	<b>Output 1</b> <b>Rejection</b>	<b>Output 2</b> <b>Flux (L/h/m2)</b>
6	Not adjusted	75	80.49%	134.96
6	Not adjusted	100	81.52%	134.96
6	Not adjusted	125	83.72%	134.59
6	Not adjusted	150	86.23%	132.79
6	Not adjusted	175	88.63%	131.57
6	Not adjusted	200	90.86%	130.19
8.5	Not adjusted	25	89.10%	128.83
8.5	Not adjusted	50	90.37%	128.00
8.5	Not adjusted	75	91.14%	125.56
8.5	Not adjusted	100	92.23%	124.78
8.5	Not adjusted	125	93.12%	123.23
8.5	Not adjusted	150	94.11%	124.78
8.5	Not adjusted	175	95.17%	123.23
8.5	Not adjusted	200	96.14%	120.97
10	Not adjusted	25	94.12%	131.04
10	Not adjusted	50	94.57%	128.00
10	Not adjusted	75	95.06%	126.36
10	Not adjusted	100	95.68%	124.00
10	Not adjusted	125	96.21%	123.72
10	Not adjusted	150	96.77%	122.95
10	Not adjusted	175	97.31%	121.45
10	Not adjusted	200	97.86%	119.27
8.5	4	25	89.40%	130.71
8.5	4	50	90.33%	128.00
8.5	4	75	91.28%	127.68
8.5	4	100	92.25%	127.17
8.5	4	125	93.20%	125.27
8.5	4	150	94.19%	124.00
8.5	4	175	95.17%	123.23
8.5	4	200	96.18%	121.71
8.5	6	25	90.28%	140.70
8.5	6	50	91.08%	139.71
8.5	6	75	91.95%	137.77
8.5	6	100	92.76%	135.89
8.5	6	125	93.71%	134.96
8.5	6	150	94.68%	133.15

<b>Input 1</b> <b>S/M ratio</b>	<b>Input 2</b> <b>pH</b>	<b>Input 3</b> <b>cumulative sampling</b> <b>volume (mL)</b>	<b>Output 1</b> <b>Rejection</b>	<b>Output 2</b> <b>Flux (L/h/m2)</b>
8.5	6	175	95.59%	131.39
8.5	6	200	96.59%	129.34
8.5	8	25	90.50%	136.43
8.5	8	50	91.31%	134.05
8.5	8	75	92.11%	132.26
8.5	8	100	93.06%	131.39
8.5	8	125	93.95%	129.34
8.5	8	150	94.97%	128.83
8.5	8	175	95.76%	126.36
8.5	8	200	96.62%	124.78
8.5	10	25	99.58%	126.87
8.5	10	50	99.70%	119.51
8.5	10	75	99.75%	111.90
8.5	10	100	99.77%	108.41
8.5	10	125	99.78%	105.53
8.5	10	150	99.81%	103.87
8.5	10	175	99.90%	102.15
8.5	10	200	99.97%	100.09



## Appendix B

Data for regression analysis (Chapter 5) are listed below.

Table B-0-1 Relationship between variables (sulfate concentration, surfactant concentration) and responses (rejection, flux, sulfate concentration in permeate)

<b>X1: SO<sub>4</sub> in feed (mM)</b>	<b>X2: CTAB in feed (mM)</b>	<b>Y1: Rejection (%)</b>	<b>Y2: flux (L/h/m<sup>2</sup>)</b>	<b>Y3: SO<sub>4</sub> in permeate (mM)</b>
10	100	93.77%	20.80	1.51
10	30	80.67%	72.37	3.89
10	80	90.11%	47.97	2.28
10	80	91.74%	30.01	1.93
10	10	67.42%	84.44	5.65
10	50	90.08%	50.66	2.29
1	15	99.50%	92.77	10.09
5	15	88.83%	64.03	1.19
10	15	66.18%	81.25	5.79
15	15	56.96%	119.62	0.01
20	15	58.51%	78.65	13.11

Table B-0-2 Relationship between variables (sulfate concentration, polymer concentration) and responses (rejection, flux, sulfate concentration in permeate)

<b>X1: SO<sub>4</sub> in feed (mM)</b>	<b>X2: PDADMAC in feed (mM)</b>	<b>Y1: Rejection (%)</b>	<b>Y2: flux (L/h/m<sup>2</sup>)</b>	<b>Y3: SO<sub>4</sub> in permeate (mM)</b>
10	10	67.83%	36.73	5.52
10	30	83.04%	32.38	3.54
10	50	87.49%	25.00	2.76
10	80	89.53%	17.29	2.37
10	100	90.21%	12.37	2.23
1	15	99.35%	57.23	0.02
5	15	86.94%	45.09	1.44
5	15	87.20%	40.91	1.41
10	15	68.82%	38.19	5.54
15	15	60.52%	33.45	9.53
20	15	61.07%	29.91	12.48

## References

- Agboola O, Mokrani T, Sadiku ER, Kolesnikov A, Olukunle OI, Maree JP (2017) Characterization of Two Nanofiltration Membranes for the Separation of Ions from Acid Mine Water. *Mine Water and the Environment* 36 (3):401-408. doi:10.1007/s10230-016-0427-z
- Ahmadi M, Vahabzadeh F, Bonakdarpour B, Mofarrah E, Mehranian M (2005) Application of the central composite design and response surface methodology to the advanced treatment of olive oil processing wastewater using Fenton's peroxidation. *Journal of Hazardous Materials* 123 (1-3):187-195. doi:10.1016/j.jhazmat.2005.03.042
- Akita S, Yang L, Takeuchi H (1997) Micellar-enhanced ultrafiltration of gold (III) with nonionic surfactant. *Journal of Membrane Science* 133 (2):189-194
- Aljeboree AM, Alshirifi AN, Alkaim AF (2017) Kinetics and equilibrium study for the adsorption of textile dyes on coconut shell activated carbon. *Arabian Journal of Chemistry* 10:S3381-S3393. doi:10.1016/j.arabjc.2014.01.020
- Almutairi FM, Williams PM, Lovitt RW (2011) Polymer enhanced membrane filtration of metals: retention of single and mixed species of metal ions based on adsorption isotherms. *Desalination and Water Treatment* 28 (1-3):130-136
- Anthati VAK, Marathe KV (2011) Selective separation of copper (II) and cobalt (II) from wastewater by using continuous cross-flow micellar-enhanced ultrafiltration and

surfactant recovery from metal micellar solutions. The Canadian Journal of Chemical Engineering 89 (2):292-298. doi:10.1002/cjce.20380

Azoug C, Sadaoui Z, Charbit F, Charbit G (1997) Removal of cadmium from wastewater by enhanced ultrafiltration using surfactants. The Canadian Journal of Chemical Engineering 75 (4):743-750

Bade R, Lee S-H (2008) Chromate Removal from Wastewater using Micellar Enhanced Ultrafiltration and Activated Carbon Fibre Processes; Validation of Experiment with Mathematical Equations. Environmental Engineering Research 13 (2):98-104. doi:10.4491/eer.2008.13.2.098

Bade R, Lee SH (2007) Micellar enhanced ultrafiltration and activated carbon fibre hybrid processes for copper removal from wastewater. Korean Journal of Chemical Engineering 24 (2):239-245. doi:10.1007/s11814-007-5035-y

Bade R, Lee SH, Jo S, Lee H-S, Lee S-E (2008) Micellar enhanced ultrafiltration (MEUF) and activated carbon fibre (ACF) hybrid processes for chromate removal from wastewater. Desalination 229 (1-3):264-278.  
doi:10.1016/j.desal.2007.10.015

Bader M (2007) Sulfate removal technologies for oil fields seawater injection operations. Journal of Petroleum Science and Engineering 55 (1-2):93-110

Baek K, Kim B-K, Yang J-W (2003) Application of micellar enhanced ultrafiltration for nutrients removal. *Desalination* 156 (1):137-144.

doi:[https://doi.org/10.1016/S0011-9164\(03\)00336-9](https://doi.org/10.1016/S0011-9164(03)00336-9)

Baek K, Yang J-W (2004a) Cross-flow micellar-enhanced ultrafiltration for removal of nitrate and chromate: competitive binding. *Journal of hazardous materials* 108 (1-2):119-123

Baek K, Yang J-W (2004b) Effect of valences on removal of anionic pollutants using micellar-enhanced ultrafiltration. *Desalination* 167:119-125

Baek K, Yang T-W (2004c) Competitive bind of anionic metals with cetylpyridinium chloride micelle in micellar-enhanced ultrafiltration. *Desalination* 167:101-110.  
doi:<https://doi.org/10.1016/j.desal.2004.06.117>

Bahmani P, Maleki A, Rezaee R, Khamfroush M, Yetilmezsoy K, Dehestani Athar S, Gharibi F (2019) Simultaneous removal of arsenate and nitrate from aqueous solutions using micellar-enhanced ultrafiltration process. *Journal of Water Process Engineering* 27:24-31. doi:10.1016/j.jwpe.2018.11.010

Balkin SD, Lin DK (2000) A neural network approach to response surface methodology. *Communications in Statistics-Theory and Methods* 29 (9-10):2215-2227

Bhatnagar A, Minocha AK, Sillanpää M (2010) Adsorptive removal of cobalt from aqueous solution by utilizing lemon peel as biosorbent. *Biochemical Engineering Journal* 48 (2):181-186. doi:10.1016/j.bej.2009.10.005

- Bowell R (2004) A review of sulfate removal options for mine waters. *Proceedings of Mine Water*:75-88
- Cai M, Zhao S, Liang H (2010) Mechanisms for the enhancement of ultrafiltration and membrane cleaning by different ultrasonic frequencies. *Desalination* 263 (1-3):133-138
- Camarillo R, Asencio I, Rincón J (2009) Micellar enhanced ultrafiltration for phosphorus removal in domestic wastewater. *Desalination and water treatment* 6 (1-3):211-216
- Canfield DE, Farquhar J (2009) Animal evolution, bioturbation, and the sulfate concentration of the oceans. *Proceedings of the National Academy of Sciences* 106 (20):8123-8127
- Cañizares P, Lucas AD, Pérez Á, Camarillo R (2005) Effect of polymer nature and hydrodynamic conditions on a process of polymer enhanced ultrafiltration. *Journal of Membrane Science* 253 (1-2):149-163. doi:10.1016/j.memsci.2004.12.042
- Chakraborty S, Dasgupta J, Farooq U, Sikder J, Drioli E, Curcio S (2014) Experimental analysis, modeling and optimization of chromium (VI) removal from aqueous solutions by polymer-enhanced ultrafiltration. *Journal of membrane science* 456:139-154

- Chang W-S, Chen S-S, Yu J-W, Hau NT, Hsu H-T, Cheng H-H (2015) Effects of co-existed anions on retention characteristics of chromate by MEUF. *Desalination and Water Treatment* 55 (10):2829-2835
- Chavalparit O, Ongwandee M (2009) Optimizing electrocoagulation process for the treatment of biodiesel wastewater using response surface methodology. *Journal of Environmental Sciences* 21 (11):1491-1496. doi:10.1016/s1001-0742(08)62445-6
- Cheryan M (1986) *Ultrafiltration handbook*. Technomic Publishing Co. Inc.,
- Chhatre A, Marathe K (2006) Dynamic analysis and optimization of surfactant dosage in micellar enhanced ultrafiltration of nickel from aqueous streams. *Separation science and technology* 41 (12):2755-2770
- Cojocar C, Zakrzewska-Trznadel G (2007) Response surface modeling and optimization of copper removal from aqua solutions using polymer assisted ultrafiltration. *Journal of Membrane Science* 298 (1-2):56-70
- Cojocar C, Zakrzewska-Trznadel G, Jaworska A (2009a) Removal of cobalt ions from aqueous solutions by polymer assisted ultrafiltration using experimental design approach. part 1: Optimization of complexation conditions. *Journal of Hazardous Materials* 169 (1-3):599-609. doi:10.1016/j.jhazmat.2009.03.145
- Cojocar C, Zakrzewska-Trznadel G, Miskiewicz A (2009b) Removal of cobalt ions from aqueous solutions by polymer assisted ultrafiltration using experimental design approach. Part 2: Optimization of hydrodynamic conditions for a crossflow

ultrafiltration module with rotating part. 169 (1-3):610-620.

doi:10.1016/j.jhazmat.2009.03.148

Czitrom V (1999) One-Factor-at-a-Time versus Designed Experiments. The American Statistician 53 (2):126-131. doi:10.1080/00031305.1999.10474445

Danis U, Aydiner C (2009) Investigation of process performance and fouling mechanisms in micellar-enhanced ultrafiltration of nickel-contaminated waters. Journal of Hazardous Materials 162 (2):577-587.

doi:<https://doi.org/10.1016/j.jhazmat.2008.05.098>

Das C, Dasgupta S, De S (2008a) Prediction of permeate flux and counterion binding during cross-flow micellar-enhanced ultrafiltration. Colloids and Surfaces 318 (1-3):125-133. doi:10.1016/j.colsurfa.2007.12.027

Das C, Maity P, DasGupta S, De S (2008b) Separation of cation–anion mixture using micellar-enhanced ultrafiltration in a mixed micellar system. Chemical Engineering Journal 144 (1):35-41

Dunaway CS, Christian SD, Tucker EE, Scamehorn JF (1998) Study of the binding of anions by a cationic polyelectrolyte using equilibrium dialysis. 1. Chromate anions. Langmuir 14 (5):1002-1012

El Zeftawy MM, Mulligan CN (2011) Use of rhamnolipid to remove heavy metals from wastewater by micellar-enhanced ultrafiltration (MEUF). Sep Purif Technol 77 (1):120-127



- Elmolla ES, Chaudhuri M, Eltoukhy MM (2010) The use of artificial neural network (ANN) for modeling of COD removal from antibiotic aqueous solution by the Fenton process. *Journal of hazardous materials* 179 (1):127-134
- Environment Canada (2011) Summary Review of Performance of Metal Mines Subject to the Metal Mining Effluent Regulations in 2011.
- Fillipi BR, Brant LW, Scamehorn JF, Christian SD (1999) Use of micellar-enhanced ultrafiltration at low surfactant concentrations and with anionic–nonionic surfactant mixtures. *Journal of colloid and interface science* 213 (1):68-80
- Foo KY, Hameed BH (2010) Insights into the modeling of adsorption isotherm systems. *Chemical engineering journal* 156 (1):2-10
- Fu F, Wang Q (2011) Removal of heavy metal ions from wastewaters: A review. *Journal of Environmental Management* 92 (3):407-418.  
doi:<https://doi.org/10.1016/j.jenvman.2010.11.011>
- Gadd GM, Griffiths AJ (1977) Microorganisms and heavy metal toxicity. *Microbial Ecology* 4 (4):303-317. doi:10.1007/bf02013274
- Garson DG (1991) Interpreting neural network connection weights. *AI Expert* 6 (7):47-51
- Geckeler KE, Volchek K (1996) Removal of Hazardous Substances from Water Using Ultrafiltration in Conjunction with Soluble Polymers. *Environmental Science & Technology* 30 (3):725-734. doi:10.1021/es950326l

- Gelardi G, Mantellato S, Marchon D, Palacios M, Eberhardt A, Flatt R (2016) Chemistry of chemical admixtures. In: Science and technology of concrete admixtures. Elsevier, pp 149-218
- Government of NL (2016) Mining in Newfoundland and Labrador. Department of natural resources, Mines Branch.
- Greenwood NN, Earnshaw A (2012) Chemistry of the Elements. Elsevier,
- Gzara L, Dhahbi M (2001) Removal of chromate anions by micellar-enhanced ultrafiltration using cationic surfactants. *Desalination* 137 (1-3):241-250
- Halake K, Birajdar M, Kim BS, Bae H, Lee C, Kim YJ, Kim S, Kim HJ, Ahn S, An SY (2014) Recent application developments of water-soluble synthetic polymers. *Journal of Industrial and Engineering Chemistry* 20 (6):3913-3918
- Hamdaoui O, Naffrechoux E (2007) Modeling of adsorption isotherms of phenol and chlorophenols onto granular activated carbonPart I. Two-parameter models and equations allowing determination of thermodynamic parameters. *Journal of Hazardous Materials* 147 (1-2):381-394. doi:10.1016/j.jhazmat.2007.01.021
- Hattab N, Hambli R, Motelica-Heino M, Mench M (2013) Neural network and Monte Carlo simulation approach to investigate variability of copper concentration in phytoremediated contaminated soils. *Journal of environmental management* 129:134-142

- Ho Y-S, McKay G (1999) Pseudo-second order model for sorption processes. *Process biochemistry* 34 (5):451-465
- Huang J-H, Zeng G-M, Zhou C-F, Li X, Shi L-J, He S-B (2010) Adsorption of surfactant micelles and  $\text{Cd}^{2+}/\text{Zn}^{2+}$  in micellar-enhanced ultrafiltration. *Journal of hazardous materials* 183 (1-3):287-293
- Huang J, Peng L, Zeng G, Li X, Zhao Y, Liu L, Li F, Chai Q (2014) Evaluation of micellar enhanced ultrafiltration for removing methylene blue and cadmium ion simultaneously with mixed surfactants. *Separation and Purification Technology* 125:83-89
- Huang J, Shi L, Zeng G, Li H, Huang H, Gu Y, Shi Y, Yi K, Li X (2019) Removal of  $\text{Cd}(\text{II})$  by micellar enhanced ultrafiltration: Role of SDS behaviors on membrane with low concentration. *Journal of Cleaner Production* 209:53-61.  
doi:10.1016/j.jclepro.2018.10.247
- Huang J, Yuan F, Zeng G, Li X, Gu Y, Shi L, Liu W, Shi Y (2017) Influence of pH on heavy metal speciation and removal from wastewater using micellar-enhanced ultrafiltration. *Chemosphere* 173:199-206
- Huang Y-C, Batchelor B, Koseoglu S (1994) Crossflow surfactant-based ultrafiltration of heavy metals from waste streams. *Separation science and technology* 29 (15):1979-1998

- Huang Y, Du J, Zhang Y, Lawless D, Feng X (2016a) Batch process of polymer-enhanced ultrafiltration to recover mercury (II) from wastewater. *Journal of Membrane Science* 514:229-240
- Huang Y, Du JR, Zhang Y, Lawless D, Feng X (2015) Removal of mercury (II) from wastewater by polyvinylamine-enhanced ultrafiltration. *Separation and Purification Technology* 154:1-10
- Huang Y, Wu D, Wang X, Huang W, Lawless D, Feng X (2016b) Removal of heavy metals from water using polyvinylamine by polymer-enhanced ultrafiltration and flocculation. *Separation and Purification Technology* 158:124-136
- INAP (2003) Treatment of Sulphate in Mine Effluents. The International Network for Acid Prevention.  
[http://www.inap.com.au/public\\_downloads/Research\\_Projects/Treatment\\_of\\_Sulphate\\_in\\_Mine\\_Effluents\\_-\\_Lorax\\_Report.pdf](http://www.inap.com.au/public_downloads/Research_Projects/Treatment_of_Sulphate_in_Mine_Effluents_-_Lorax_Report.pdf)
- Iqbal J, Kim H-J, Yang J-S, Baek K, Yang J-W (2007) Removal of arsenic from groundwater by micellar-enhanced ultrafiltration (MEUF). *Chemosphere* 66 (5):970-976. doi:10.1016/j.chemosphere.2006.06.005
- Isa MHM, Frazier RA, Jauregi P (2008) A further study of the recovery and purification of surfactin from fermentation broth by membrane filtration. *Separation and Purification Technology* 64 (2):176-182

- Jaishankar M, Tseten T, Anbalagan N, Mathew BB, Beeregowda KN (2014) Toxicity, mechanism and health effects of some heavy metals. *Interdisciplinary toxicology* 7 (2):60-72
- Jana DK, Roy K, Dey S (2018) Comparative assessment on lead removal using micellar-enhanced ultrafiltration (MEUF) based on a type-2 fuzzy logic and response surface methodology. *Separation and Purification Technology* 207:28-41. doi:10.1016/j.seppur.2018.06.028
- Järup L (2003) Hazards of heavy metal contamination. *British Medical Bulletin* 68 (1):167-182. doi:10.1093/bmb/ldg032
- Jing L, Chen B, Zhang B (2014) Modeling of UV-induced photodegradation of naphthalene in marine oily wastewater by artificial neural networks. *Water, Air, & Soil Pollution* 225 (4):1-14
- Juang R-S, Chen M-N (1996) Retention of copper (II)—EDTA chelates from dilute aqueous solutions by a polyelectrolyte-enhanced ultrafiltration process. *Journal of membrane science* 119 (1):25-37
- Juang R-S, Xu Y-Y, Chen C-L (2003) Separation and removal of metal ions from dilute solutions using micellar-enhanced ultrafiltration. *Journal of Membrane Science* 218 (1-2):257-267

- Jung J, Yang J-S, Kim S-H, Yang J-W (2008) Feasibility of micellar-enhanced ultrafiltration (MEUF) or the heavy metal removal in soil washing effluent. *Desalination* 222 (1-3):202-211
- Kalteh AM, Hjorth P, Berndtsson R (2008) Review of the self-organizing map (SOM) approach in water resources: Analysis, modelling and application. *Environmental Modelling & Software* 23 (7):835-845
- Kamble S, Marathe K (2005) Membrane characteristics and fouling study in MEUF for the removal of chromate anions from aqueous streams. *Separation science and technology* 40 (15):3051-3070
- Karate VD, Marathe K (2008) Simultaneous removal of nickel and cobalt from aqueous stream by cross flow micellar enhanced ultrafiltration. *Journal of hazardous materials* 157 (2-3):464-471
- Kim BK, Baek K, Yang JW (2004) Simultaneous removal of nitrate and phosphate using cross-flow micellar-enhanced ultrafiltration (MEUF). *Water Science and Technology* 50 (6):227-234. doi:10.2166/wst.2004.0380
- Kim H, Baek K, Kim B-K, Shin H-J, Yang J-W (2008) Removal characteristics of metal cations and their mixtures using micellar-enhanced ultrafiltration. *Korean Journal of Chemical Engineering* 25 (2):253-258
- Kiran B, Kaushik A, Kaushik CP (2007) Response surface methodological approach for optimizing removal of Cr (VI) from aqueous solution using immobilized

cyanobacterium. Chemical Engineering Journal 126 (2-3):147-153.

doi:10.1016/j.cej.2006.09.002

Körbahti BK, Aktaş N, Tanyolaç A (2007) Optimization of electrochemical treatment of industrial paint wastewater with response surface methodology. Journal of Hazardous Materials 148 (1-2):83-90. doi:10.1016/j.jhazmat.2007.02.005

Kumar KV, Porkodi K (2006) Relation between some two- and three-parameter isotherm models for the sorption of methylene blue onto lemon peel. Journal of Hazardous Materials 138 (3):633-635. doi:<https://doi.org/10.1016/j.jhazmat.2006.06.078>

Lagergren S (1898) About the theory of so-called adsorption of soluble substances. Sven Vetenskapsakad Handlingar 24:1-39

Landaburu-Aguirre J, García V, Pongrácz E, Keiski RL (2009) The removal of zinc from synthetic wastewaters by micellar-enhanced ultrafiltration: statistical design of experiments. Desalination 240 (1-3):262-269. doi:10.1016/j.desal.2007.11.077

Landaburu-Aguirre J, Pongrácz E, Perämäki P, Keiski RL (2010) Micellar-enhanced ultrafiltration for the removal of cadmium and zinc: use of response surface methodology to improve understanding of process performance and optimisation. Journal of hazardous materials 180 (1-3):524-534

Landaburu-Aguirre J, Pongrácz E, Sarpola A, Keiski RL (2012) Simultaneous removal of heavy metals from phosphorous rich real wastewaters by micellar-enhanced

ultrafiltration. Separation and Purification Technology 88:130-137.

doi:10.1016/j.seppur.2011.12.025

Langmuir I (1918) The adsorption of gases on plane surfaces of glass, mica and platinum.  
Journal of the American Chemical society 40 (9):1361-1403

Lee SH, Shrestha S (2014) Application of micellar enhanced ultrafiltration (MEUF)  
process for zinc (II) removal in synthetic wastewater: Kinetics and two-parameter  
isotherm models. International Biodeterioration & Biodegradation 95:241-250

Leung PS (1980) Surfactant micelle enhanced ultrafiltration. In: Ultrafiltration  
membranes and applications. Springer, pp 415-421

Li C-W, Liu C-K, Yen W-S (2006) Micellar-enhanced ultrafiltration (MEUF) with mixed  
surfactants for removing Cu (II) ions. Chemosphere 63 (2):353-358

Li X, Zeng G-M, Huang J-H, Zhang C, Fang Y-Y, Qu Y-H, Luo F, Lin D, Liu H-L  
(2009) Recovery and reuse of surfactant SDS from a MEUF retentate containing  
Cd<sup>2+</sup> or Zn<sup>2+</sup> by ultrafiltration. Journal of Membrane Science 337 (1-2):92-97

Li X, Zeng G-M, Huang J-H, Zhang D-M, Shi L-J, He S-B, Ruan M (2011) Simultaneous  
removal of cadmium ions and phenol with MEUF using SDS and mixed  
surfactants. Desalination 276 (1):136-141.

doi:<https://doi.org/10.1016/j.desal.2011.03.041>



- Li Z, Ma Z, Van Der Kuijp TJ, Yuan Z, Huang L (2014) A review of soil heavy metal pollution from mines in China: Pollution and health risk assessment. *Science of The Total Environment* 468-469:843-853. doi:10.1016/j.scitotenv.2013.08.090
- Lima ÉC, Adebayo MA, Machado FM (2015) Kinetic and equilibrium models of adsorption. In: *Carbon Nanomaterials as adsorbents for environmental and biological applications*. Springer, pp 33-69
- Lin W, Jing L, Zhu Z, Cai Q, Zhang B (2017) Removal of Heavy Metals from Mining Wastewater by Micellar-Enhanced Ultrafiltration (MEUF): Experimental Investigation and Monte Carlo-Based Artificial Neural Network Modeling. *Water, Air, & Soil Pollution* 228 (6). doi:10.1007/s11270-017-3386-5
- Maree JP, Hlabela P, Nengovhela R, Geldenhuys AJ, Mbhele N, Nevhulaudzi T, Waanders FB (2004) Treatment of Mine Water for Sulphate and Metal Removal Using Barium Sulphide. *Mine Water and the Environment* 23 (4):195-203. doi:10.1007/s10230-004-0062-y
- Michaels AS (1968) Ultrafiltration. In: Perry ES (ed) *Progress in Separations and Purification*, vol 1. New York: Interscience, pp 297-334
- MMER (2012) Metal Mining Effluent Regulations. <http://laws-lois.justice.gc.ca>.
- Montgomery DC (2017) *Design and analysis of experiments*. John Wiley & sons,

- Mosler R, Hatton TA (1996) Surfactants and polymers for environmental remediation and control. *Current Opinion in Colloid & Interface Science* 1 (4):540-547
- Mulder J (1996) Basic principles of membrane technology. Springer Science & Business Media,
- Mungray AA, Kulkarni SV, Mungray AK (2012) Removal of heavy metals from wastewater using micellar enhanced ultrafiltration technique: a review. *Central European Journal of Chemistry* 10 (1):27-46
- Nagy E (2019) Chapter 15 - Nanofiltration. In: Nagy E (ed) *Basic Equations of Mass Transport Through a Membrane Layer (Second Edition)*. Elsevier, pp 417-428.  
doi:<https://doi.org/10.1016/B978-0-12-813722-2.00015-7>
- Pezhhan A, Pezhhan A (2015) Removal of heavy metals from wastewater by membrane processes: A review.
- Pookrod P, Haller KJ, Scamehorn JF (2005) Removal of Arsenic Anions from Water Using Polyelectrolyte-Enhanced Ultrafiltration. *Separation Science and Technology* 39 (4):811-831. doi:10.1081/ss-120028448
- Purkayastha D, Mishra U, Biswas S (2014) A comprehensive review on Cd(II) removal from aqueous solution. *Journal of Water Process Engineering* 2:105-128.  
doi:10.1016/j.jwpe.2014.05.009

Rahmanian B, Pakizeh M, Esfandiyari M, Heshmatnezhad F, Maskooki A (2011a) Fuzzy modeling and simulation for lead removal using micellar-enhanced ultrafiltration (MEUF). *Journal of hazardous materials* 192 (2):585-592

Rahmanian B, Pakizeh M, Mansoori SAA, Abedini R (2011b) Application of experimental design approach and artificial neural network (ANN) for the determination of potential micellar-enhanced ultrafiltration process. *Journal of hazardous materials* 187 (1-3):67-74

Rahmanian B, Pakizeh M, Mansoori SAA, Esfandiyari M, Jafari D, Maddah H, Maskooki A (2012a) Prediction of MEUF process performance using artificial neural networks and ANFIS approaches. *Journal of the Taiwan Institute of Chemical Engineers* 43 (4):558-565. doi:10.1016/j.jtice.2012.01.002

Rahmanian B, Pakizeh M, Maskooki A (2012b) Optimization of lead removal from aqueous solution by micellar-enhanced ultrafiltration process using Box-Behnken design. *Korean Journal of Chemical Engineering* 29 (6):804-811. doi:10.1007/s11814-011-0240-0

Rangabhashiyam S, Anu N, Giri Nandagopal MS, Selvaraju N (2014) Relevance of isotherm models in biosorption of pollutants by agricultural byproducts. *Journal of Environmental Chemical Engineering* 2 (1):398-414. doi:10.1016/j.jece.2014.01.014

- Rengaraj S, Moon S-H (2002) Kinetics of adsorption of Co(II) removal from water and wastewater by ion exchange resins. *Water Research* 36 (7):1783-1793.  
doi:10.1016/s0043-1354(01)00380-3
- Rivas BL, Pereira ED, Palencia M, Sánchez J (2011) Water-soluble functional polymers in conjunction with membranes to remove pollutant ions from aqueous solutions. *Progress in Polymer Science* 36 (2):294-322
- Roach JD, Zapien JH (2009) Inorganic ligand-modified, colloid-enhanced ultrafiltration: A novel method for removing uranium from aqueous solution. *Water Research* 43 (18):4751-4759. doi:10.1016/j.watres.2009.08.007
- Sadeghalvad B, Azadmehr A, Hezarkhani A (2016) Enhancing adsorptive removal of sulfate by metal layered double hydroxide functionalized Quartz-Albitophire iron ore waste: preparation, characterization and properties. *RSC Advances* 6 (72):67630-67642
- Sadri Moghaddam S, Alavi Moghaddam MR, Arami M (2010) Coagulation/flocculation process for dye removal using sludge from water treatment plant: Optimization through response surface methodology. *Journal of Hazardous Materials* 175 (1-3):651-657. doi:10.1016/j.jhazmat.2009.10.058
- Samper E, Rodríguez M, De la Rubia M, Prats D (2009) Removal of metal ions at low concentration by micellar-enhanced ultrafiltration (MEUF) using sodium dodecyl

sulfate (SDS) and linear alkylbenzene sulfonate (LAS). Separation and purification technology 65 (3):337-342

Sánchez J, Rivas BL (2011) Arsenate retention from aqueous solution by hydrophilic polymers through ultrafiltration membranes. Desalination 270 (1-3):57-63

Scamehorn JF, Christian SD, El-Sayed DA, Uchiyama H, Younis SS (1994) Removal of divalent metal cations and their mixtures from aqueous streams using micellar-enhanced ultrafiltration. Separation science and technology 29 (7):809-830

Scamehorn JF, Christian SD, Tucker EE, Tan BI (1990) Concentration polarization in polyelectrolyte-enhanced ultrafiltration. Colloids and Surfaces 49:259-267

Schwarze M (2017) Micellar-enhanced ultrafiltration (MEUF)—state of the art. Environmental Science: Water Research Technology 3 (4):598-624

Schwarze M, Groß M, Moritz M, Buchner G, Kapitzki L, Chiappisi L, Gradzielski M (2015) Micellar enhanced ultrafiltration (MEUF) of metal cations with oleylthoxycarboxylate. Journal of Membrane Science 478:140-147.  
doi:<https://doi.org/10.1016/j.memsci.2015.01.010>

Schwarze M, Le D, Wille S, Drews A, Arlt W, Schomäcker R (2010) Stirred cell ultrafiltration of aqueous micellar TX-100 solutions. Separation and Purification Technology 74 (1):21-27

- Schwarze M, Rost A, Weigel T, Schomäcker R (2009) Selection of systems for catalyst recovery by micellar enhanced ultrafiltration. *Chemical Engineering and Processing: Process Intensification* 48 (1):356-363.  
doi:<https://doi.org/10.1016/j.cep.2008.04.014>
- Shi X, Tal G, Hankins NP, Gitis V (2014) Fouling and cleaning of ultrafiltration membranes: a review. *Journal of Water Process Engineering* 1:121-138
- Shon H, Phuntsho S, Chaudhary D, Vigneswaran S, Cho J (2013) Nanofiltration for water and wastewater treatment-a mini review. *Drinking Water Engineering and Science*
- Silva R, Cadorin L, Rubio J (2010) Sulphate ions removal from an aqueous solution: I. Co-precipitation with hydrolysed aluminum-bearing salts. *Minerals Engineering* 23 (15):1220-1226. doi:10.1016/j.mineng.2010.08.016
- Sriratana S, Scamehorn JF, Chavadej S, Saiwan C, Haller KJ, Christian SD, Tucker EE (1996) Use of poly electrolyte-enhanced ultra filtration to remove chromate from water. *Separation science and technology* 31 (18):2493-2504
- Tabatabai A, Scamehorn JF, Christian SD (1995) Economic feasibility study of polyelectrolyte-enhanced ultrafiltration (PEUF) for water softening. *Journal of membrane science* 100 (3):193-207
- Tait S, Clarke WP, Keller J, Batstone DJ (2009) Removal of sulfate from high-strength wastewater by crystallisation. *Water Research* 43 (3):762-772.  
doi:10.1016/j.watres.2008.11.008

- Tangvijitsri S, Saiwan C, Soponvuttikul C, Scamehorn JF (2002) Polyelectrolyte-enhanced ultrafiltration of chromate, sulfate, and nitrate. *Separation science and technology* 37 (5):993-1007
- Tanhaei B, Pourafshari Chenar M, Saghatoleslami N, Hesampour M, Kallioinen M, Sillanpää M, Mänttari M (2014) Removal of nickel ions from aqueous solution by micellar-enhanced ultrafiltration, using mixed anionic–non-ionic surfactants. *Separation and Purification Technology* 138:169-176.  
doi:<https://doi.org/10.1016/j.seppur.2014.10.018>
- Tansel B, Bao W, Tansel I (2000) Characterization of fouling kinetics in ultrafiltration systems by resistances in series model. *Desalination* 129 (1):7-14
- Tchounwou PB, Yedjou CG, Patlolla AK, Sutton DJ (2012) Heavy Metal Toxicity and the Environment. In. Springer Basel, pp 133-164. doi:10.1007/978-3-7643-8340-4\_6
- Tortora F, Innocenzi V, Prisciandaro M, Mazziotti di Celso G, Vegliò F (2016a) Analysis of membrane performance in Ni and Co removal from liquid wastes by means of micellar-enhanced ultrafiltration. *Desalination and Water Treatment* 57 (48-49):22860-22867
- Tortora F, Innocenzi V, Prisciandaro M, Vegliò F, di Celso GM (2016b) Heavy Metal Removal from Liquid Wastes by Using Micellar-Enhanced Ultrafiltration. *Water, Air, & Soil Pollution* 227 (7):1-11

- Tung C-C, Yang Y-M, Chang C-H, Maa J-R (2002) Removal of copper ions and dissolved phenol from water using micellar-enhanced ultrafiltration with mixed surfactants. *Waste management* 22 (7):695-701
- Urbański R, Góralaska E, Bart H-J, Szymanowski J (2002) Ultrafiltration of Surfactant Solutions. *Journal of Colloid and Interface Science* 253 (2):419-426.  
doi:<https://doi.org/10.1006/jcis.2002.8539>
- USEPA (1972) Clean Water Act. Appendix A to Part 423-126 Priority Pollutants.  
[https://www.ecfr.gov/cgi-bin/text-idx?SID=15e352a79a295dd3e0f1699119f82c04&mc=true&node=pt40.31.423&rgn=div5#\\_top](https://www.ecfr.gov/cgi-bin/text-idx?SID=15e352a79a295dd3e0f1699119f82c04&mc=true&node=pt40.31.423&rgn=div5#_top). Accessed May 2019
- USEPA (2002) National Recommended Water Quality Criteria.  
<https://pdfs.semanticscholar.org/8b2f/d7c89be7249c0726831635b30c85da34495a.pdf>
- Van de Ven W, van't Sant K, Pünt I, Zwijnenburg A, Kemperman AJ, van der Meer WGJ, Wessling M (2008) Hollow fiber dead-end ultrafiltration: Influence of ionic environment on filtration of alginates. *Journal of Membrane Science* 308 (1-2):218-229
- Verma SP, Sarkar B (2017) Rhamnolipid based micellar-enhanced ultrafiltration for simultaneous removal of Cd(II) and phenolic compound from wastewater. *Chemical Engineering Journal* 319:131-142. doi:10.1016/j.cej.2017.03.009



- Vibhandik AD, Marathe KV (2014) Removal of Ni (II) ions from wastewater by micellar enhanced ultrafiltration using mixed surfactants. *Frontiers of Chemical Science and Engineering* 8 (1):79-86
- Volchek K, Krentsel E, Zhilin Y, Shtereva G, Dytnersky Y (1993) Polymer binding/ultrafiltration as a method for concentration and separation of metals. *Journal of membrane science* 79 (2-3):253-272
- Wang J-P, Chen Y-Z, Ge X-W, Yu H-Q (2007) Optimization of coagulation–flocculation process for a paper-recycling wastewater treatment using response surface methodology. *Colloids and Surfaces A: Physicochemical and Engineering Aspects* 302 (1-3):204-210. doi:10.1016/j.colsurfa.2007.02.023
- Xiarchos I, Jaworska A, Zakrzewska-Trznadel G (2008) Response surface methodology for the modelling of copper removal from aqueous solutions using micellar-enhanced ultrafiltration. *Journal of Membrane Science* 321 (2):222-231
- Xu K, Zeng G-M, Huang J-H, Wu J-Y, Fang Y-Y, Huang G, Li J, Xi B, Liu H (2007a) Removal of Cd<sup>2+</sup> from synthetic wastewater using micellar-enhanced ultrafiltration with hollow fiber membrane. *Colloids and Surfaces A: Physicochemical and Engineering Aspects* 294 (1-3):140-146. doi:10.1016/j.colsurfa.2006.08.017
- Xu K, Zeng G-m, Huang J-h, Wu J-y, Fang Y-y, Huang G, Li J, Xi B, Liu H (2007b) Removal of Cd<sup>2+</sup> from synthetic wastewater using micellar-enhanced

- ultrafiltration with hollow fiber membrane. *Colloids and Surfaces A: Physicochemical and Engineering Aspects* 294 (1):140-146
- Yang J-S, Baek K, Yang J-W (2005) Crossflow ultrafiltration of surfactant solutions. *Desalination* 184 (1-3):385-394
- Yang JS, Kwon TS, Baek K, Yang JW (2006) Centrifugal Polyelectrolyte Enhanced Ultrafiltration for Removal of Copper-Citrate Complexes from Aqueous Solutions. *Separation science and technology* 41 (8):1583-1592
- Zhang Z, Zheng G, Huan J, Fang Y, Xu K, Qu Y, Yang C, Li J (2007) Removal of zinc ions from aqueous solution using micellar- enhanced ultrafiltration at low surfactant concentrations. *Water SA* 33 (1). doi:10.4314/wsa.v33i1.48787
- Zhu X, Choo K-H, Park J-M (2006) Nitrate removal from contaminated water using polyelectrolyte-enhanced ultrafiltration. *Desalination* 193 (1-3):350-360
- Zhu X, Tian J, Liu R, Chen L (2011) Optimization of Fenton and electro-Fenton oxidation of biologically treated coking wastewater using response surface methodology. *Separation and Purification Technology* 81 (3):444-450. doi:10.1016/j.seppur.2011.08.023